Aus der Kinderklinik und Kinderpoliklinik im Dr. von Haunerschen Kinderspital
Abteilung für Pädiatrische Infektiologie
der Ludwig-Maximilians-Universität München
Direktor: Prof. Dr. med. Dr. sci. nat. Christoph Klein

Identification of the AI-2 binding protein in the Quorum Sensing system of *Enterococcus faecalis*

Dissertation
zum Erwerb des Doktorgrades der Medizin
an der Medizinischen Fakultät der
Ludwig-Maximilians-Universität München

vorgelegt von
Victoria Riedl

aus
Santa Maria im Münstertal
Schweiz

Jahr
2023

Mit Genehmigung der Medizinischen Fakultät
der Ludwig-Maximilians-Universität München

Berichterstatter:	Prof. Dr. med. Johannes Hübner
Mitberichterstatter:	Prof. Dr. Jürgen Heesemann Prof. Dr. Markus Gerhard Prof. Barbara Stecher
Mitbetreuung durch den promovierten Mitarbeiter:	Dr. Luis Felipe Romero Saavedra
Dekan:	Prof. Dr. med. Thomas Gudermann
Tag der mündlichen Prüfung:	04.05.2023

Content

List of abbreviations

α-LTA..... antibodies raised against lipoteichoic acid from *E. faecalis* 12030
α-T2..... antibodies raised against the whole bacterium of *E. faecalis* Type
α-V583 ..... antibodies raised against the whole bacterium of *E. faecalis* V583
ABC..... ATP-binding cassette
Abneg ..... without antibodies
AI-1 ..... autoinducer 1 (N-3-hydroxybutanoyl-L-homoserine lactone)
AI-2 ..... autoinducer 2 (2R,4S-2-methyl-2,3,3,4-tetrahydroxytetrahydrofuran)
AHLs ..... acyl-homoserine lactones
AIPs..... autoinducing peptides
Ala ..... alanine
AMC..... active methyl cycle
Amp^R ..... ampicillin resistance
Arg ..... arginine
Asn ..... asparagine
Asp ..... aspartate
BHI..... brain heart infusion
BHIA ..... brain heart infusion agar
bp..... base pair
BSA ..... bovine serum albumin
°C ..... degree Celsius
CDM..... chemically defined media
Cm^R..... chloramphenicol resistance
Cneg ..... without complement
ColE1..... origin of replication
Cyl ..... cytolysin
$CylL_S$ ..... cytolysin small subunit
$CylL_L$ ..... cytolysin large subunit
C. saccharobutylicum..... *Clostridium saccharobutylicum*
Δ ..... deletion mutation
dCACHE ..... double calcium channel and chemotaxis receptor
DNA ..... deoxyribonucleic acid
dNTPs..... deoxyribonucleotide triphosphates
DPD..... 4,5-dihydroxy-2,3-pentanedione
EDTA ..... ethylenediamine tetraacetic acid
et al. ..... et alii
EARS-Net ..... European Antimicrobial Resistance Surveillance Network
FBS..... fetal bovine serum

FRET ..... fluorescence resonance energy transfer

FsR ..... *(E.) faecalis* system regulator

FW ..... forward

g ..... gram

GBAP ..... gelatinase biosynthesis activating pheromone

GelE ..... gelatinase

GI ..... gastrointestinal tract

Gly ..... glycine

Gln ..... glutammine

Glc ..... glucose

H ..... enthalpy

His ..... histidine

Ile ..... isoleucine

IPTG ..... isopropyl β-D-1-thiogalactopyranoside

ITC ..... isothermal titration calorimetry

K ..... equilibrium association constant

Kd ..... dissociation constant

Kan^R ..... kanamycin resistance

kb ..... kilobase pair

kV ..... kilovolt

L ..... liter

LAB ..... lactic acid bacteria

Lac ..... lactose

LB Agar ..... Luria/Miller agar

LB Broth ..... Luria/Miller broth

Lsr ..... LuxS regulated

LuxS ..... S-ribosyl-L-homocysteine lyase

Lys ..... lysin

MCS ..... multiple cloning site

Mg^{2+} ..... magnesium

min ..... minute

mini-prep ..... Mini-preparation

mL ..... milliliter

mm ..... millimeter

MRSA ..... methicillin-resistant *Staphylococcus aureus*

ms ..... milliseconds

MTA/SAH ..... methylthioadenosine/S-adenosylhomocysteine

N ..... reaction stoichiometry

Na ..... natrium

NCBI ..... National Center for Biotechnology Information

NEB ..... New England BioLabs

ng ..... nanogram

Ω ..... omega

OD ..... optical density

OD_{430} ..... optical density at 430nm

OD_{485} ..... optical density at 485nm

OD_{527} ..... optical density at 527nm

OD_{595} ..... optical density at 595nm

OD_{600} ..... optical density at 600nm

OD_{660} ..... optical density at 660nm

O-lac ..... lac operator

Oligo ..... oligonucleotides

ON ..... overnight

OPA ..... opsonophagocytic killing assay

PBS ..... phosphate buffered saline

PCR ..... polymerase chain reaction

Pfs ..... methylthioadenosine/S-adenosylhomocysteine nucleosidase

Phe ..... phenylalanine

pmol ..... picomole

PMNs ..... polymorphonuclear neutrophils

PMNneg ..... without polymorphonuclear neutrophils

Pro ..... proline

PT5 ..... phage T5 promoter

QS ..... Quorum Sensing

R^2 ..... coefficient of the determination

RBS ..... ribosomal binding site

RbsB ..... ribose binding proteins

rEF0907 ..... recombinant protein EF0907

R-DHMF 2R,4S-methyl-2,4-dihydroxydihydrofuran-3-one

RNA ..... ribonucleic acid

rpm ..... revolutions per minute

RPMI ..... Roswell Park Memorial Institute

RT ..... room temperature

R-THMF 2R,4S-2-methyl-2,3,3,4-tetrahydroxytetrahydrofuran

RV ..... reverse

S ..... entropy

s ..... seconds

SAH ..... S-adenosylhomocysteine

SAM ..... S-adenosyl-L-methionine

S-DHMF-borate 2S,4S-2-methyl-2,4-dihydroxydihydrofuran-3-one

SDS-PAGE ..... sodium dodecyl sulfate-polyacrylamide gel electrophoresis

Ser ..... serine

$Spec^R$ ..... spectinomycin resistance

spp ..... species pluralis

SprE ..... serine protease

SRH ..... S-ribosyl-L-homocysteine

S-THMF-borate 2S,4S-2-methyl-2,3,3,4-tetrahydroxytetrahydrofuran-borate

Str^R ..... streptomycin resistance

STSB ..... TSB with 0.5M sucrose

S. enterica ser. typhimurium .. *Salmonella enterica* serovar typhimurium

T_0 ..... transcriptional terminator

TBE ..... Tris-borate-EDTA

Tc^R ..... tetracycline resistance

Thr ..... threonine

Tm ..... melting temperature

Tris ..... Tris(hydroxymethyl)aminomethane

Trp ..... tryptophan

TSA ..... tryptic soy agar

TSA-S ..... tryptic soy agar-sheep blood

TSB ..... tryptic soy broth

UG ..... urogenital

UTI ..... urinary tract infection

UV light ..... ultraviolet light

V ..... volt

Val ..... valin

V. harveyi ..... *Vibrio harveyi*

VR ..... vancomycin-resistant

VRE ..... vancomycin-resistant *Enterococci*

X-gal 5-bromo-4-chloro-3-indolyl-β-D-galactopyranoside

xxx ..... single point mutation

xylA ..... xylose inducible promoter

µF ..... microfarad

µg ..... microgram

µL ..... microliter

Index of tables

Index of figures

I. Introduction

I.1. Enterococci

I.1.1. General characteristics of enterococci

Enterococci are Gram-positive, catalase-negative, non-sporulating, and facultative anaerobic bacteria, that are able to grow in single colonies, in pairs, or in short chains [1]. Enterococci are found ubiquitously in nature, i.e. in water, soil, plants, and aliments [2]. Although the natural habitat of enterococci is the gastrointestinal (GI) tract of humans and other higher organism, there they live as beneficial commensals in large numbers [3]. Of the 10^{11} bacterial cells/gram feces found in the human intestinal microbiome [4], about 10^5 to 10^7 bacterial cells/gram feces are enterococci [3]. The capacity of enterococci to colonize such vast niches is related with their ability to survive under harsh conditions [1]. Such conditions are extreme temperatures (5–50°C and 60°C for 30min), wide pH ranges (4.6–9.9), high salinity (6.5% NaCl and 40% bile salts), and oxidative stresses [1,5,6]. Furthermore, enterococci are resistant to dehydration and can withstand detergents, disinfection agents, and antimicrobials, thus they are able to survive on abiotic surfaces for weeks to months [1,7]. Moreover, enterococci possess enormous genomic plasticity. Since they can transfer and integrate mobile resistance elements [7,8], they are able to achieve and distribute resistance to all currently used antibiotics [5,9]. Along with the ability to form biofilms on medical devices [10], enterococci have become feared hospital pathogens [11].

I.1.2. History and taxonomy of enterococci

The first documentation of enterococci dates back to 1899 when Thiercelin described a Gram-positive coccus of intestinal origin [12]. In 1903, Thiercelin and Jouhaud named those coccus "*Enterococcus*" [13]. Because of their ability to grow in chains, Andrewes and Horder (1906) assigned *Enterococcus* to the genus *Streptococcus* [14]. Another effort to classify enterococci was made by Lancefield in 1933, who developed a serological method for the typing of streptococci based on group antigens. From then on, enterococci were also classified as group D streptococci [9]. Later in 1937, enterococci were included in Sherman's classification system for streptococci as so-called “fecal streptococci” [15]. Finally, Schleifer and Kilpper-Bälz used DNA-DNA and DNA-rRNA hybridization to demonstrate the fundamental differences between enterococci and streptococci, that is why enterococci received genus status in 1984 [16]. In the following years, the division was confirmed by 16S rRNA sequence analyses [17,18]. Actually, Bacteria of the genus

Enterococcus are considered as members of the *Enterococcaceae* family who are representatives of the *Lactobacillales* order who in turn belong to the Bacilli class of the low G+C content branch of the Firmicutes phyla [19]. In the last report from 2021, 60 species of enterococci and two subspecies had been identified [20–22].

I.1.3. Pathogenicity of enterococci

Most enterococci are considered as non-virulent [23], for a long time they were expected to be sole beneficial commensals within the GI tract of humans and other higher organism [1,24–26]. Similar to other representatives of the *Lactobacillales* order (lactic acid bacteria, LAB), some enterococcal strains are even administered as probiotics and are supplemented to artisanal foods to favor fermentation [19,27,28]. However, they have been reported to cause life-threatening opportunistic and nosocomial infections [29]. Among the genus *Enterococcus*, *E. faecalis* (60–95%) and *E. faecium* (5–40%) are the two most commonly isolated species in human infections [1,9,30]. For this reason they are considered as the enterococcal species with the greatest clinical relevance worldwide [7,31,32]. Urinary tract infections (UTI) are the most common disease caused by enterococci [33]. Such enterococcal UTIs are more likely to be acquired in hospitals or in long-term care facilities [33]. Enterococci are also frequently isolated in polymicrobial intraabdominal, pelvic, and soft tissue infections [33]. Among the less common infections associated with enterococci are osteomyelitis and meningitis [33]. Feared infections caused by enterococci are bacteremia and endocarditis [33]. Although enterococcal endocarditis is more likely to present as a subacute infection [34], rapid progressions have been described [33].

I.1.4. Antibiotic resistance of enterococci

Besides the intrinsic antibiotic resistance enterococci often possess acquired antibiotic resistances, generally obtained through integration of foreign genetic material or through sporadic gene mutation [35]. Intrinsic resistances of enterococci are listed in table 1.

Table 1: Intrinsic resistances of enterococci [7,36].

Intrinsic resistance to	Species
Aminoglycosides	*Enterococcus* spp.
β-lactams (all cephalosporins, semisynthetic penicillins, monobactams)	*Enterococcus* spp.
Mupirocin	only *E. faecalis*
Lincosamides	*Enterococcus* spp.
Polymyxins	*Enterococcus* spp.
Streptogramine	only *E. faecalis*
Vancomycin	only *E. gallinarum*, *E. casseliflavus*

spp., species pluralis.

With the epidemic of the methicillin-resistant *Staphylococcus aureus* (MRSA) in the 1980s and with the enhanced use of invasive devices, increased usage of Vancomycin arose [6]. As a result, just 15 years after vancomycin's clinical introduction (1954), the first vancomycin-resistant (VR) *E. faecium* strain was isolated from dialysis patients in France and England in 1986 [6,8,37,38]. This was followed by the isolation of the first VR *E. faecalis strain* in the US in 1987 [39,40]. Subsequently, a rapid rise of antibiotic-resistant *Enterococcus* species could be observed in the US in the 1990s and in Europe in the 2000s [8,41]. In the European countries, the rapid expansion of VRE was attributed to the excessive use of avoparcin in animal husbandry, which was added to animal feed as a growth promoter, spreading vancomycin resistance throughout the food chain [9,28,40]. Whereas in America the uncritical usage of antibiotics and the resulting colonization pressure are regarded as the largest contributors for the emergence of VRE populations [28,40].

Today, VRE, also known as glycopeptide-resistant enterococci (GER) [1], are among the pathogens with special resistances and multi-resistances that have to be reported and controlled in German hospitals and outpatient surgery facilities according to the Robert Koch Institute [42]. The risk of VRE colonization depends on the antimicrobial exposure (largest predictor of VRE colonization) and the host characteristics (e.g. hospitalization, contact to colonized or infected patient, insufficient hygiene management,

immunosuppression, severe comorbidities, coinfections, amongst others) [8]. The primary reservoir of VRE is the large intestine [6], where VRE persist for months to years and decolonization efforts are often very difficult to implement [8]. However, skin contamination and colonialization of the genitourinary (GU) tract, and the oral cavity occur regularly [8,40]. Nosocomial VRE are transmitted through the hands of health care professionals [8,24,40].

As mentioned before, *E. faecalis* (60–95%) and *E. faecium* (5–40%) are the most commonly isolated species in human enterococcal infections [1,30]. Although *E. faecalis* is the more frequently isolated because of its higher pathogenicity, *E. faecium* has a broader spectrum of antibiotic resistances than *E. faecalis* [1,7,8]. According to the European Antimicrobial Resistance Surveillance Network (EARS-Net) data, there continued to be an increasing trend in the population-weighted mean percentage of invasive *E. faecium* isolates with vancomycin resistance, increasing from 11.6% in 2016 to 16.8% in 2020 [43]. Regarding the VR *E. faecalis* isolates, the population-weighted mean percentage varies significantly between 0.0 and 7.2% among European countries [44]. In Germany, the resistance rates of invasive VR *E. faecium* isolates even increased to 22.3%, while those of VR *E. faecalis* isolates remain below 1% [45,46].

I.2. Quorum Sensing

In 1994, Fuqua et al. were the first to describe an intra- and interspecies communication system, called Quorum Sensing (QS) which enables bacteria to regulate collective behaviors through specific gene expression [47]. Behaviors regulated by QS include metabolic pathways [48], antibiotic susceptibility [49], virulence [50–52], biofilm formation [52–55], modulation of the gut microbiome [56,57], inflammatory response, and bioluminescence [58]. The first bacterium in which QS has been characterized was the marine bacterium *Vibrio fischeri* [59]. During the colonization of the light organs of several marine animals, this bioluminescent bacteria lives in symbiosis with its hosts and is responsible for the production of light [29]. Autoinducers are low-molecular-weight signaling molecules involved in the QS cell-to-cell communication [60]. Autoinducers are produced endogenously depending on the cell population density and can be actively or passively transported in and out of the cell [60]. So far, three different classes of autoinducers have been described: Acylated homoserine lactones (AHLs) (in Gram-negative bacteria), Autoinducing peptides (AIPs) (in Gram-positive bacteria), and DPD (4,5-dihydroxy-2,3-pentanedione)-derived furanosyl borate diesters (see Figure 2, B, blue branch) or furanones (see Figure 2, B, red branch), which are generally named Autoinducer 2 (AI-

2) (in Gram-negative and Gram-positive bacteria) [29,61]. Based on the different autoinducers classes, three QS systems are characterized (see Figure 1): i. the LuxI/LuxR-type QS system (a), ii. the Oligopeptide-type QS system (b), iii. and the LuxS/AI-2-type QS system (c) [29,61].

I.2.1. LuxI/LuxR-type Quorum Sensing system

The LuxI/LuxR-type QS system (Figure 1, a) has been described for Gram-negative bacteria and uses as autoinducer different AHLs (red triangle) [30]. AHLs are composed of homoserine-lactone rings which are acylated at their N-termini with four to eighteen modified acyl chains [62]. AHLs can be detected by LuxR-type proteins (solid ellipse), which in bound state can bind specific promoter DNA elements (open arrow) and let to transcription of target genes (xyz) [63]. Since the bacterial cell membrane is permeable to AHLs, they are passively secreted [63].

I.2.2. Oligopeptide-type Quorum Sensing system

The Oligopeptide-type QS system (Figure 1, b) has been described for Gram-positive bacteria and uses as autoinducer different AIPs (red waves) [30]. Typically, AIPs are precursor peptides consisting from five to seventeen amino acids which are modified intracellularly and actively secreted in the environment by cell-surface oligopeptide transporters (open ellipse) since the bacterial cell membrane is not permeable to AIPs [63]. The cognate AIPs can be detected by a two-component signal transduction circuit: AIPs are bound by a sensor kinase (open circle) and consequently, phosphorylation of a response regulator protein (closed ellipse) takes place [63]. In its phosphorylated state, the regulator protein binds promoter DNA (open arrow) leading to transcription of target genes (xyz) [63].

I.2.3. The LuxS/AI-2-type Quorum Sensing System

The LuxS/AI-2-type QS system is normally found in Gram-negative and Gram-positive bacteria and uses as signaling molecules DPD derivates which are synthesized by the LuxS enzyme and are generally named AI-2 [30]. To date, AI-2-like activity has been observed only in strains possessing a LuxS-like gene [63]. Interestingly, in over half of all sequenced bacterial genomes LuxS-like genes have been found [64]. However, AI-2 was first described in the bioluminescent marine bacterium *Vibrio harveyi* (*V. harveyi*) [65]. The AI-2 used from *V. harveyi* is a furanosyl borate diester which together with its cognate AHL autoinducer 1 (AI-1) regulates bioluminescence (see Figure 1, c) [66]. While AI-1 (blue triangles) is produced by the LuxLM protein (open square with blue labeling), the

AI-2 (red circles) is synthesized by the LuxS protein. For internalization, the autoinducers bind to the autoinducer sensors LuxN (cap) or to LuxP/LuxQ (cap/open rectangle with curved side edges), both kinases [63]. In bound state, dephosphorylation of the phosphotransferase LuxU (open square) and the response regulator protein LuxO (open rectangle with curved side edge) take place resulting in the transcription of the luciferase gene luxCDABE [63]. Additionally, the activator protein LuxR (open circle) is required for sufficient gene expression. [63] Interestingly, different bacteria recognize different DPD derivatives (see Figure 3, B) [63]. Presumably, the perpetual interconversion between the different forms of the signal molecule accomplished by the bacteria to respond not only to their own AI-2 but also to AI-2 produced by other bacterial species [67]. Thus, AI-2 enables intra- and interspecies communication and becomes one of the central molecules of QS systems [68].

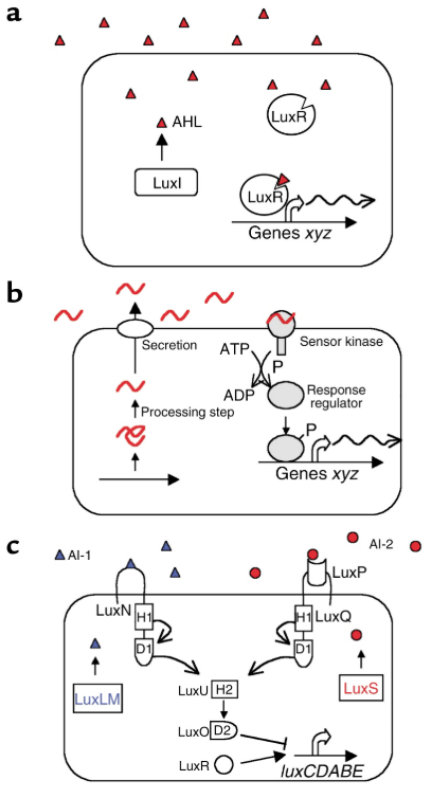

Figure 1: The different bacterial QS systems. [a] QS system in Gram-negative bacteria: AHLs (red triangles), LuxI-type protein (open square), LuxR-type proteins (open ellipse), specific promoter DNA element (open arrow), target gene (xyz); [b] QS system in Gram-positive bacteria: AIPs (red waves), oligopeptide transporter (open ellipse), sensor kinase (closed circle), response regulator protein (closed ellipse), promoter DNA (open arrow), target gene (xyz); [c] LuxS/AI-2-type QS system on the example *V. harveyi*, which harbours two parallel two- component systems (LuxN, LuxP/LuxQ): LuxLM protein (open square with blue labeling), LuxS protein (open square with red labeling), autoinducer sensors LuxN (cap), autoinducer sensors LuxP/LuxQ (cap/open rectangle with curved side edges), phosphotransferase LuxU (open square), response regulator protein LuxO (open rectangle with curved side edge), activator protein LuxR (open circle), promoter DNA (open arrow), luciferase gene (luxCDABE). [63]

I.2.3.1. AI-2 synthesis

According to preliminary structural studies and biosynthetic pathway analysis, Schauder et al. described AI-2 as a simple small molecule which becomes enzymatically synthesized and spontaneously transformed from the AI-2 precursor DPD [30,69]. DPD is a by-product of the activated methyl cycle (AMC) [64] generated while recycling methionine from S-adenosyl-L-methionine (SAM), an essential donor of methyl groups [30,70]. As observed in figure 2 panel A, for the synthesis of DPD from SAM three nucleosidase enzymes are involved of the AMC [70]: i. Besides a methyltransferase, ii. the 5'-methylthioadenosine/S-adenosylhomocysteine (MTA/SAH nucleosidase, Pfs enzyme), iii. as well as the S-ribosylhomocysteine lyase (SRH lyase, LuxS enzyme) [29,69]. The methyltransferase demethylates SAM into the toxic S-adenosylhomocysteine (SAH) [30]. Subsequently, the Pfs enzyme detoxicates SAH by hydrolyzation yielding adenine and S-ribosyl-L-homocysteine (SRH) [63]. Afterward, the LuxS enzyme cleaves SRH into the unstable DPD and the stable L-homocysteine [71].

As observed in figure 2 panel B, DPD is an unstable molecule that spontaneously cyclizes into the two enantiomers 2R,4S- and 2S,4S-2-methyl-2,4-dihydroxydihydrofuran-3-one (R- and S-DHMF), considered as Pro-AI-2 [72]. Spontaneous hydration gives rise to the final AI-2 2R,4S-2-methyl-2,3,3,4-tetrahydroxytetrahydrofuran (R-THMF) recognized by *Enterobacteriaceae*, *Pasteurellaceae*, *Bacillaceae* and *Alphaproteobacteria*. In the presence of borate is transformed into 2S,4S-2-methyl-2,3,3,4-tetrahydroxytetrahydrofuran-borate (S-THMF-borate) that is recognized by *Vibrionaceae* [65,70].

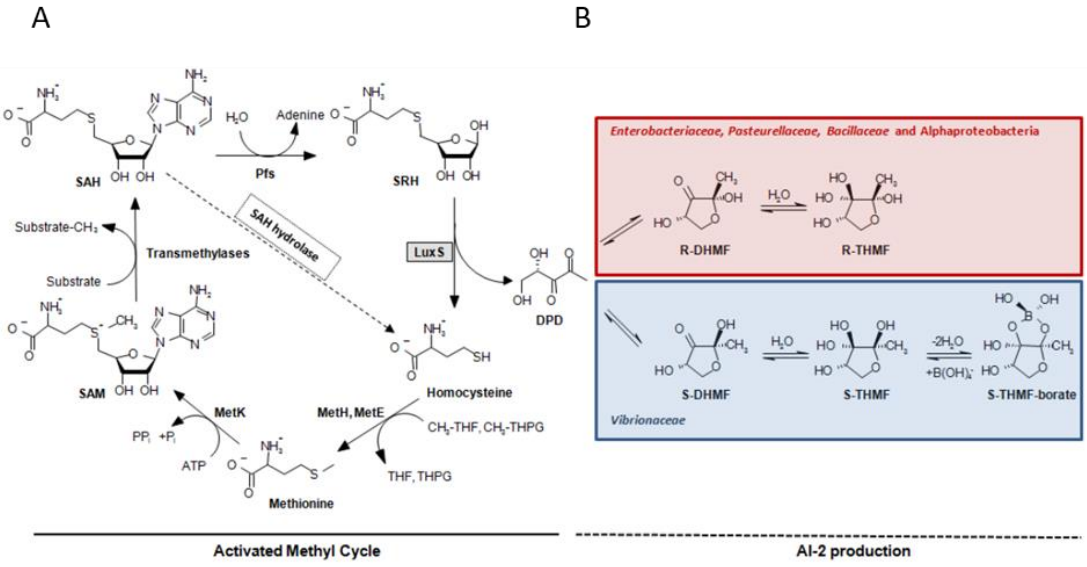

Figure 2: Relationship between the AMC and AI-2 production in bacteria. [A] Bacterial AMC: During the salvage of Methionine, the Pfs and LuxS enzyme lead to the by-product DPD; [B] Proposed interconversion of DPD: R-THMF is the recognized AI-2 from *Enterobacteriaceae*, *Pasteurellaceae*, *Bacillaceae*, and *Alphaproteobacteria* (red square), S-THMF-borate is the AI-2 form recognized by *Vibrionaceae* (blue square). [59,64]

I.2.3.2. Types of AI-2 receptors

Although the role of AI-2 as a universal signaling molecule in the QS system has been assumed in many instances [29,63,69], its recognition and signal transduction have not been investigated in detail yet. So far, two classes of AI-2 receptors have been characterized: i. the LuxP receptor, described first in *Vibrio* spp., and ii. the LsrB (LuxS regulated) receptor, described first in *Salmonella enterica* serovar typhimurium (*S. enterica* ser. typhimurium) [72,73]. Both receptors are members of the ribose binding protein family and recognize the corresponding AI-2 derivate in the periplasm [62]. Their structures and sequences have been described, revealing low sequence identity (11%) but high similarity in the overall protein folding (see Figure 3) [58,62]. Even though a high affinity for AI-2 was found for both receptors, the bound AI-2 derivate and thus also the binding sites of LuxP and LsrB differ considerably [72,74]. Whereas the LuxP-type receptors bind the furanosyl borate diester S-THMF-borate (see Figure 3, left branch), LsrB-type receptors recognize the furanone R-THMF (see Figure 3, right branch) [58,74].

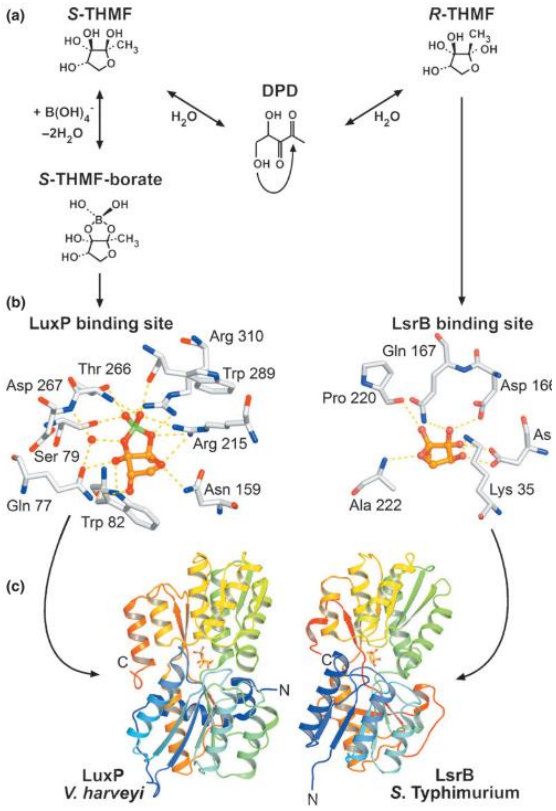

Figure 3: Crystal structure of LuxP receptor found in *V. harveyi* and LsrB receptor found in *S. enterica* ser. typhimurium with respective AI-2 signaling molecules. [a] DPD spontaneously rearrange in aqueous solution into the final AI-2 R-THMF (detected by *S. enterica* ser. typhimurium) or in the presence of borate into the final AI-2 S-THMF-borate (detected by *V. harveyi*). [b] LuxP and LsrB binding sites binding respective AI-2 derivates with different amino acids residues by hydrogen bonds or salt bridges (dashed yellow lines); [c] LuxP and LsrB ribbon diagram colored in rainbow showing high similarity between their overall folding. [58]

Stabilization of the negatively charged S-THMF-borate in the LuxP binding site is enabled by the positively charged arginine residues (Arg_{215} and Arg_{310}) of the LuxP binding pocket (see Figure 3, b) [58]. Furthermore, binding is forced by hydrogen bonds between AI-2 and the two previously mentioned amino acids as well as the polar amino acids Gln_{77}, Ser_{79}, Trp_{82}, Thr_{266}, and Asn_{159} [58]. In contrast to the positively charged binding pocket of LuxP, the LsrB binding pocket is charged negatively [58]. The negative charge occurs because only two of the three amino acids (Lys_{35} and Asp_{166}) in the LsrB binding pocket can form an AI-2 stabilizing salt bridge and can neutralize their respective charges, while the third amino acid (Asp_{166}) having no salt bridge partner leaves a net negative charge (see Figure 3, b) [58]. Thereby binding between a negatively charged AI-2 derivate such as S-THMF-borate to the negatively charged LsrB receptor becomes unlikely [58].

Further studies revealed that six residues (Lys_{35}, Asp_{116}, Asp_{166}, Gln_{167}, Pro_{220}, and Ala_{222}) are completely conserved within all bacterial species having orthologues to the *S. enterica* ser. typhimurium LsrB protein (sequence identity about more than 60%) [72,74]. Meanwhile, LsrB-type receptors have been described in various members of the *Enterobacteriaceae*, the *Rhizobiaceae*, the *Pasteurellaceae* and the *Bacillaceae* family, while the LuxP-type receptors have only been found in the *Vibrionaceae* [58,59].

I.2.4. Quorum Sensing in *E. faecalis*

So far, three different QS mechanisms have been reported in *E. faecalis* (see Table 2). Two of them, the Cytolysin-type (Cyl-type) QS system and the *E. faecalis* system regulator-type (Fsr-type) QS system, have been already well described and have been demonstrated to contribute to virulence [29]. Both are belonging to the Oligopeptide-type QS model using AIPs as autoinducers [29]. The third, the LuxS/AI-2-type QS system and its role in virulence, have not been investigated in detail yet [29].

Table 2: QS systems of *E. faecalis* [29].

Strain	QS system(s)	Autoinducer(s)	Regulated phenotypes
E. faecalis	Fsr	GBAP	GelE and SprE, biofilm
	Cyl	$CylL_S$	$CylL_S$, $CylL_L$, biofilm
	LuxS	AI-2	Biofilm, ATP generation, translation, cell wall/membrane biogenesis, and nucleotide transport and metabolism [30]

AI-2, autoinducer 2; Cyl, cytolysin; $CylL_S$, cytolysin small subunit; $CylL_L$, cytolysin large subunit; Fsr, *(E.) faecalis* system regulator; GBAP, gelatinase biosynthesis activating pheromone; GelE, gelatinase; SprE, serin protease; LuxS, Lux synthesis.

I.2.4.1. Fsr-type Quorum Sensing system in *E. faecalis*

Quin et al. (1990) were the first to describe the Fsr-type QS system in *E. faecalis* [75]. The Fsr-type QS is a major virulence regulator in *E. faecalis*, similar to the Agr-type QS in *Staphylococcus aureus* [71]. It includes four genes namely *fsrA, fsrB, fsrC and fsrD* that are responsible for the extracellular accumulation of the gelatinase biosynthesis-activating pheromone, GBAP [30]. GBAP is a cyclic peptide which acts as an autoinducer in the Fsr-type QS system [76]. As observed in figure 4, it proceeds from the propeptide FsrD through FsrB before being released in the surrounding of *E. faecalis* [76]. The extracellular concentration of GBAP is sensed by the histidine kinase FsrC that responds to GBAP by phosphorylating the intracellular response regulator FsrA [77]. Activated FsrA acts as a transcription factor for *fsr* genes as well as for two genes (*gelE* and *sprE*) encoding for two extracellular proteases, the gelatinase GelE and the serine protease SprE [77]. Together with the Fsr-type QS, GelE and SprE contribute to the virulence of *E. faecalis*, by producing inflammation, damage of host's tissue and biofilm formation [76,78].

I.2.4.2. Cyl-type Quorum Sensing systems in *E. faecalis*

Haas et al. (2002) were the first to verify the Cyl-type QS systems in *E. faecalis* [79]. In the Cyl-type QS systems a major virulence factor of *E. faecalis* is produced, the hemolytic toxin cytolysin (Cyl), being lethal for a number of prokaryotic and eukaryotic cells [29, 30]. In figure 4 can be observed that the mature Cyl is composed of two mature subunits, the cytolysin small subunit ($CylL_S$") and the cytolysin large subunit ($CylL_L$") [77]. The subunit's precursors ($CylL_S$ and $CylL_L$) are intracellularly modified by the lanthionine synthetase CylM to be then exported in the environment by the CylB transporter where their proteolytic activity is activated by the serine protease CylA [77]. Only in the absence

of target cells, the mature subunits form inactive complexes corresponding to Cyl [77]. Since $CylL_L$ binds with a higher affinity to the cellular membrane than to $CylL_S$, in the presence of target cells, the last will accumulate in the environment [77]. As soon as a certain threshold of free mature $CylL_S$ is reached, $CylL_S$ starts to act as an autoinducer for the Cyl-type QS system, suppressing the regulatory proteins CylR1 and CylR2 and leading to transcription of the *cyl* operon [29,77].

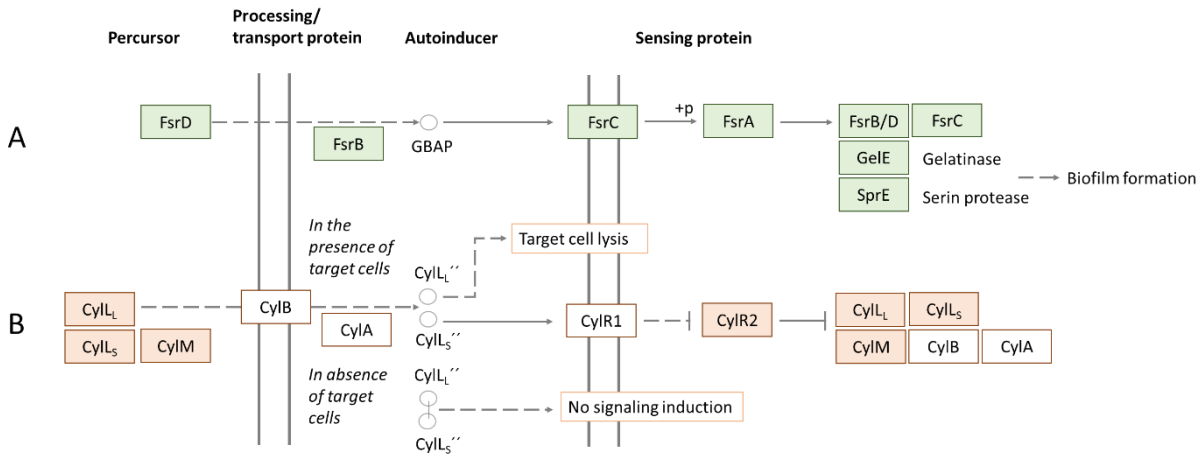

Figure 4: Fsr-type and Cyls-type QS systems in *E. faecalis*. [A] Fsr-type QS system in *E. faecalis*; [B] Cyls-type QS systems in *E. faecalis*. Gene product (pen squares), chemical compound (open circles), molecular interaction/relation (arrows), indirect link/unknown reaction (dashed arrows), gene expression (dotted arrows), gene depression (lines ending with bars), phosphorylation (+p). [80]

I.2.4.3. LuxS/AI-2-type Quorum Sensing system in *E. faecalis*

Already in 2001, Schauder et al. reported evidence that *E. faecalis* is using the same biosynthetic pathways in the production of DPD as *S. enterica* ser. typhimurium, *E. coli*, *V. harveyi*, and *V. cholerae* (see Figure 2) [69]. Three years later, Sun et al. (2004) verified the presence of a *luxS* homolog in *E. faecalis* V583 strain [81]. In 2012, Shao et al. confirmed the ability of *E. faecalis* V583 to synthesize a functional AI-2 molecule, which is dependent on the growth phase [30]. Moreover, the influence of AI- 2 on biofilm formation was proved by the increases in biofilm with the addition of AI-2 in a concentration-dependent manner [30]. Also the ability to induce virulence genes via phage release, and the dispersal of preformed biofilms after the addition of AI-2 in high concentrations has been described in the LuxS/AI-2-type QS system of *E. faecalis* V583ΔABC by Rossmann et al. (2015) [52].

Recently, the role of the *luxS* gene in *E. faecalis* V583ΔABC was investigated further by Gaspar et al. (2018), revealing that deletion of *luxS* leads to differences in the utilization

of galactose and to a delayed death in the *Drosophila* septic injury model, while no statistically significant differences in biofilm formation, adhesion to Caco-2 cells, resistance to oxidative stress and survival inside J-774 macrophages could be observed [82]. So far *E. faecalis* has responded only to boron-free AI-2 derivates [30,52,83], leading to the conclusion that *E. faecalis* recognizes R-THMF as final AI-2 form, which seems very likely since recognition of R-THMF has been demonstrated as well for other enteric bacteria [62,65,70].

I.2.4.3.1. AI-2 ABC transport systems of *E. faecalis*

So far, in *E. faecalis* as in most Gram-positive bacteria, no AI-2 specific receptor had been identified. It seems that *E. faecalis* is using an analogical AI-2 transport system as *S. enterica* ser. typhimurium, *E. coli*, *V. harveyi*, and *V. cholerae* since they are using the identical biosynthetic pathway in AI-2 biosynthesis [69]. The rational that *E. faecalis* possess an LsrB-type and not a LuxP-type AI-2 receptor can be justified by the fact that *E. faecalis* is responding to boron-free AI-2 derivates [30,52,83] which usually are bound by LsrB-type receptors (described above in the *Types of AI-2 receptors* chapter). Importantly, the LsrB-type receptors have been proven in various members of enteric bacteria and in the phyllum of *Firmicutes* [57,74,84] to which *E. faecalis* belongs, while the LuxP-type receptors have only been found in the *Vibrionaceae* [58,59].

I.2.5. Quorum Sensing-based therapy

Since QS mechanism has been discovered to be relevant for human pathogens to promote virulence and pathogenicity in vivo [29,53,62,84] the disruption of the bacterial intra- and intercommunication would be a potential alternative to conventional antibiotic therapy. Infections could be treated without the use of resistance inducing agents. To date, various treatment strategies targeting the interference of QS have been evaluated [85] including the interference in autoinducer synthesis, accumulation, and detection. Especially for the AHL-mediated intraspecies QS systems have been already developed different QS pathways inactivating enzymes, called quorum quenching enzymes (QQE), as well as disrupting chemicals, called Quorum Sensing inhibitors (QSI) [86–88]. Nonetheless, none of them has been tested clinically until now [86].

I.3. *Enterococcus faecalis*

I.3.1. *E. faecalis* V583ΔABC

E. faecalis V583ΔABC is a plasmid-free derivate from *E. faecalis* V583 [5] and the main strain used in this study. This strain is cured of its three naturally occurring plasmids avoiding plasmid-related problems, that may be caused, for example, by self-replication [89]. *E. faecalis* V583 was collected from an American patient in 1987. It is the first clinical isolate of an *E. faecalis* species with vancomycin resistance in the US [39] and it became one of the first enterococci to be completely sequenced [5,90]. Intensive studies about V583 revealed that a quarter of V583s genome consists of mobile and foreign DNA, including the DNA of seven prophages and several pathogenicity islands [2,5,23]. The apparent genomic plasticity of V583 (and also of other enterococcal strains) enables them to achieve and distribute resistance to all presently used antibiotics [5,9], that is why it becomes really necessary to find new therapeutic options besides antibiotics to treat multidrug-resistant *E. faecalis* infections.

I.3.1.1. Gene *ef0907* from *E. faecalis* V583ΔABC

The presence of the *ef0907* gene has been demonstrated to be conserved among *E. faecalis* strains [91], including the *E. faecalis* V583ΔABC strain [31]. The *ef0907* gene encodes a surface-located lipoprotein [5] that is a substrate-binding domain of a multicomponent ABC transporter [23]. This kind of proteins have been demonstrated to be responsible for the import into the cell of several molecules such as peptides [23], amino acids, amines, metallic ions, and pheromones [91]. In addition, EF0907 protein is known to be attached within the cell membrane by a lipid anchor [31], to be surface accessible [23], and to have a solute-binding domain (Pfam accession PF00496) [2]. The crystal structure of EF0907 can be observed in figure 5 represented as a ribbon diagram (rainbow colored ribbons) interacting with a sodium ion (blue sphere) [92]. The expression of the *ef0907* gene has been investigated by analyzing extracellular proteomes of *E. faecalis* V583 and V583ΔABC. Interestingly, a decrease in EF0907 expression has been observed when bacteria were cultured in erythromycin [28], while its expression has increased when cultured in urine [93] or human blood [32]. In the context of Quorum Sensing, unpublished transcriptome analysis of our research group on *E. faecalis* V583ΔABC revealed significant up-regulation of *ef0907* gene 6h after incubation with 100µM AI-2.

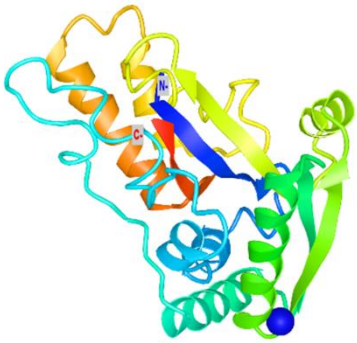

Figure 5: 3D crystal structure of EF0907 ABC transporter peptide-binding protein in *E. faecalis* V583. Overview of EF0907ABC transporter peptide-binding protein. The ribbon diagram is colored in rainbow. The ribbons represent the organization of the protein backbone in 3D. The blue sphere represents a sodium ion which interacts with the protein. The N- terminus of the protein is labeled in blue whereas the C-terminus is labeled in red. [92]

I.3.1.2. Role of Pfs in *E. faecalis* V583ΔABC

In *E. faecalis* the *ef2694* gene encodes for the Pfs enzyme, a 5'-methylthioadenosine/S-adenosylhomocysteine (MTA/SAH) nucleosidase, which plays a role in the bacterial S-methyl-5‘-thioadenosine degradation, the L-cysteine biosynthesis, the AMC and the AI-2 biosynthesis (see Figure 2) [48]. As described previously, bacteria using Pfs enzyme to detoxify SAH in the AMC and to recycle SAM, are generating as an additional byproduct the AI-2 precursor SRH and DPD, respectively (see Figure 2) [64]. For that, Pfs cleaves irreversibly the glycosidic bond in SAH to produce adenine and the corresponding thioribose SRH. Finally, the Pfs reaction product and LuxS substrate, SRH, can proceed to homocysteine and active AI-2 species [69,94]. In fact, in different bacteria, AI-2 production is strongly correlated with the transcription of *ef2694* gene [48]. Nonetheless, AI-2 is not regulating the transcription of *ef2694* gene [94].

I.4. Biofilm

Biofilms are formed when microbes aggregate on biotic or abiotic surfaces, surrounded by a matrix of extracellular polymeric substances (EPSs), including polysaccharides, proteins, and nucleic acids [95,96]. The ability to form biofilm is related to bacterial pathogenicity and virulence, since compared to their planktonic (free-floating) form, bacteria in a biofilm show increased resistance to antimicrobial substances such as antibiotics and disinfectants [97]. Therefore, biofilm promotes infections that are difficult to eradicate [98]. The four stages during the biofilm development are: i. initial attachment of single cells, ii. the formation of microcolonies surrounded by an extracellular matrix, iii. the biofilm maturation increasing the complexity of biofilm architecture, and iv. the

biofilm dispersal (see Figure 6) [99]. Especially the biofilm matrix is important regarding the biofilm stability and as a defense mechanism against antimicrobials and immune cells [10].

I.4.1. Biofilm formation of *E. faecalis*

E. faecalis and *E. faecium* are a frequent cause of nosocomial infections, mainly attributed to their ability to form biofilm on surfaces of indwelling medical devices [10]. Since enterococcal biofilm forms a reservoir of bacteria and antibiotic resistance genes, they are hardly eradicable [10]. Therefore, enterococcal infections that are difficult to treat, such as UG infections, GI infections, surgical site infections, bacteremia, and endocarditis, are associated with biofilm.

Recently, biofilm of *E. faecalis* was extensively reviewed by Ch'ng et al. (2019) [99], explaining more detailed the single stages of biofilm development (see Figure 6). Biofilm formation of *E. faecalis* starts with the attachment of planktonic cells to any surface, involving adhesins, proteases and glycolipids (see Figure 6, b) [99]. Important adhesins involved in the attachment process are Ebp (Endocarditis and biofilm-associated pilus), Agg (Aggregation substance), Esp (Enterococcal surface protein) and Ace (Adhesin to collagen from *E. faecalis*) [99]. After attachment, *E. faecalis* typically generates biofilm sheets formed out of microcolonies and released extracellular polysaccharides (see Figure 6, a). Within maturation, accumulation of extracellular DNA (eDNA), lipoteichoic acid (LTA), autolysin AtlA, gelatinase GelE, and serine protease SprE in the matrix, makes the sheets thicker and more complex (see Figure 6, c) [99]. The triggering factors for the dispersal of the enterococcal biofilm remain poorly understood. Rossmann et al. (2015) speculated that high concentrations of AI-2 can initiate the dispersal of bacteria from mature biofilms [52] but this has not been confirmed yet.

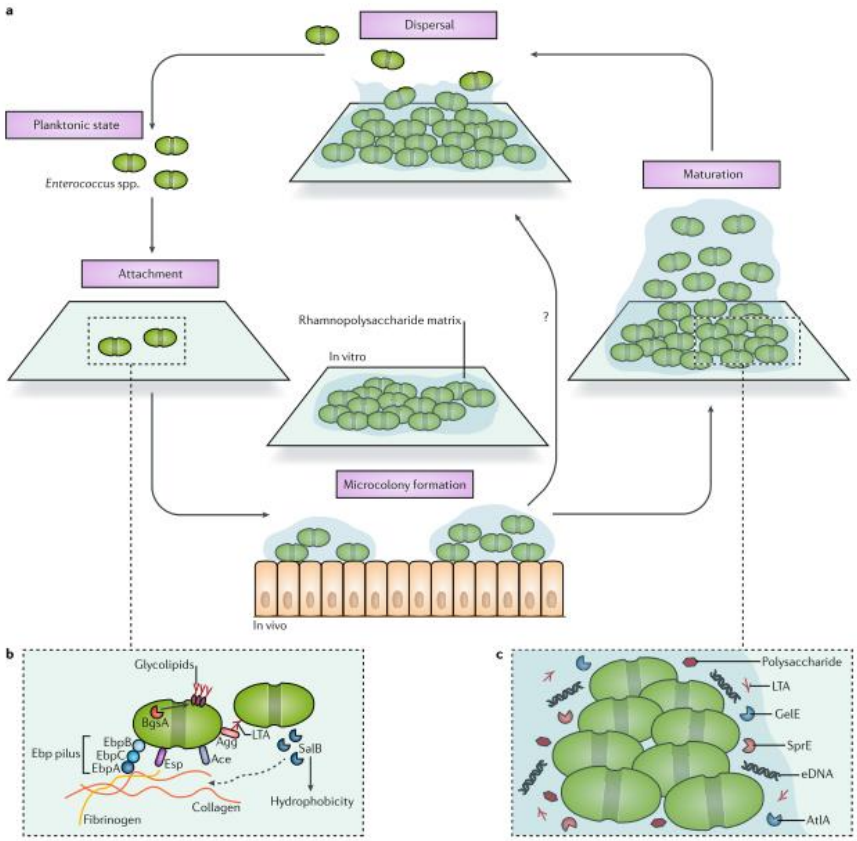

Figure 6: Enterococcal biofilm development. [a] Single stages of biofilm development, including cell attachment, microcolony formation, biofilm maturation and biofilm dispersal; [b] Attachment on a surface enabled by adhesins such as Endocarditis- and biofilm-associated pilus (Ebp), Aggregation substance (Agg), Enterococcal surface protein (Esp), Adhesin to collagen from *E. faecalis* (Ace), proteases and glycolipids; [c] Mature biofilm with a complex architecture of the surrounding extracellular matrix formed out of extracellular DNA (eDNA), lipoteichoic acid (LTA), autolysin AtlA, gelatinase GelE, and serine protease SprE. [99]

I.4.2. Biofilm formation and Quorum Sensing

The influence of population density-dependent signaling on the formation and the dispersion of bacterial biofilm has been confirmed in several instances [10,98,100,101]. Generally, an increased biofilm OD was measured when low concentrations of AI-2 were added exogenously to bacterial culture [102]. Considering that the present work focuses on the AI-2-mediated QS system in *E. faecalis*, it is of particular interest to consider previous studies in which AI-2 contributes to enterococcal biofilm [30,52,55,103]. Also in *E. faecalis* an increase of the in vitro biofilm formation could be observed with the external addition of AI-2 in low concentrations [103]. In comparison, it was described the dispersal of biofilm when high concentrations of AI-2 were added [52]. Additionally, *luxS* deficient *E. faecalis* mutants, which are no longer able to produce AI-2, demonstrated abnormal aggregation and dense biofilm formation [99], leading to apparently different results in the wet biofilm assay after external AI-2 supplementation [55,103].

II. Objectives

With the discovery of the bacterial intra- and interspecies communication system, called QS [1], new therapeutic opportunities to fight bacterial infections emerged. At a time when multi-resistant pathogens are on the rise, the disruption of the bacterial communication seems to be a promising potential alternative to conventional antibiotic therapy, especially since QS has been reported to be relevant for the regulation of collective behaviours such as virulence, inflammatory response, and biofilm formation [61,76]. A better understanding of QS is required to identify novel druggable molecular targets, including signaling molecules, enzymes involved in the signal synthesis, regulators of the signal response, and receptors involved in signal transduction [104]. Among the different QS systems described so far, the LuxS/AI-2-type QS system might be the most promising for novel anti-infectives. This presumption derives from the fact that AI-2, in contrast to all other QS signal molecules known to date, is considered universal, since it can be produced and detected by a wide variety of both Gram-positive and Gram-negative bacteria.

Since enterococci belong to the most important multi-resistant pathogens [105], it might be of particular interest to delete or suppress genes involved in enterococcal QS. Among enterococci, *E. faecalis* is the most commonly isolated species (60–95%) in human infections [1,9,30], hence it is considered as the species with the greatest clinical relevance [7,31]. Consequently, *E. faecalis* is considered to be well suited for further molecular QS studies. Although it is already known that *E. faecalis* synthesizes and responds to AI-2 [30,52,83], and this autoinducer affects enterococcal biofilm formation [30,103], no genes encoding for the AI-2 transport system in *E. faecalis* have been identified so far. Therefore, the aim of the present thesis was to identify the AI-2 binding protein in the LuxS/AI-2-type QS system of *E. faecalis.*

Combining the facts that our literature research and unpublished *in silico* analyses suggests that *E. faecalis* has an AI-2 specific transport system belonging to the family of ABC-transporters family and that our previous unpublished transcriptomic analysis revealed a series of genes significantly up-regulated 6h after incubation with 100µM AI-2, we hypothesize that the *ef0907* gene might encode for the AI-2 binding protein. Following this rational we decided to investigate and characterize the role of EF0907 protein in the AI-2 transport of *E. faecalis*.

More specifically, the following objectives were pursued:

- Apply bioinformatic analysis to compare the amino acid sequence of already described AI-2 binding proteins with those of *ef0907* gene (see Chapter III.4. and IV.1.).

- Apply a combination of different genetic, biochemical and biophysical strategies to prove that the *ef0907* gene is encoding for the putative AI-2 binding protein in the LuxS/AI-2-type QS system of *E. faecalis* V583ΔABC (see Chapter III.4.–III.11., IV., and V.).

- Use the overexpression vector pQE30 to recombinantly express the putative AI-2 binding protein EF0907 in the *E. coli* BL21ΔluxS strain (see Chapter III.3.1.1., III.6.1.–III.6.3., III.9., IV.2., IV.7., IV.10., and IV.11.).

- Create an in-frame knock out of the *ef0907* gene encoding the putative AI-2 binding protein (EF0907) in the well-studied *E. faecalis* V583ΔABC strain using site-directed mutagenesis (see Chapter III.5., IV.3., and IV.4.).

- Create a single point mutation of the *ef2694* gene encoding the MTA/SAH nucleosidase (Pfs) in the well-studied *E. faecalis* V583ΔABC strain using site-directed mutagenesis to use as negative control (see Chapter III.5., IV.3., and IV.5.).

- Complement the ΔEF0907 mutant by plasmid-encoded gene EF0907 in vector pEU327 (see Chapter III.3.1.4, III.5.1.1., and IV.6.).

- Study growth behavior of the wildtype *E. faecalis* V583ΔABC, and its mutants and derivates (see Chapter III.7., IV.8., and IV.9.).

- Verify that AI-2 can be used as a carbon source growing the wildtype *E. faecalis* V583ΔABC, and its derivates in chemically defined media containing AI-2 as the only carbon source (see Chapter IV.9.).

- Verify the binding between the rEF0907 protein and AI-2 by isothermal titration calorimetry (see Chapter III.8. and IV.10.).

- Verify that ΔEF0907 mutant is no longer able to internalize AI-2 by measuring the external AI-2 concentration in the supernatants of *E. faecalis* wildtype, mutants and derivates by fluorescence resonance energy transfer-based AI-2 assay (see Chapter III.9. and IV.11.).

- Assess the impact of ΔEF0907 in the in vitro biofilm formation performing a microtiter plate biofilm assay (see Chapter III.10., and IV.12.).

- Additionally, asses putative changes in the bacterial surface of the wildtype *E. faecalis* V583ΔABC, and its mutants by opsonophagocytic killing assay (see Chapter III.11., and IV.13.).

In a long-term perspective, the study should contribute to a better understanding of the AI-2-mediated QS system of the vancomycin-resistant *E. faecalis* and help to identify new targets for antimicrobial therapy.

III. Materials and methods

III.1. General

To prepare media, buffers or solutions, deionized, sterile water (Milli Q, Millipore) or nuclease-free water (Millipore) was used. Additionally, all non-sterile utensils and solutions were either filter sterilized (0.22µm, Millipore) or autoclaved at 121°C for 1.5h. Preparation of the special media, buffers or solutions is described in the corresponding section.

III.2. Bacterial strains and culture conditions

The main strain of study was *Enterococcus faecalis* V583ΔABC, a plasmid-free descendant of the *E. faecalis* V583 [5]. Different strains used in this study and their characteristics are described in table 3.

Table 3: Different strains used in this study.

Strain(s)	Description	Company/Reference
Species: *E. coli*		
TOP10	Gram-negative cloning host; lacZΔM15 (deleted β-galactosidase; for functional enzyme a vector expressing a complementation of the β-galactosidase when plated on X-gal is required; used in blue-white screening of recombinants) [106]	invitrogen
TOP10+pLT06	Gram-negative cloning host; harboring the pLT06 plasmid	[107]
TOP10+pQE30	Gram-negative cloning host; harboring the pQE30 plasmid	Qiagen
TOP10+pREP4	Gram-negative cloning host; harboring the pREP4 plasmid	Qiagen
TOP10+pEU327	Gram-negative cloning host; harboring the pEU327 plasmid	[108]

BL21	Gram-negative cloning host; presence of recombinant phage λ BL21 (enabling controlled transcription through the T7 RNA polymerase); ΔompT and Δlon (deleted outer membrane proteases, avoiding external protein degradation); lack of O-antigen polysaccharide (emerging in enhanced permeability) [109]	invitrogen
DH5α	Gram-negative cloning host; lacZΔM15 deleted β-galactosidase; for functional enzyme a vector expressing a complementation of the β-galactosidase when plated on X-gal is required (used in blue-white screening of recombinants) [110]	invitrogen
BL21ΔluxS	Gram-negative overexpression host; with a deletion in the *luxS* gene (used to overproduce the rEF0907)	[60]
BL21ΔluxS+pREP4+pQE30::EF0907	Gram-negative derivate; with a deletion in the *luxS* gene; harboring the expression vector pREP4 (constitutively expresses the lac repressor protein encoded by the lac I gene, Amp^R) and the repressor vector pQE30 (allowing the overexpression of the rEF0907 in the presence of IPTG); Kan^R	this study
BL21ΔluxS+pQE30::CLPY	Gram negative derivate; with a deletion in the *luxS* gene (used to quantify AI-2 concentration); harboring vector pQE30::CLPY; Kan^R	[111]
Top10+pEU327::EF0907	Gram-negative derivate; harboring vector pEU327::EF0907; $Spec^R$	this study

DH5α+pLT06::ΔEF0907	Gram negative derivate; harboring vector pLT06::ΔEF0907; CM^R	this study
BL21+pLT06::xxxEF2694	Gram-negative derivate; harboring vector pLT06::xxxEF2694; CM^R	this study
Species: *E. faecalis*		
V583ΔABC	Gram-positive cloning host and derivate of *E. faecalis* V583 cured of plasmids A, B, and C; presence of prophage 1, 2, 3, 4, 5, 6, 7	[89,112]
V583ΔABC+PLT06::ΔEF0907	Gram-positive derivate; harboring vector PLT06::ΔEF0907; CM^R	this study
V583ΔABC+PLT06::xxxEF2694	Gram-positive derivate; harboring vector PLT06::xxxEF2694; CM^R	this study
V583ΔABCΔEF0907	Gram-positive derivate; with the in-frame deletion of 81,3% of the *ef0907* gene	this study
V583ΔABCxxxEF2694	Gram-positive derivate; with three single point mutation to stop the transcription of the *ef2694* gene	this study
V583ΔABC+pEU327	Gram-positive cloning host; harboring vector pEU327; $Spec^R$	this study
V583ΔABCΔEF0907+pEU327	Gram-positive derivate; with the deletion mutation of gene *ef0907*; harboring vector pEU327; $Spec^R$	this study
V583ΔABCΔEF0907+pEU327::EF0907	Gram-positive derivate; with the deletion mutation of gene *ef0907*; harboring vector pEU327::EF0907; $Spec^R$	this study

Amp^R, ampicillin resistance; Cm^R, chloramphenicol resistance; Kan^R, kanamycin resistance; $Spec^R$, spectinomycin resistance; Str^R, streptomycin resistance; Tc^R, tetracycline resistance, X-gal, 5-bromo-4-chloro-3-indolyl-β-D-galactopyranoside.

III.2.1. Culture conditions for *E. coli* strains

E. coli strains were cultured under vigorous shaking at 37°C in LB broth (Luria/Miller; Carl Roth). As solid media LB agar plates (Luria/Miller; Carl Roth) were used. When required, either ampicillin (100µg/mL), kanamycin (50µg/mL), chloramphenicol (20µg/mL) or spectinomycin (100µg/mL) were added to the medium. The exact composition of the media is shown in table 4.

Table 4: Composition of LB medium.

LB broth	LB Agar
Tryptone 10g/L Yeast extract 5g/L Sodium chloride 10g/L pH 7.0 ± 0.2	Tryptone 10g/L Yeast extract 5g/L Sodium chloride 10g/L Agar 15g/L pH 7.0 ± 0.2

III.2.2. Culture conditions for *E. faecalis* strains

Enterococci were grown without agitation at 37°C in liquid media, either in tryptic soy broth (TSB; CASO broth; Carl Roth), in brain heart infusion (BHI; Carl Roth) or chemically defined media (CDM, prepared as described in chapter III.2.4). As solid media were used tryptic soy agar (TSA; CASO agar; Carl Roth) or brain heart infusion agar (BHIA; Carl Roth). When required chloramphenicol (20µg/mL) or spectinomycin (100µg/mL) were added to the medium. The exact composition of the different media is shown in table 5.

Table 5: Composition of TSB medium.

TSB	TSA
Casein peptone (pancreatic digest.) 17g/L Soya peptone (papain digest.) 3g/L Dipotassium hydrogen phosphate 2.5g/L Sodium chloride 5g/L Glucose 2.5g/L	Casein peptone (pancreatic digest.) 15g/L Soya peptone (papain digest.) 5g/L Sodium chloride 5g/L Agar 15g/L

pH 7.3 ± 0.2	pH 7.3 ± 0.2
BHI	**BHIA**
Calf brain infusion 7.5g/L Beef heart infusion 10g/L Gelatin peptone 10g/L Dextrose 2g/L Sodium chloride 5g/L Disodium phosphate 2.5g/L pH 7.4 ± 0.2	Calf brain infusion 7.5g/L Beef heart infusion 10g/L Gelatin peptone 10g/L Dextrose 2g/L Sodium chloride 5g/L Disodium phosphate 2.5g/L Agar 15g/L pH 7.4 ± 0.2

III.2.3. Bacterial stocks

Bacterial stocks were prepared in order to have sufficient quantities of all tested strains easily available at all times. A single colony was picked up from an agar plate and resuspended in 7mL of freshly prepared liquid media. If necessary, an antibiotic was added. The liquid culture was grown overnight (ON) at 37°C. Next day, 1mL of ON culture was transferred to a 1.5mL cryovial and mixed with 350µL of sterile 80% glycerol. Vials were immediately stored at -80°C.

III.2.4. Chemically defined media

A 1L of double concentrated CDM without carbon sources was prepared. All reagents used for preparing double concentrated CDM are listed in table 6.

Table 6: Reagents for CDM used in this study.

Reagent	Weight	Storage	Company
Adenine	70mg	RT	Sigma-Aldrich
Alanine	0.48g	RT	Sigma-Aldrich
Ammonium citrate	1.2g	RT	Carl Roth
Arginine	0.25g	RT	Merck
Asparagine	0.2g	RT	Carl Roth
$CaCl_2$	100mg	RT	Merck

$CoSO_4$	5mg	RT	Sigma-Aldrich
$CuSO_4 . 5H_2O$	7.8mg	RT	Merck
Cystine	100mg	RT	Carl Roth
Cysteine	0.26g	RT	Carl Roth
D-Biotin	5mg	+4°C	Sigma-Aldrich
$FeCl_3 . 6H_2O$	10mg	RT	Sigma-Aldrich
$FeCl_2 . 4H_2O$	15.8mg	RT	Carl Roth
Glutamic acid	1g	RT	Carl Roth
Glutamine	0.4g	RT	Sigma-Aldrich
Glycine	0.35g	RT	Sigma-Aldrich
Guanine	54mg	RT	Sigma-Aldrich
Histidine	0.25g	RT	Sigma-Aldrich
Inosine	10mg	RT	Sigma-Aldrich
Isoleucine	0.42g	RT	Merck
K_2HPO_4	2g	RT	Merck
KH_2PO_4	10g	RT	Sigma-Aldrich
Leucine	0.95g	RT	Sigma-Aldrich
Lipoic acid	5mg	RT	Sigma-Aldrich
Lysine chlorohydrate	1.1g	RT	Merck
Methionine	0.25g	RT	Sigma-Aldrich
$MgCl_2 . 6H_2O$	853.2mg	RT	Carl Roth
$MnCl_2 . 4H_2O$	47.2mg	RT	Sigma-Aldrich
$(NH_4)_6Mo_7O_{24} . 4H_2O$	5.3mg	RT	Sigma-Aldrich
Nicotinic acid	2mg	RT	Sigma-Aldrich
Sodium acetate	2g	RT	Sigma-Aldrich
Orotic acid	10mg	RT	Sigma-Aldrich
p-aminobenzoic acid	20µg	+4°C	Sigma-Aldrich
Pantothenate	2mg	RT	Carl Roth
Phenylalanine	0.55g	RT	Sigma-Aldrich

Proline	1.35g	RT	Carl Roth
Pyridoxamine-HCl	10mg	RT	Carl Roth
Pyridoxine	4mg	RT	Carl Roth
Riboflavin	2mg	RT	Sigma-Aldrich
Serine	0.68g	RT	Carl Roth
Thiamine	2mg	RT	Sigma-Aldrich
Threonine	0.446g	RT	Sigma-Aldrich
Thymidine	10mg	RT	Sigma-Aldrich
Tryptophan	0.1g	RT	Sigma-Aldrich
Tyrosine	0.5g	RT	Merck
Uracil	44mg	RT	Sigma-Aldrich
Valine	0.65g	RT	Merck
Vitamin B12	2mg	+4°C	Sigma-Aldrich
Xanthine	100mg	RT	Sigma-Aldrich
$ZnSO_4$	10mg	RT	Carl Roth

A 1L glass flask was filled first with 250mL of Milli-Q water. All reagents were carefully weighted in the flask. At the same time, the water was heated at 50°C and was mix with a magnetic stirrer in a hot plate stirrer. Another 250mL of Milli-Q-Water were added to the flask and solution heated up until 70°C under constant mixing. When the reagents were completely dissolved, the CDM was cool down to RT. Finally, the media was filtered sterile in the hood using a Stericup® 500mL Millipore Express®Plus 0.22µm PES filter (Millipore).

III.3. Plasmids, genes of interest and primers

III.3.1. Plasmids

The plasmids used in this study and their more important characteristics are shown in table 7.

Table 7: Plasmids used in this study.

Plasmid(s)	Characteristics	Company/Reference
pREP4	Allows the production of high levels of the lac repressor protein to repress the transcription of the recombinant proteins encoded in the pQE30 [113]; Kan^R	Qiagen
pQE30	Allows the cloning and overproduction of N-terminally 6xHis-tagged proteins for their purification [113]; Amp^R	Qiagen
pQE30::EF0907	pQE30 carrying the *ef0907* gene downstream of a multiple cloning site encoding for six histidines, allowing the overproduction and the purification of the 6xHis-tagged recombinant protein EF0907; Amp^R	this study
pLT06	Allows the construction of the isogenic, in-frame deletion and single point mutants used in this study [107]; Cm^R	[107]
pLT06::xxxEF2694	pLT06 harboring the *ef2694* gene with three single point mutations; Cm^R	this study
pLT06::ΔEF0907	pLT06 harboring the in-frame deletion 81,3% of the *ef0907* gene; Cm^R	this study
pEU327	Allows the extrachromosomal expression of proteins controlled by a xylose-inducible promoter (PxylA), pSH71 replicon [108]; $Spec^R$	[108]
pEU327::EF0907	pEU327 harboring the *ef0907* gene; $Spec^R$	this study

Amp^R, ampicillin resistance; Cm^R, chloramphenicol resistance; Kan^R, kanamicyn resistance; $Spec^R$, spectinomycin resistance.

III.3.1.1. The pQE30 vector

The pQE30 vector of Qiagen is a low-copy plasmid equipped amongst others with an upgraded promoter-operator element, a 6xHis-tagged coding sequence, a synthetic ribosomal binding site (RBS), a multiple cloning site (MCS) and strong transcriptional terminator (T_0) [113]. In addition, pQE30 is harboring a β-lactamase coding sequence and a ColE1 origin of replication [114]. The promoter-operator element can be recognized by *E.coli* RNA polymerases and consists out of a potent phage T5 promoter (PT5) and two lac operator sequences (O-lac) [114]. The two lac operator sequences allow the attachment of Lac repressors, avoiding a constant overexpression of the PT5 given that any RNA polymerase can anymore attach [114]. Lac repressor can be encoded from the bacteria by

itself or by an additional harbored vector, for example from the plasmid pREP4 [114]. The RBSII allows the RNA polymerase to bind and to transcribe the DNA into mRNA at high rates [115].

The MCS is located downstream a sequence which encodes for six histidines [113]. Like this, the transcript will be an N-terminal 6xHis-tagged recombinant protein that can afterward easily be purified by affinity chromatography [116]. To ensure a controlled overproduction Isopropyl β-D-1-thiogalactopyranoside (IPTG; AppliChem) can be added [113]. IPTG replace the Lac repressor from the lac operons, giving the starter shot for the overproduction of the recombinant protein [113,114]. The strong t_0 are needed to avoid reading through transcription of the recombinant protein [117]. The *β-lactamase* gene allows screening for bacteria which have internalized the pQE30 plasmid, assuring them an ampicillin resistance [113]. The ColE1 origin of replication can be used from the plasmid to replicate itself [114]. A schematic vector map of pQE30 can be seen in figure 7.

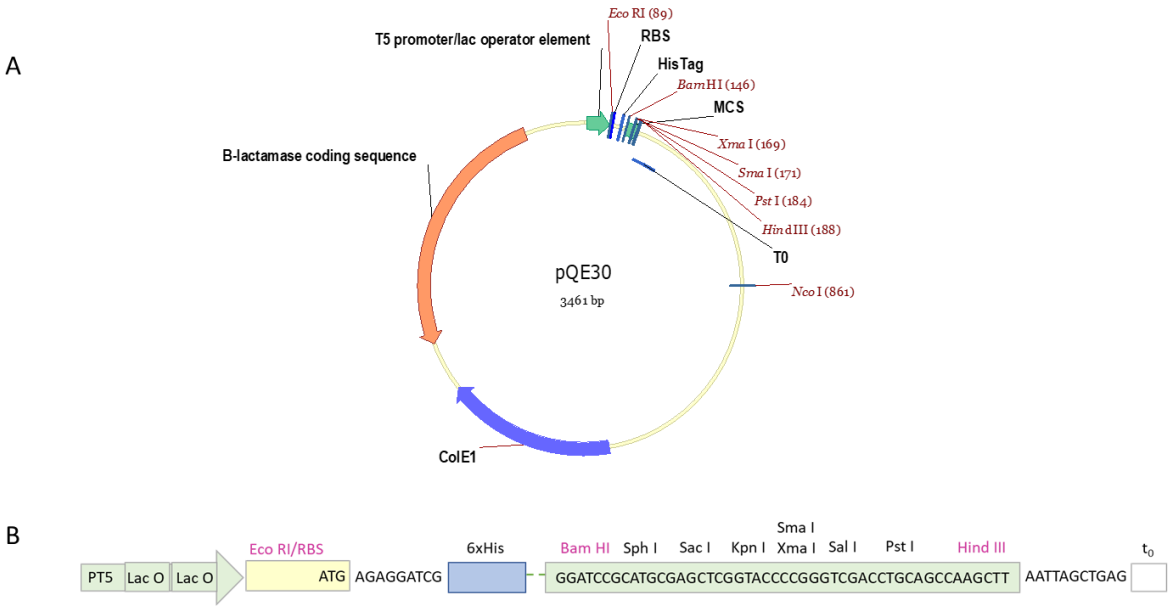

Figure 7: Schematic vector map of pQE30. [A] Plasmid map of pQE30 with unique restriction sites (red) in the multiple cloning sites of the plasmid; [B] Up scaled multiple cloning site of pQE30. [113]

III.3.1.2. The pREP4 vector

The pREP4 vector of Qiagen is a low-copy plasmid which constitutively expresses the lac repressor protein, encoded by the *lacI* gene [60]. It can be combined with any other plasmid having the ColE1 origin of replication [114]. Together with the pQE30 vector, it forms a special "double-operator" system, where multiple copies of pREP4 let to high levels of lac repressor protein production, which are able to bind the synthetic ribosomal

binding site RBSII of the pQE30 vector, regulating the expression of 6xHis-tagged recombinant proteins [114]. In addition, it carries the p15A replicon and it is kanamycin resistant [113]. A schematic vector map of pREP4 can be seen in figure 8.

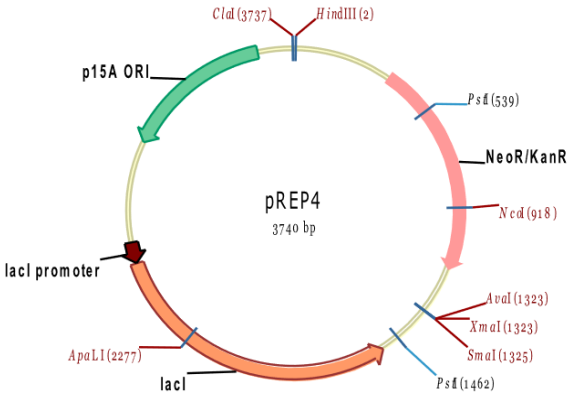

Figure 8: Schematic vector map of pREP4. Unique restriction sites in the multiple cloning sites of the plasmid (red); multiple restriction sites in the multiple cloning sites (black). [113]

III.3.1.3. The pLT06 vector

The pLT06 vector is an improved vector system created by Thurlow et al. [107] combining the properties of three different plasmids: pCJK47 [118], pGB354 [119] , and pCASPER [120]. It has been designed to be a more versatile vector for mutagenesis in *E. faecalis*. But also for other bacteria such as for *E. coli*, the plasmid is a suitable cloning vector. From the pCJK47 plasmid, the pLT06 vector obtained the *p-pheS* gene encoding for the counter-selectable marker P-pheS and the *lacZ* reporter gene encoding for a β-galactosidase used for blue-white screening [118]. From the pGB354 plasmid, the pLT06 vector obtained the chloramphenicol acetyltransferase (*cat*) gene used for antibiotic selection [119]. And from the pCASPER plasmid, the pLT06 vector obtained the *orfB*, *orfC*, *orfD* and the *repA*(Ts) gene [120]. The latter encodes for the temperature sensitive replication protein RepA used for temperature selection. With RepA the best replication rate is achieved when the cloning host is cultured at 30°C but the replication is inhibited when cultured at temperatures superior to 42°C [107]. A schematic vector map of pLT06 can be seen in figure 9.

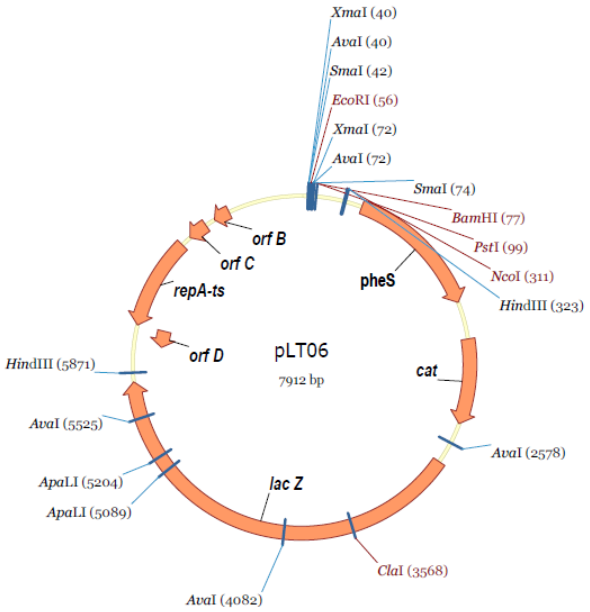

Figure 9: Schematic vector map of pLT06. Unique restriction sites in the multiple cloning sites of the plasmid (red); multiple restriction sites in the multiple cloning sites (black). [118]

III.3.1.4. The pEU327 vector

The pEU327 vector is a gram-positive expression host created by Eichenbaum et al. [108]. It is harboring a xylose-inducible promoter (xylA) which is controlled through the XylR repressor and is constitutively expressed by *E. faecalis* [121]. The initiator protein RepA is required for vector replication [122]. The RepB protein is necessary for plasmid stability and regulation of copy number [123]. Additionally, it is harboring a glucose-lactose-controlled expression system. In the presence of glucose, the expression of lacA promotor is repressed [108]. While in the presence of lactose (Lac), expression of the repressor LacR is repressed, allowing gene transcription after the lacA promotor [108]. Additionally, it contains a spectinomycin resistance (*add9*) gene used for antibiotic selection. A schematic vector map of pEU327 can be seen in figure 10.

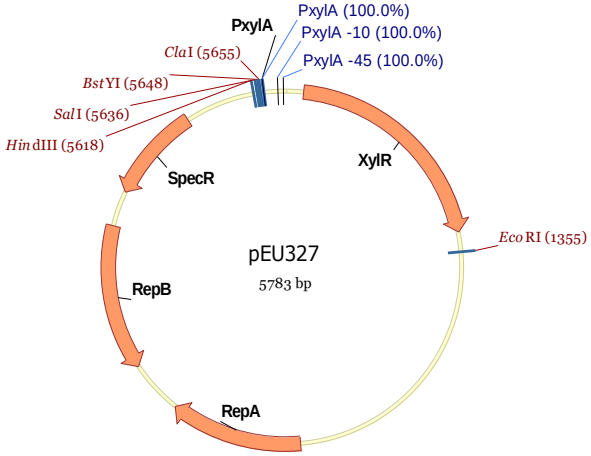

Figure 10: Schematic vector map of pEU327. Unique restriction sites in the multiple cloning sites of the plasmid (red). [108]

III.3.2. Genes of study

The National Center for Biotechnology Information (NCBI) (https://www.ncbi.nlm.nih.gov/gene) enables public access to the sequenced genome of *E. faecalis* V583. The genome of *E. faecalis* V583 was studied, importing the genome sequence to Vector NTI Advance Sequence Analysis Software (Thermo Fisher Scientific).

The main genes of interest were the *ef0907* gene, encoding for the putative AI-2 binding protein in *E. faecalis*, and the *ef2694* gene, encoding for the 5'-methylthioadenosine/S-adenosylhomocysteine (MTA/SAH) nucleosidase in the LuxS/AI-2-type Quorum Sensing system allowing AI-2 synthesis in *E. faecalis* [30,52]. Genes used in this study are shown in table 8.

Table 8: Genes of interest in this study.

Systematic gene name	Gene product (name)	Accession number gene / protein	Gen length [bp]	Reference
ef0907	ABC transporter peptide-binding protein (EF0907)	NC_004668.1 / NP_814645.1	1,671	[28]
ef2694	MTA/SAH nucleosidase (Pfs)	NC_004668.1 / NP_816328.1	696	[124]

MTA/SAH, methylthioadenosine/S-adenosylhomocysteine.

III.3.3. Primers

The primers were purchased from Eurofins Genomics. Primers used in this study are shown in table 9.

Table 9: Primers used in this study.

Primer name	5´–3´sequence	Restriction site	Use
Recombinant protein EF0907 (rEF0907)			

EF0907_pQE_BamHI	aggcGGATCCGCTTGTGGAGGCGGCG	BamHI (GGATCC)	To introduce the restriction site to integrate the fragment into the plasmid
EF0907_pQE30_HindIII	aggcAAGCTTTTATTCTGAAATGTATGCCCAT	Hind III (AAGCTT)	To introduce the restriction site to integrate the fragment into the plasmid

***ef0907* mutant**

EF0907_33_HindIII	agacAAGCTTTTAAATGCAGAGAAAACGAT	Hind III (AAGCTT)	To introduce the restriction site to make the deletion by PCR with oligo 66
EF0907_66_RV	CCTCTACCATCTCGGTTCGAATAAA		To amplify the fragment downstream of the gene of interest by PCR with oligo 33
EF0907_22_HindIII	agacAAGCTTTTTCTTGTTGTTCTGTGACA	Hind III (AAGCTT)	To introduce the restriction site to make the deletion by PCR with oligo 5
EF0907_5_FW	AGAAGCGGGATCGATATAAAGTCG		To amplify the fragment upstream of the gene of interest by PCR with oligo 22
EF0907_44_BamHI	agacGGATCCTTGTAATAATACCGCGAA	BamHI (GGATCC)	To introduce the restriction site in the construction to integrate it in the plasmid by PCR with oligo 1
EF0907_1_EcoRI	agacGAATTCTTGAAAAACGTAGGGGCG	EcoRI (GAATTC)	To introduce the restriction site in the construction to integrate it in the plasmid by PCR with oligo 44
EF0907_seq1_FW	GGCAAGTGGCGAACAAGTTTTA		To verify the deletion mutation by sequencing
EF0907_seq2_FW	CACTTTGTGGTTAATCGCAACGAT		To verify the deletion mutation by sequencing
EF0907_seq3_RV	GCCAATTATTACAGCCGTTATTTCC		To verify the deletion mutation by sequencing

EF0907_seq4_RV	CATAGTGTTGCCTCCTAAAATAATGCA		To verify the deletion mutation by sequencing
***ef2694* mutant**			
EF2694_2_RV	AATCACCATATTTACGCCCTATTGATGAAT CTATTAAGTCGTGGTCACAGCTGA		To amplify the gene of interest and insert the single point mutation in one DNA strand by PCR with oligo 5
EF2694_5_FW	CAGTAGCTATGATTCCGTTAACCGCAG		To amplify the gene of interest and insert the single point mutation in one DNA strand by PCR with oligo 2
EF2694_3_FW	TCAGCTGTGACCACGACTTAATAGATTCAT CAATAGGGCGTAAATATGGTGATT		To amplify the gene of interest and insert the single point mutation in one DNA strand by PCR with oligo 6
EF2694_6_RV	CCAGGCAAAGAAGCCAATGTTTTACTAA		To amplify the gene of interest and insert the single point mutation in one DNA strand by PCR with oligo 3
EF2694_1_BamHI	agcaGGATCCGTATCTGTCACCAGGATTTGCTAATG	BamHI (GGATCC)	To amplify the gene of interest and insert the single point mutation in both DNA strands and to introduce the restriction site in the construction by PCR with oligo 4
EF2694_4_NcoI	agcaCCATGGCTTTTACGGTGGCTATACAACTGAGC	NcoI (CCATGG)	To amplify the gene of interest and insert the single point mutation in both DNA strands and to introduce the restriction site in the construction by PCR with oligo 1
EF2694_7_FW_Verif	CGACTTAATAGATTCATCAATAG		To verify the insertion of the single point mutations by PCR with oligos 4 or 6

EF2694_seq1_FW	GGTTCGTTCAG GAATTGGTAAA GTG		To verify the insertion of the single point mutations by sequencing
EF2694_seq2_RV	TTCGCAATTTCC ATCCGCA		To verify the insertion of the single point mutations by sequencing

***ef0907* in pEU327**

EF0907_FW_pEU327_ SalI	accaGTCGACAG GAGGCAACACT ATGAA	SalI (GTCGAC)	To insert the *ef0907* gene into the plasmid pEU327 in order to complement the mutant
EF0907_RV_pEU327_ HindIII	accaAAGCTTTTA TTCTGAAATGT ATGCC	HindIII (AAGCTT)	To insert the *ef0907* gene into the plasmid pEU327 in order to complement the mutant
EF0907_seqPE_FW	GAACTTGTTCC AAGATGGACAA ACA		To verify the insertion of *ef0907* gene into the plasmid pEU327 by sequencing
EF0907_seqPE_RV	GGGCTAATTCA CCAGAAAGAAC GA		To verify the insertion of *ef0907* gene into the plasmid pEU327 by sequencing

Primers for cloning verification

pQE30_FW	GTGAGCGGATA ACAATTTCAC		To check the insert on the plasmid by PCR with oligo pQE30_RV
pQE30_RV	GAGTTCTGAGG TCATTACTG		To check the insert on the plasmid by PCR with oligo pQE30_FW
pEU327_FW	GTATTTGAATG CCGGATCGAT		To check the insert on the plasmid by PCR with oligo pEU327_RV
pEU327_RV	CTCTTGCCAGTC ACGTTACGTTAT		To check the insert on the plasmid by PCR with oligo pEU327_FW
pLT06_FW	CAATAATCGCA TCCGATTGCAG		To check the insert on the plasmid by PCR with oligo pLT06_RV
pLT06_RV	CCTATTATACCA TATTTTGGAC		To check the insert on the plasmid by PCR with oligo pLT06_FW

pREP4_FW	TTCGGTATCGTC GTATCCCA		To check the presence of pREP4 on a specific strain by PCR with oligo pREP4_RV
pREP4_RV	GGTGGTGTCGA TGGTAGAAC		To check the presence of pREP4 on a specific strain by PCR with oligo pREP4_FW

FW, forward; Oligo, oligonucleotides; RV, reverse.

Note: Lowercase bases are not complementary to the target sequence. Underlined bases correspond to the restriction sites. Yellow shaded bases correspond to the single point mutations.

III.4. Bioinformatic analysis

III.4.1. Homology search of the binding sites of LsrB AI-2 receptors

The amino acid sequences corresponding to the LsrB-**type** receptor of *S. enterica* ser. typhimurium (WP_000090739.1) [72] and the LsrB-**like** receptor of *Clostridium saccharobutylicum (C. saccharobutylicum)* (WP_022746280) [125] were retrieved from the NCBI data base (https://www.ncbi.nlm.nih.gov/protein) and compared by BLASTp (https://blast.ncbi.nlm.nih.gov/Blast.cgi) with the amino acid sequence of the putative AI-2 binding protein EF0907 of *E. faecalis* V583.

III.5. Genetic and molecular biology methods

III.5.1. Extraction of nucleic acids

III.5.1.1. Extraction of the plasmid DNA

Plasmid DNA from the different *E. coli* strains was extracted using the PureYield™ Plasmid Miniprep System (Promega) according to the manufacturer's instructions.

III.5.1.2. Extraction of chromosomal DNA

Genomic DNA from *E. faecalis* V583ΔABC was extracted using the MasterPure™ Gram Positive DNA Purification Kit (Epicentre) according to the manufacturer's instructions.

III.5.2. Polymerase chain reaction (PCR)

III.5.2.1. General PCR conditions

Depending on the further processing of the polymerase chain reaction (PCR) product, different kits were used to perform polymerase chain reactions in the T100™ Thermal Cycler (Bio-Rad). If the PCR products were used for cloning or sequencing the experiments were performed using the Q5® High-Fidelity PCR Kit (New England

BioLabs, NEB). For all the other routine PCRs the Gotaq® G2 Hot Start Polymerase Kit (Promega) was used. The reagents used to perform the different PCR reactions are listed in table 10.

Table 10: Reagents and their volume for PCR reaction with GoTaq® and Q5® enzymes.

	GoTaq®	**Q5® High-Fidelity**
Master Mix: Thermostable DNA Polymerase, dNTPs, $Mg^{2+}$and reaction buffer	12.5µL	12.5µL
Forward primer	1µL	1.25µL
Reverse primer	1µL	1.25µL
DNA template	15µL (<250ng)	15µL (<1000ng)
Nuclease-free water	To 25µL	To 25µL

dNTPs, deoxyribonucleotide triphosphates; Mg^{2+}, magnesium.

An online Tm-Calculator (NEB), considering the DNA polymerase used and sequence of the primers, calculated annealing temperature. The melting temperature chosen was approximately the same for sense and antisense primers with differences of less than 5°C. Time of polymerization was calculated according to the size of the desired PCR product: While GoTaq® polymerase needs 1min to elongate 1000bp, the Q5® High-Fidelity polymerase needs 20–30s to elongate 1000bp. The temperature programs for the PCR reactions are listed in table 11.

Table 11: General conditions for the amplifications by PCR with GoTaq® and Q5® enzymes.

Step	No. Cycles	**GoTaq®**		**Q5® High-Fidelity**	
		Temperature	Time	Temperature	Time
Initial Denaturation	1	95°C	2min	98°C	30s
Denaturation	35	95°C	30s	98°C	8s
Annealing	35	X	30s	X	20s
Elongation	35	72°C	**1min/1kb**	72°C	**2030s/1kb**
Final Elongation	1	72°C	5min	72°C	2min

If required, the amplified DNA was purified using the Wizard® SV Gel and PCR Clean-Up-System (Promega) according to the manufacturer's instructions.

III.5.3. Agarose gel electrophoresis

Agarose gel electrophoresis was performed according to Sambrook et al. [126]. A 1% agarose gel solution was prepared with 1g of agarose (Merck) in 100mL of boiling Tris-Borate-EDTA buffer (TBE: 10.8g Tris base, 5.5g boric acid and 0.7g EDTA-Na_2 per liter). To make DNA visible under UV light, a 1µL of Midori Green Advance DNA Stain (Nippon Genetics Europe) were added to the boiling mixture. Gel solution was cast into an acrylic chamber (Bio-Rad). After cooldown and solidification, the gel was covered with TBE Buffer in a Mini-Sub® cell GT (Bio-Rad) chamber and 5µL of the samples were loaded into each well. To analyze the size of the DNA fragments 5µL of the O´GeneRuler 1kb DNA ladder (Thermo Fisher Scientific) were added in one well. DNA fragments were separated with a constant voltage of 120V for 35min using a PowerPac Basic supply (Bio-Rad, Hercules). DNA bands were detected under UV illuminator (ChemiDoc™ MP Imaging System).

III.5.4. DNA manipulations using modification enzymes

III.5.4.1. DNA digestion by endonucleases

All restriction enzymes were purchased from NEB and were used following the manufacturer's instructions. In general, 5–20 units of restriction enzymes were used to digest 0.7–1µg of DNA. Digested DNA was purified using the Wizard® SV Gel and PCR Clean-Up-System (Promega) according to the manufacturer's instructions.

III.5.4.2. DNA ligation

Ligation was performed using the T4 DNA Ligase purchased from NEB following the manufacturer's instructions. For the reaction were used 30–50ng of the digested vector and a 5–7 molar excess of the insert.

III.5.5. Transformation

III.5.5.1. Preparation of electrocompetent *E. coli* cells

Electrocompetent *E. coli* cells were prepared according to the protocol described by Dower et al. [127]. Briefly, A 10mL ON culture of the respective *E. coli* strain was inoculated in 500mL of fresh LB and incubated with agitation at 37°C until an OD_{600} of 0,6–0,8. After the bacterial suspension was centrifuged (4000rpm, 30min, at 4°C), the

supernatant was discarded and the cell pellet was resuspended with 500mL of ice-cold sterile Milli-Q water. The centrifugation and resuspension steps were repeated with 250mL of ice-cold sterile Milli-Q water, 125mL, and 50mL of ice-cold sterile 10% glycerol. After the last washing step, the bacterial pellet was drained well with a pipet before resuspending it in 1mL of ice-cold sterile 10% glycerol. Electrocompetent cells suspension was then aliquoted in 100µL portions and stored at -80°C.

III.5.5.2. Transformation of recombinant plasmids into electrocompetent *E. coli* cells

To transform the ligated plasmids into electrocompetent *E. coli* cells, electroporation was performed as described by Dower et al. [127]. A 100µL aliquot of electrocompetent cells thawed on ice was gently mixed with 2µL of plasmid ligation mixture in a sterile 2mm electroporation cuvette (Carl Roth). To electroporate, the Electro Cell Manipulator® ECM 630 (BTX Harvard apparatus) was used under the conditions listened in table 12.

Table 12: General conditions for electroporation of *E. coli* cells.

Resistance	200Ω
Capacitance	25µF
Voltage	2.5kV
Time constant	4–6ms

Immediately after pulsing, cells were resuspended in 1mL of fresh LB and incubated under vigorous shaking for 30min at 37°C. Subsequently, 50, 100, and 200µL of the culture were spread out on LB agar plates containing the corresponding antibiotic and 5-bromo-4-chloro-3-indolyl-β-D-galactopyranoside (X-gal) (AppliChem) at 20µg/mL when needed. Finally, plates were incubated ON at 37°C.

III.5.5.3. Blue-white screening

After transformation, blue-white selection was performed to differentiate between colonies that integrated or not the pLT06 plasmid [128]. Blue-white screening was performed according to the method described by Sambrook et al. [129]. As follows, 20µg/mL X-gal (AppliChem) was added to the corresponding agar plates when screening *E. coli* colonies and 40µg/mL X-gal (AppliChem) were added when screening for *E. faecalis* colonies.

III.5.5.4. DNA sequencing and DNA sequence analyses

Purified PCR products and plasmid DNA samples were sent to sequence according to the method of Sanger [130] using the sequencing service of Eurofins Genomics (Germany). Samples were prepared in 1.5mL Eppendorf tubes as seen in table 13.

Table 13: Preparation of PCR and plasmid DNA samples for sequencing.

	Sample Volume	Sample Concentration
Primer	2µL	10pmol/µL primer
Plasmid	15µL	50–100ng/µL
PCR product	15µL	4–20ng/µL

The sequenced fragments were analyzed using Vector NTI 11.0 (Invitrogen, USA) software. After the sequencing analysis, bacterial stocks were made from the clones that harbor the desired recombinant plasmid or mutation.

III.5.5.5. Preparation of electrocompetent *E. faecalis* cells

Electrocompetent *E. faecalis* cells were prepared according to the protocol described by Taeok et al. Briefly, 10mL of an ON culture of the desire *E. faecalis* strain was inoculated into 90mL of fresh BHI or TSB and incubated without agitation at 37°C until an OD_{600} reached 0.8. Cells were chilled on ice for 20min and centrifuged at 4000rpm for 15min at 4°C. Supernatant was discarded and the cell pellet was resuspended in 3mL of ice-cold sterile 10% glycerol. Bacterial suspension was then split into two Eppendorf tubes and centrifuge at 13000rpm for 1min at 4°C. Pellets were resuspended in 500µL of lysozyme buffer (see Table 14), containing freshly added lysozyme at 25µg/mL (Sigma Aldrich) and mutanolysin at 2µg/mL (Sigma Aldrich). The suspensions were incubated for 30min at 37°C before centrifuging at 13000rpm for 1min at 4°C. After, the cells were washed three times with 1mL ice-cold sterile electroporation buffer (see Table 14), between each washing step cells were harvested by centrifugation at 13000rpm for 1min at 4°C. After the washing steps, the bacterial pellet was drained well before resuspending it in 300µL of ice-cold sterile electroporation buffer and aliquoted in 70µL portions before storage at -80°C. Lysozyme solution and the Electroporation buffer were prepared with the reagents listed in table 14.

Table 14: Composition of electroporation reagents.

Lysozyme buffer	Electroporation Buffer
10mM Tris base pH 8.0	0.5M Sucrose
20% Sucrose	10% Glycerol
10mM EDTA	
50mM NaCl	

III.5.5.6. Transformation of recombinant plasmids into electrocompetent *E. faecalis* cells

To transform recombinant plasmids into electrocompetent *E. faecalis* cells, electroporation was performed as described by Dower et al. [127]. A 70µL aliquot of electrocompetent cells thawed on ice was gently mixed with 1µL of purified recombinant plasmid in a sterile 1mm electroporation cuvette (Carl Roth). To electroporate, the Electro Cell Manipulator® ECM 630 (BTX Harvard apparatus) was used under the conditions listened in table 15.

Table 15: General conditions for electroporation of electrocompetent *E. faecalis* cells.

Resistance	200Ω
Capacitance	25µF
Voltage	1.6kV
Time constant	44.7ms

Immediately after pulsing, electrocompetent cells were mixed with 400µL of fresh STSB (0.5M sucrose, TSB) and incubated without shaking for 2h at 37°C. Subsequently, 50µL, 100µL, and 200µL of the culture were spread out on BHIA plates with the respective antibiotic and X-gal at 50µg/mL (AppliChem) when needed. Plates were incubated 23 days at 37°C. Colonies were stroked out with a sterile tip on fresh TSA plates containing the corresponding antibiotic and incubated ON at 37°C. Next day, a part of the each grown colony was suspended in 100µL of sterile ultra-pure water. Colonies suspected to harbor the recombinant plasmid were screened by PCR using 1µL of this suspension as a template and the primers corresponding to the plasmid transformed.

Purified PCR products and plasmid DNA samples were proceeded as described in chapter III.5.5.4. After the sequencing analysis, bacterial stocks were made from the *E. faecalis* clones that harbor the desired recombinant plasmid or mutation.

III.5.6. Mutagenesis by double-crossover in *E. faecalis* V583ΔABC

III.5.6.1. First crossover

For the first crossover, 10mL BHI supplemented with 20µg/mL of chloramphenicol were pre-warmed at 43°C in a water bath. In the prepared media *E. faecalis* V583ΔABC strain harboring the correct pLT06 derivate was inoculated and grown ON at 43°C. Next day, 10mL BHI supplemented with 20µg/mL of chloramphenicol were pre-warmed at 43°C and re-inoculated with 10µL of the ON culture from the day before. Bacterial cultures were grown ON at 43°C. This procedure was repeated five times and when possible the correct integration of the recombinant pLT06 vector into the enterococcal genome was confirmed by PCR.

III.5.6.2. Second crossover

For the first day of the second crossover, 10mL BHI without antibiotic were pre-warmed up to 30°C and were inoculated with 10µL of the ON culture from the last day of the first crossover. Bacteria were allowed to grow for 45h at 30°C. Afterward, culture was switched into a pre-warmed water bath and grown ON at 43°C. On day two of the second crossover, 10mL of fresh BHI without antibiotic were pre-warmed at 30°C and inoculated with 10µL of the bacterial culture from the day before. After, bacteria were allowed to grow for 45h at 30°C and switched into a pre-warmed water bath at 43°C to grow ON. At the same time, 10µL of the ON culture from the first day were diluted to 10^{-5} and 10^{-6} in 1.5mL Eppendorf tubes. Bacterial dilutions were quickly stroke out on prewarmed (43°C) BHIA plates supplemented with X-gal 50µg/mL (AppliChem) and were grown ON at 43°C. From the third day of the second crossover, the ON plates were screened for white colonies indicating the loss of the pLT06 plasmid. White Colonies were plated in two BHIA plates supplemented with either X-gal 50µg/mL (AppliChem) or X-gal 50µg/mL (AppliChem) and chloramphenicol 20µg/mL and incubated ON at 43°C. Additionally, 10µL of the ON culture from day two were treated in the same way as the culture from the first day of the second crossover. For the fourth day of the second crossover, colonies that only grew in the plates without antibiotic and white were considered positive for screening. Each selected colony was re-suspended in 100µL of sterile Milli-Q-water and 1µL of each bacterial suspension was used as a template in a PCR. Clones that yield PCR products with the appropriate molecular size were further inoculated in 10mL BHI with

and without chloramphenicol 20µg/mL to verify the loss of plasmid. Putative positive clones that grew only in the BHI without antibiotic were again tested for loss of vector pLT06 and persistence of recombinant gene fragment in the enterococcal genome by PCR. Purified PCR products were sent to sequence to verify the mutations. After the sequencing analysis, bacterial stocks were prepared from the *E. faecalis* clones that harbor the desired modification. The second crossover was continued at least for six days.

III.5.7. Construction of the recombinant plasmid pQE30::EF0907 and transformation into *E. coli* BL21ΔluxS

The *ef0907* gene was amplified by PCR using Q5® enzyme. Amplification was started from the 64th bp of *ef0907* gene excluding the sequence corresponding to the signal peptide. As template, the purified DNA of *E. faecalis* V583ΔABC was used. The primer pair EF0907_pQE_BamHI / EF0907_pQE30_HindIII was used to amplify a fragment of about 1.6kb. After purification, the construct was cloned downstream of an IPTG-inducible promotor and a 6xHis-codon sequence in the pQE30 expression vector using the restriction enzymes BamHI and HindIII. To transform recombinant plasmid pQE30::EF0907 together with plasmid pREP4 into electrocompetent *E. coli* BL21ΔluxS cells, plasmid DNA was purified as described in chapter III.5.1.1. To verify transformation, colonies grown on LB agar plates supplemented with ampicillin 100µg/mL and kanamycin 50µg/mL were screened for plasmids using the primer pairs pQE30_FW / pQE30_RV and pREP4_FW / pREP4_RV generating a fragment of about 1.7kb and 0.6kb, respectively. Plasmid DNA samples of potential clones containing the desired construct were confirmed by sequencing as described in chapter III.5.5.4 using the primers pQE30_FW, pQE30_RV, EF0907_seq1_FW, and EF0907_seq1_RV. A bacterial stock of the E. *coli* BL21ΔluxS+pREP4+pQE30::EF0907 was prepared.

III.5.8. Construction of the recombinant plasmid pLT06::ΔEF0907 and transformation into *E. faecalis* V583ΔABC

An 81,3% portion of the *ef0907* gene of *E. faecalis* V583ΔABC was deleted in-frame using site-directed mutagenesis as described by Ho et al. [131]. Restriction sites were used to introduce a complementary sequence in the primers to generate DNA fragments with overlapping ends which can anneal in further ligation reactions (see Chapter IV Figure 15). Two independent PCRs with Q5® enzyme were performed, using as template the purified DNA of *E. faecalis* V583. While the primer pair EF0907_5_FW / EF0907_22_HindIII was used to amplify a fragment of about 1kb upstream of the *ef0907* gene, the primer pair EF0907_33_HindIII / EF0907_66_RV was used to amplify a

fragment of about 1.3kb downstream of the *ef0907* gene. After purification, cleaned amplicons were digested with the enzyme HindIII and ligated with the T4 DNA Ligase. The ligation product was diluted 1:100 in nuclease-free water and used as DNA template for a PCR with Q5® enzyme using the primer pair EF0907_1_EcoRI / EF0907_44_BamHI generating a fragment of about 2.1kb. After purification, the cleaned construct was cloned into shuttle vector pLT06 by digestion with EcoRI and BamHI enzymes and ligation using the T4 DNA Ligase. The ligation was transformed into *E. coli* DH5α electrocompetent cells as described in chapter III.5.5.2. Colonies that grow blue in LB agar plates supplemented with 20µg/mL chloramphenicol and 20µg/mL X-gal (AppliChem) were screened for recombinant plasmid using the primer pair pLT06_FW / pLT06_RV generating a fragment of about 2.5kb. Plasmid DNA samples of potential clones containing the desire construct were confirmed by sequencing as described in chapter III.5.5.4 using the primers pLT06_FW, pLT06_RV, EF0907_seq1_FW, EF0907_seq2_FW, EF0907_seq3_RV, and EF0907_seq4_RV. A bacterial stock of the *E. coli* DH5α+pLT06::ΔEF0907 was prepared. To transform the recombinant plasmid into electrocompetent *E. faecalis* V583ΔABC cells, plasmid DNA was purified as described in chapter III.5.1.1 and electroporation was made as described in I.5.5.6. Colonies that grow blue in TSB agar plates supplemented with 20µg/mL chloramphenicol and 50µg/mL X-gal (AppliChem) were screened for recombinant plasmid using the primer pair pLT06_FW / pLT06_RV generating a fragment of about 2.5kb. A bacterial stock of *E. faecalis* V583ΔABC+pLT06::ΔEF0907 was prepared.

III.5.9. Construction of the recombinant plasmid pLT06::xxxEF2694 and transformation into *E. faecalis* V583ΔABC

The *ef2694* gene in *E. faecalis* V583ΔABC was single point mutated using site-directed mutagenesis as described by Ladjouzi et al. [132] (see Chapter IV, Figure 20). Three codons from the original gene were transformed into stop codons by introducing specific mutations in the nucleotide sequence using overlapping primers which already incorporate the respective nucleotide changes. Two independent PCRs with Q5® enzyme were performed, using as template the purified DNA of *E. faecalis* V583 as template. The primer pairs EF2694_5_FW / EF2694_2_RV and EF2694_3_FW / EF2694_6_RV were used to amplify fragments of about 1kb up- and downstream targeted mutation site in the *ef2694* gene. Amplificons were purified and diluted 1:100 in nuclease-free water. The dilutions in a 1:1 mix were used as a template to perform an overlapping PCR using the Q5® enzyme and the primer pair EF2694_1_BamHI / EF2694_4_NcoI generating a gene fragment of about 1.6kb. After purification, the cleaned construct was cloned into shuttle

vector pLT06 by digestion and ligation using BamHI and NcoI enzymes. The ligation was transformed into *E. coli* BL21 electrocompetent cells as described in chapter III.5.5.2. Colonies that grow blue in LB agar plates supplemented with 20µg/mL chloramphenicol and 20µg/mL X-gal (AppliChem) were screened for recombinant plasmid using the primer pair pLT06_FW / pLT06_RV generating a fragment about 1.7kb. Correct cloning in the plasmid was confirmed by DNA sequencing as described in chapter III.5.5.4 using the primers pLT06_FW, pLT06_RV, EF2694_seq1_FW, and EF2694_seq2_RV. A bacterial stock of the *E. coli* BL21+pLT06::xxxEF2694 was prepared. To transform the recombinant plasmid into electrocompetent *E. faecalis* V583ΔABC cells, plasmid DNA was purified as described in chapter III.5.1.1 and electroporation was made as described in I.5.5.6. Colonies that grow blue in TSB agar plates supplemented with 20µg/mL chloramphenicol and 50µg/mL X-gal (AppliChem) were screened for recombinant plasmid using the primer pair pLT06_FW / pLT06_RV generating a fragment about 1.7kb. A bacterial stock of *E. faecalis* V583ΔABC+pLT06::xxxEF2694 was prepared.

III.5.10. Disruption of the *ef0907* gene and *ef2694* gene by double-crossover

Positive clones containing the desire pLT06-gene plasmid were exposed to different antibiotic and temperature pressures for a certain time to promote the mutagenesis by homologous recombination. The first crossover was performed over one week at high temperatures to force the integration of the plasmid DNA into the enterococcal genome. The second crossover was performed several days by removing the antibiotic pressure to get rid of the plasmid after the first crossover. For first crossover, blue colonies were cultured as described in chapter III.5.6.1. For second crossover, blue colonies from the first crossover were cultured as described in chapter III.5.6.2. White grown colonies were screened for loss of plasmid by PCR using the primer pair pLT06_FW / pLT06_RV. Additional, disruption of *ef0907* and *ef2694* gene was confirmed by PCR using the primer pairs EF0907_seq1_FW / EF0907_seq3_RV and EF2694_7_FW_Verif / EF2694_6_RV generating a fragment of about 0.7kb and 1kb, respectively. While no sequencing confirmation of the deletion of *ef0907 gene* was required, *ef2694* gene was screened for the single point mutations by DNA sequencing using the primers EF2694_seq1_FW and EF2694_seq2_RV. A bacterial stock of *E faecalis* V583ΔABCΔEF0907 and *E. faecalis* V583ΔABCxxxEF2694 was prepared (further named as ΔEF0907 and xxxEF2694 mutants).

III.5.11. Complementation of the ΔEF0907 deletion mutant using pEU327 plasmid

The complementation of the *E. faecalis* ΔEF0907 mutant was constructed cloning the whole *ef0907* gene into the vector pEU327 [108]. The *ef0907* gene was amplified by PCR using Q5® enzyme. Amplification was started from the 1st bp of the *ef0907* gene including the sequence corresponding to the signal peptide. As template, the purified DNA of *E. faecalis* V583 was used. The primer pair EF0907_FW_pEU327_SalI / EF0907_RV_pEU327_HindIII was used to amplify a fragment of about 1.7kb. After purification, DNA was cloned downstream of the xylose-inducible promoter of the vector pEU327 by digestion with SalI and HindIII and ligation with T4 DNA Ligase. The recombinant plasmid pEU327::EF0907 was transformed into *E. coli* Top10 electrocompetent cells as described in chapter III.5.5.2. Colonies that grow white in LB agar plates supplemented with 100µg/mL spectinomycin were screened for recombinant plasmid using the primer pair pEU327_FW / pEU327_RV generating a fragment of about 1.8kb. Positive clones were sent to sequencing as described in chapter III.5.5.4 using the primers pEU327_FW, and pEU327_RV, EF0907_seqPE_FW, and EF0907_seqPE_RV. A bacterial stock of *E. coli* Top10+pEU327::EF0907 was prepared. To transform the recombinant plasmid into electrocompetent *E. faecalis* ΔEF0907 cells, plasmid DNA was extracted as described in chapter III.5.1.1. Colonies that grow white in TSB agar plates supplemented with 100µg/mL spectinomycin were screened for recombinant plasmid using the primer pair pEU327_FW / pEU327_RV generating a fragment of about 1.8kb. A bacterial stock of *E. faecalis* V583ΔABCΔEF0907+pEU327::EF0907 (further named as ΔEF0907+pEU327::EF0907 mutant) was prepared.

To exclude plasmid related effects on the phenotype of the plasmid-based-complementation of ΔEF0907 mutant, the empty pEU327 plasmid was transformed into wildtype *E. faecalis* V583ΔABC and ΔEF0907 mutant. As described previously, the pEU327 plasmid was extracted from *E. coli* Top10+pEU327 by mini-prep. A 2µL of plasmid yield was added to a 100µL aliquot of electrocompetent *E. faecalis* V583ΔABC and ΔEF0907 cells. Colonies that grow white in TSB agar plates supplemented with 100µg/mL spectinomycin were screened for recombinant plasmid using the primer pair pEU327_FW / pEU327_RV generating a fragment of about 0.1kb. A bacterial stock of *E. faecalis* V583ΔABC+pEU327 and *E. faecalis* V583ΔABCΔEF0907+pEU327 (further named as ΔEF0907 +pEU327::EF0907 mutant) was prepared.

III.6. Methods of biochemical analysis

III.6.1. Purification of the N-terminally 6xHis-tagged recombinant protein rEF0907 under native conditions using HisTalon Metal Affinity Resin

The 6xHis-tagged recombinant protein rEF0907 from *E. coli* was extracted and purified using the HisTALON™ Gravity Column Purification Kit (Clontech) according to the manufacturer's instructions. Bacterial strain *E. coli* BL21ΔluxS+pREP4+pQE30::EF0907 was inoculated in 20mL of LB liquid media supplemented with 100µg/mL ampicillin and 25µg/mL kanamycin. Bacterial culture was grown at 37°C ON under vigorous shaking. The whole ON culture was transferred into a 1 Liter Erlenmeyer flask filled with 200mL fresh LB liquid media supplemented with 100µg/mL ampicillin, 25µg/mL kanamycin and glucose 5%. The culture was grown at 37°C with vigorous shaking (250rpm) between 2 and 3h. When the culture reached an OD_{600nm} between 0.5 and 0.7, IPTG (AppliChem) at a final concentration of 0,5mM was added. Bacteria were grown for two more hours at 37°C with vigorous shaking. To harvest the cells, the culture was centrifuged (4000rpm, 30min, 4°C) and the supernatant was discarded. All the subsequent steps were performed on ice to avoid proteolysis. The cell pellet was resuspended with 10mL of PBS and centrifuged once more under the same conditions. To lyse the bacteria, cells were resuspended in 20mL of HisTalon xTractor Buffer for each gram of pellet. A 40µL of 5units/µL DNase I solution (Sigma-Aldrich) and 200µL of lysozyme 10mg/mL solution (Sigma-Aldrich) was added and carefully mixed by pipetting up and down. The suspension was incubated with gentle shaking at 4°C for 2h and centrifuged (12.000xg, 20min, 4°C). The clarified lysate harboring the rEF0907 was mixed with 3mL of Talon® Metal Affinity Resin (Clontech) and placed in a falcon tube. To enable binding between rEF0907 to the cobalt charged resin, the tube was fixed on a platform shaker under gentle agitation for 20min at 4°C. After incubation, the tube was centrifuged (700xg, 5min, 4°C). After centrifugation, the supernatant was carefully removed without disturbing the resin pellet. The resin was washed with 12mL of Equilibration Buffer. The tube was fixed on a platform shaker under gentle agitation for 10min at 4°C. After incubation, the mix was poured into a plastic column and allowed to drain by gravity. The column was washed two times by the gentle addition of 20 mL of Washing buffer. The His-tagged protein was eluted from the cobalt resin with 8 mL of Elution Buffer. The buffer was allowed to flow through the HisTALON™ Gravity Column and the flow-through was collected in 1mL fractions. The correct purification of the rEF0907 was verified by SDS-PAGE. After electrophoresis, the Elution Buffer was replaced for the same buffer in which the synesthetic DPD (OMM scientific) (Buffer for

ITC) is dissolved by diafiltration as follows. The eluate was transferred into a 50mL Amicon diafiltration device with a 3kDa membrane (Millipore). The tube was centrifuged (3200rpm, 40min, 4°C) and the flow-through was discarded. To ensure a complete buffer exchange the membrane containing the protein was washed by adding 10mL of the Buffer for ITC followed by centrifugation (3200rpm, 40min, 4°C). The washing step was repeated 10 times. Finally, the solution was concentrated to 1 mL, transferred into 2mL Eppendorf tubes in 100µL aliquots and stored at -80°C. A 10µL from the solution was used to quantify the final concentration of the protein.

III.6.2. Sodium dodecyl sulfate-polyacrylamide gel electrophoresis (SDS-PAGE)

III.6.2.1. General conditions for SDS-PAGE

The proteins were separated by Sodium dodecyl sulfate-polyacrylamide gel electrophoresis (SDS-PAGE) under denaturing conditions as described by the method of Laemmli [133]. Briefly, 10µL of protein samples (usually 2–10µg) were mixed with 3µL of 5x Laemmli sample buffer (Bio-Rad) and heated at 95°C on a heating block (Stuart SBH200D). While protein samples were let to cool down to RT, a freshly cast 12% SDS-PAGE gel was placed in the electrophoresis chamber (Bio-Rad) and completely covert with Tris/Glycine/SDS Running Buffer (25 mM Tris, 192 mM Glycine, 0.1% SDS, pH 8.3). The wells were loaded with 13µL of the protein samples and one well with 7µL of the precision plus™ Dual Color Protein Standard (Bio-Rad). Electrophoresis was run at 170V for 50min using the PowerPac™ (Bio-Rad) as a power supply.

III.6.2.2. Coomassie Blue protein staining

SDS-PAGE gels were stained using the InstantBlue protein stain (expedeon) according to the manufacturer's instructions. After electrophoresis, gels were placed in three times for 5min with water. After washing, gels were completely covered with 7mL of InstantBlue protein stain and gentle agitation for 1h. To make protein bands more visible after the staining process, the background was cleared by rinsing the gel with water for 30min.

III.6.3. Determination of protein concentration by Bradford assay

Total protein concentration was determined by the Bradford dye-binding method [134] using the Roti®-Nanoquant Protein Quantification Assay (Carl Roth) according to the manufacturer's instructions. Briefly, protein samples were diluted with water in 1,5mL Eppendorf tubes in a dilution of 1:50, 1:100, and 1:200. For the calibration curve, Bovine Serum Albumin (BSA) Standard (Carl Roth) was diluted with water ranging from

1µg/mL to 100µg/mL. A 50µL of the diluted samples and 50µL of prepared BSA Standards were pipetted in an ELISA 96-well plate (Sarstedt). Subsequently, a 200µl of Roti®-Nanoquant solution was added to each well and the plate was stored in the dark for 5min at RT. The plate was measured at 590nm and 450nm using CLARIOstar® reader (BMG-LABTECH). A calibration curve was generated and protein concentration in the sample was determined by comparing the quotient OD_{590}/OD_{450} of each sample to the calibration curve. All samples were measured in duplicate and plate was read at least two times.

III.7. Growth curve analysis

III.7.1. Growth curves with TSB (or BHI)

Growth curves of the wildtype *E. faecalis* V583ΔABC and corresponding mutants and derivatives were performed as follows: A 10µL from every bacterial stock was stroke out on a TSB (or BHI) agar plate to let them grow ON at 37°C. One single colony was inoculated in 7mL of TSB (or BHI) in 15mL Falcon tubes and let grow ON at 37°C. The cultures were re-inoculated in glass tubes filled with 7mL of fresh media (TSB or BHI) to obtain an OD_{600nm} of 0.05 for all tested strains. The glass tubes were incubated at 37°C. At certain time points (0, 1, 2, 3, 4, 5, 6, 7, 8 and 24h), the optical density at 600nm was measured using GENESYS^{TM}20 Vis-Spectrophotometer (Thermo Fisher Scientific).

III.7.2. Growth curves with chemically defined media

Growth curves of the wildtype *E. faecalis* V583ΔABC and its corresponding mutants and derivatives were performed as follows: A 10µL from every bacterial stock was stroke out on a TSB agar plate to let them grow ON at 37°C. One single colony was inoculated in 7mL of fresh TSB in 15mL Falcon tubes and let growth ON at 37°C. Cells were harvest by centrifugation of 2mL of the ON culture (4°C, 4000rpm, and 4min) and the cell pellet was resuspended in 1mL of PBS. Bacteria were re-inoculated in glass tubes filled with 4.5mL of fresh chemically defined media (CDM, prepared as described in chapter III.2.3). The OD_{600nm} was measured and adjusted to 0.05 for all tested strains. For each sample, 45µL were transferred into three 8.5mm UV cuvettes (Sarstedt). To obtain a final volume of 75µL, either 30µL of DPD (12 µL DPD OMM scientific 0.52g/L diluted with 18µL Milli-Q-Water), which is spontaneously converted to AI-2 when dissolved in water and is therefore referred by the following simply as AI-2 (0.08% final concentration), 30µL of Milli-Q-Water (negative control) or 30µL of glucose 0.2% (0.08% final concentration; positive control) were added. Cuvettes were incubated at 37°C. At certain time points (0,

1, 2, 3, 4, 5, 6, 7, 8 and 24h), the optical density at 600nm was measured using GENESYS^{TM}20 Vis-Spectrophotometer (Thermo Fisher Scientific). As blanc were used either CDM supplemented with AI-2 or CDM supplemented glucose 0.2% or CMD supplemented with Milli-Q-Water.

III.8. Isothermal titration calorimetry (ITC)

Binding between rEF0907 and AI-2 was studied by isothermal titration calorimetry (ITC) using the MicroCal^{TM} ITC200 microcalorimeter (Malvern) according to the manufacturer's instructions. The reagents prepared for ITC experiment are listed in table 16.

Table 16: Recipes to perform ITC experiments.

	Ligand	**Binding protein**
Name	AI-2	rEF0907
Amount of substance	500µM	50µM
Total volume	250µL	1mL

III.8.1. ITC sample application

The reference cell was filled with tap water and the sample cell was filled with 200µL of rEF0907 at a concentration of 50µM. Both cells were heated up to equal temperature (25°C). A 40µL of AI-2 (OMM scientific) at a concentration of 500µM was filled into the syringe. Every 3min, aliquots of 2µl of AI-2 were injected from the syringe into the sample cell. Measurements were performed with the reference power at 10µcal/s.

III.8.2. ITC analysis

The power needed to restore isothermal conditions between the reference and the sample cell was measured by the ITC instrument. Measurements were evaluated by Microcal^{TM} ITC200 analysis software (Malvern). Binding affinities were quantified by calculating the binding constants (K, association constant, or K_d, dissociation constant), the reaction stoichiometry (n), the enthalpy (ΔH) and the entropy (ΔS).

III.9. Fluorescence resonance energy transfer (FRET)-based AI-2 assay

To detect and quantify the AI-2 concentration in filter-sterilized supernatants of *E. faecalis* V583ΔABC and its corresponding mutants and derivatives a fluorescence resonance energy transfer (FRET)-based AI-2 assay was performed as described by Rajamani et al. [135].

Briefly, the FRET assay is based on a modified version of an AI-2 receptor protein purified from an *E. coli* strain by Ni-NTA affinity chromatography (see Figure 6). On the external C- and N-termini of the AI-2 receptor protein were fused a cyan fluorescent protein (CFP) and a yellow fluorescent protein (YFP) [135]. The fusion protein is called CLPY [135]. When AI-2 binds to CLPY changes in the protein conformation are induced, pointing in a dose-dependent decrease in FRET of CFP and YFP [135]. The CLPY protein was prepared for the assay in a final concentration of 0.025mg/mL in reaction buffer (25mM sodium phosphate buffer pH 8.0, 35mM sodium chloride and 1mM boric acid) [52]. The FRET ratio (YFP/CFP or $OD_{527nm/485nm}$) was determined measuring the fluorescence at 540nm and 485nm upon excitation at 430nm [52]. Purchased DPD (ITQB) was used at concentrations between 1–60µM to establish a calibration curve, corresponding to the linear range of this assay. The FRET ratio of each sample was compared with the calibration curve, when necessary bacterial supernatants were diluted with TSB.

III.9.1. Preparation of supernatants from *E. faecalis* strains for FRET-based AI-2 assay

ON cultures of a single colony of *E. faecalis* V583ΔABC and its corresponding mutants and derivatives were grown without agitation in 7mL TSB. For each strain, two TSB agar plate were stroke out and incubated ON at 37°C. After incubation, bacteria were scratched from the plate with a cotton swap and resuspend in 1.5mL Eppendorf tubes filled with 1mL TSB. Tubes were centrifuged (4000rpm, 4min, 4°C) the supernatant was discarded and the cell pellet was resuspended in 1mL of fresh TSB. Bacteria were inoculated in 50 mL of fresh TSB and adjusted to an OD_{600} of 0.05 using GENESYS^{TM}20 Vis-Spectrophotometer (Thermo Fisher Scientific). At certain time points (0, 1, 2, 3, 4, 5, 6, 7, and 8h) a 700µL aliquots were taken and centrifuged (9000rpm, 4min, 4°C). The supernatant was collected with a syringe (Braun) and filtered using a Rotilabo®-syringe filters of 0.22µm (Carl Roth). After filtering, the samples were rapidly stored until usage at -80°C.

III.10. Microtiter plate biofilm assay

Biofilm formation of the wild type *E. faecalis* V583ΔABC and its corresponding mutants and derivatives were performed as described by Paganelli et al. in the presence or absence of AI-2 [136].

Bacteria were grown on TSA-sheep blood (TSA-S) plates at 37°C. A bacterial suspension was prepared on PBS from agar plates. OD_{660} of suspension culture was measured to prepare a dilution at 0.01 in 1mL TSB supplemented with glucose 1%. A 100µl of each dilution was pipetted in four replicates in a Costar® polystyrene TC-treated 96-well plate (Corning). The AI-2 (OMM scientific) was supplemented to obtain final concentrations of up to 500µM. As negative control TSB supplemented with glucose 1% was used. The plate was incubated ON at 37°C without shaking. After incubation, culture supernatants were removed and 195µl PBS were carefully pipetted along the side walls of the wells to remove the remaining media. Washing was repeated two times more with 195µl of PBS. Afterward wells were stained with 170µl 0.2% crystal violet (Gram-Hucker's Crystal Violet Oxalate solution from AppliChem mixed with PBS) for 15min. Then, crystal violet was carefully pipetted off and discarded. Wells were washed 2 times with PBS as described before. After PBS was removed, the stained biofilm was eluted by incubating each well with 170µl 96% ethanol for 1h at RT. Eluted biofilm was measured at 595nm in Elisa reader (CLARIOstar® B).

III.11. Opsonophagocytic killing assay (OPA)

The in vitro opsonophagocytic killing assay (OPA) was performed of the wildtype *E. faecalis* V583ΔABC and its corresponding mutants and derivatives as described by Kropec et al. [137]. The four main compounds used in OPA were prepared at the same time (see Table 17). The reagents and buffers used in OPA are listed in table 18.

Table 17: Four main compounds used in OPA.

Main compounds	Obtained from	Use
Lyophilized complement	Sera of baby rabbits (Cedarlane Laboratories)	Complement source
Antibodies at different dilutions	Heat-inactivated sera of rabbits	Antibody source
Bacterial suspension	Bacterial stock of the respective strain	Target surface structure

PMNs	Freshly taken blood of healthy adult volunteers	Neutrophils (mediate the opsonic killing)

PMNs, polymorphonuclear neutrophils.

Table 18: Buffer and reagents used in OPA.

Buffer and reagents	Composition
Heparin-dextran buffer	4.5g NaCl, 32.5mg Heparin-sulfate, 10g dextran 500 filled up to 500mL dH_2O; filtered sterile
Lysis buffer	2,5g NH_4Cl in 250mL dH_2O; filtered sterile
RPMIF	RPMI (Thermo Fisher Scientific) supplemented with 15% FBS (Thermo Fisher Scientific)

FBS, fetal bovine serum; RPMI media, Roswell Park Memorial Institute media.

III.11.1. Preparation of the four main components used in OPA

The PMNs were prepared from freshly drawn human blood of a healthy adult volunteer. Collected blood was mixed 1:1 with Heparin-dextran buffer and incubated at 37°C for 45min. While the sedimented erythrocytes were discarded, the leucocyte-containing upper phase was centrifuged (2.700rpm, 10min, 10°C). Afterwards, supernatant was discarded and the leucocyte pellet was washed by gently resuspended it in 10mL RPMIF. The suspension was centrifuged (2.700rpm, 10 min, 10°C), supernatant was removed and cell pellet was resuspended in 10mL Lysis buffer. The mixture was incubated for 20min at RT. After incubation, suspension was centrifuged (2.700rpm, 10 min, 10°C) and washed with 10mL of RPMIF. Finally, supernatant was discarded and the leucocyte pellet was resuspended in 3mL of RPMIF. The PMNs were stored on ice until usage at a final concentration of approximately $2x10^7$ cells/mL. All tested bacterial strains were taken from freshly inoculated TSA plates with a cotton swap and adjust to an OD_{650} of 0.1 in 7ml of TSB. The bacterial cultures were allowed to grow at 37°C until an OD_{650} of 0.4. For each tested strain an aliquot of 1mL was taken and centrifuged (13.000rpm, 5min, 10°C). After centrifugation, supernatants were discarded and cell pellets were resuspended in 1mL of RPMIF. The bacterial suspension was diluted 1:100 in RPMIF and stored on ice until usage. Lyophilized baby rabbit complement (Cedarlane Laboratories) was diluted 1:15 in RPMIF and absorbed with the corresponding target *E. faecalis* strain taken from a freshly grown plate with a cotton swab. The mixture was

incubated on a rotor rack for 1h at 4°C. After incubation, mix was centrifuged (2700rpm, 10min, 4°C). The supernatant was taken with a syringe and filtered sterile using Rotilabo®-syringe filters 0.22µm CME (Carl Roth). Finally, the complements were stored on ice until usage. Polyclonal antibodies produced in rabbit were heat-inactivated and diluted with RPMIF at dilutions ranging from 1:50 to 1:200. The antibodies were stored on ice until usage.

III.11.2. The OPA assay

The opsonophagocytic killing assay was performed combining 100µL of leukocytes ($2x10^7$/mL), 100µL of bacteria ($2x10^7$cfu/mL), 100µL of the complement solution, and 100µL of heat-inactivated rabbit immune serum raised against whole-bacteria as a source of antibody at various dilutions. Controls without PMNs (PMNneg), complement (Cneg), or antibody (Abneg) where included to monitor the assay. The mixtures were incubated on a rotor rack at 37°C for 90min. Afterwards, the tubes were vortexed for 10s, diluted in TSB to 10^{-2}, and 10µL of the dilutions plated in quadruplicates on TSA plates. Percent killing (%Killing) was calculated by comparing the colony counts at 90min (t90) to the ones of the PMNneg control using the following formula: {[(mean cfu PMNneg at t90) - (mean cfu at t90)]/(mean cfu PMNneg at t90)}×100 [137].

III.12. Statistics

For statistical analysis the software program PRISM version 5.00 (GraphPad, San Diego, California, USA) was used. Differences between AI-2 concentrations of the wildtype and the ΔEF0907 mutant at each time point in FRET-based AI-2 assay as well as differences between the biofilm formation in the presence and absence of AI-2 of the wildtype and the mutants ΔEF0907 and xxxEF2694 were analyzed by the nonparametric Mann-Whitney U-Test. Mean and standard deviations are shown. Statistical significant results are signed with * for $p<0.05$. Statistical analysis of the %Killing of the bacterial counts of the OPA was done by the Kruskal-Wallis nonparametric analysis of variance (multigroup comparison, nonparametric test) with the Dunn procedure (pairwise comparisons). Mean and standard deviations are shown. Statistical significant results are signed with * for $p<0.05$.

III.13. Buffers, reagents, and enzymes

III.13.1. Buffer and reagents

Table 19: Buffer and reagents.

Name	Composition/Company/Reference	Storage
α-LTA	[138]	-20°C
α-V583	[89]	-20°C
α-T2	[139]	-20°C
Acrylamide/Bis-solution 30%	Carl Roth	+4°C
Agarose	Merck	RT
Ampicillin	Carl Roth	+4°C
APS 20%	Sigma-Aldrich	+4°C
Baby rabbit complement, lyophilized	Cedarlane Laboratories	-20°C
Boric acid	Merck	RT
Bradford Standard	Thermo fisher scientific	+4°C
Chloramphenicol	Carl Roth	RT
DPD	OMM scientific, Texas or ITQB, Portugal	-80°C
FBS (Gibco)	Thermo Fisher Scientific	-20°C
Glucose	Sigma-Aldrich	+4°C
Gram-Hucker's Crystal Violet Oxalate solution	AppliChem	RT
Heparin-sulfate	Sigma-Aldrich	RT
InstantBlue™ Protein Stain	expedeon	+4°C
IPTG	AppliChem	-20°C
Kanamycin sulfate	Carl Roth	+4°C
Laemmli Sample Buffer	Bio-Rad	-20°C
O´GeneRuler 1kb DNA ladder	Thermo Fisher Scientific	+4°C

PBS	1L distilled H_2O 80g of NaCl 2g of KCl 14.4g of Na_2HPO_4 2.4g of KH_2PO_4	RT
Precious plus™ Dual Color Protein Standards marker	Bio-Rad	-20°C
RPMI 1640 Medium, GlutaMAX™ Supplement	Thermo Fisher Scientific	+4°C
SDS 10%	Sigma-Aldrich	RT
Spectinomycin	AppliChem	RT
Sulfuric acid	Carl Roth	-20°C
TEMED	Sigma-Aldrich	RT
Tris base	Sigma-Aldrich	RT
TBE	1L distilled H_2O 0.7g EDTA-Na_2 5.5g boric acid 10.8g Tris base	RT
X-gal	AppliChem	-20°C
10X Tris/Glycine/SDS Buffer	Bio-Rad	RT

α-LTA, antibodies raised against lipoteichoic acid from *E. faecalis* 12030; α-V583, antibodies raised against the whole-bacterium of *E. faecalis* V583; α-T2, antibodies raised against the whole-bacterium of *E. faecalis* Type 2; APS, Ammonium-persulfate; DPD, 4,5-dihydroxy-2,3-pentanedione; FBS, fetal bovine serum; IPTG, isopropyl β-D-1-thiogalactopyranoside; ITC, isothermal titration calorimetry; PBS, phosphate buffered saline; RPMI, Roswell Park Memorial Institute; SDS, Na-lauryl-sulfate; TBE, Tris-borate-EDTA; TEMED, N,N,N´,N´- tetramethyl-ethylenediamine; X-gal, 5-bromo-4-chloro-3-indolyl-β-D-galactopyranoside.

III.13.2. DNA modifying enzymes

Table 20: Enzymes.

Enzyme	Company
DNA polymerases	
▪ Gotaq®	Promega
▪ Q5®	NEB
DNAse I	Sigma-Aldrich
T4 DNA Ligase	NEB

Lysozyme	Sigma-Aldrich
Restriction enzymes	
▪ HindIII	NEB
▪ BamHI	NEB
▪ EcoRI	NEB
▪ NcoI	NEB
▪ SalI	NEB

III.13.3. Commercially available Kits

Table 21: Kits used in this study.

Name	Company
HisTALON™ Gravity Column Purification Kit	Clontech
MasterPure™ Gram Positive DNA Purification Kit	Epicentre
PureYield™ Plasmid Miniprep System	Promega
Roti®-Nanoquant Protein Quantification Assay	Carl Roth
Wizard® SV Gel and PCR Clean-Up System	Promega

III.13.4. Instruments

Table 22: Instruments used in this study.

Instrument(s)	Company
Centrifuges	
▪ Centrifuge 5417 R	Eppendorf
▪ Centrifuge 5424 R	Eppendorf
▪ Centrifuge 5810 R	Eppendorf
▪ Centrifuge Avanti J-26 XPI	Beckman Coulter
Clean Bench	
▪ Camfil MXLA-GW	BDK Luft- und Reinraumtechnik
Cuvettes	
▪ UV cuvette, min. sample vol.: 50µL, 2 sides optical	Sarstedt
▪ UV cuvette, 4mL, made of PS, 4 sides optical	Sarstedt

Electrophoresis	
▪ Mini-PROTEAN® Tetra Cell	Bio-Rad
Electroporation	
▪ Electroporation cuvettes 2mm	Carl Roth
▪ Electro Cell manipulator® ECM 630	BTX Harvard apparatus
▪ Safety Stand 630B	BTX Harvard apparatus
ELISA Readers	
▪ CLARIOstar®	BMG Labtech
▪ Synergy H1 Hybrid Multi-Mode Micro-plate Reader	BioTek
Agarose gel electrophoresis	
▪ Universal Hood III 731BR00955	Bio-Rad
▪ PowerPac™ Basic	Thermo Fisher Scientific
▪ Wide Mini-Sub® Cell GT 258BR012074	Bio-Rad Bio-Rad
DNA quantification	
▪ NanoDrop™ 2000	Thermo Fisher Scientific
Heating block	
▪ Stuart SBH200D	Stuart
Incubators	
▪ Temperature-controller kelvitron® T	Heraeus
▪ IN30	Memmert
▪ CO_2 Incubator ThermoForma	Thermo Fisher Scientific
▪ KS 4000 ic control	IKA
Hot plate Stirrer	
▪ Magnetic mini-stirrer IKA® topolino	IKA
Microscopy	
▪ VWR VisiCam® 3.0	ZEISS
Microliter syringe	
▪ Syringes inject 10mL, 20mL, 50mL	Braun
Needles	
▪ Sterican needles Ø 0,90*40mm; Gr 1	Braun
PCR-Maschine	
▪ T100™ Thermal Cycler	Bio-Rad
Pipetboys	

▪ accu-jet® 04 A 2303	Brand
▪ pipetus®	Hirschmann
Pipette Eppendorf research plus	
▪ 0.5–10µL	Eppendorf
▪ 10–100µL	Eppendorf
▪ 100–1000µL	Eppendorf
Power supply	
▪ PowerPac™ Basic Power Supply	Bio-Rad
Scales	
▪ Electronic balance Typ ABJ 80-4M	Kern und Sohn
▪ sartorius	VWR
Thermomixers	
▪ ThermoMixer® 5436	Eppendorf
▪ ThermoMixer® 5437	Eppendorf
▪ ThermoMixer® comfort	Eppendorf
Vortexer	
▪ Vortex-Genie 2®	Scientific industries
Water bath	
▪ VWB 12	VWR
Spectrophotometer	
▪ Thermo Scientific GENESYS™20 Vis-Spectrophotometer	Thermo Fisher Scientific
Isothermal titration calorimetry	
▪ MicroCal™ ITC200	Malvern

III.13.5. Software programs

Table 23: Software programs used in this study.

Name	Company
ChemiDoc™ MP Imaging System	Bio-Rad
GraphPad Software	GraphPad
Image Lab™ Software	ZEISS
MARS Datenanalyse Software	BMG Labtech
Mendeley	Elsevier

Microcal™ ITC200 analysis software	Malvern
Nanodrop™ 2000	ZEISS
Spark® multimode microplate reader	Tecan
Vector NTI Advance® Sequence Analysis Software	Thermo Fisher Scientific

IV. Results

The *ef0907* gene in *E. faecalis* V583ΔABC encodes for a putative EF0907 ABC transporter peptide-binding protein. Unpublished data in *E. faecalis* V583ΔABC using transcriptome analysis revealed in RNA-seq data various genes significantly up-regulated 6h after incubation with 100µM AI-2. As one of this up-regulated genes was the *ef0907* gene and as the usage of ABC transporter for AI-2 internalization have been already reported for other bacteria such as *S. enterica* ser. typhimurium, *E. coli*, and *V. harveyi* [140], we hypothesized that EF0907 protein could be a putative AI-2 binding protein in *E. faecalis*. Following this rational we decided to investigate the role of EF0907 in the AI-2 transport as is described in detail in the subsequent sections.

IV.1. Homology search of the binding sites of LsrB AI-2 receptors

In order to find homologies between the amino acid sequence of the EF0907 protein of *E. faecalis* V583 and those of the LsrB-type receptor of *S. enterica* ser. typhimurium and the LsrB-like receptor of *C. saccharobutylicum*, bioinformatic analysis as described in the materials and methods section was used.

In the BLASTp analysis we found that the amino acid sequence corresponding to the EF0907 protein showed a sequence identity of 37.21% to the binding sites of the LsrB-type receptor of *S. enterica* ser. typhimurium and a sequence identity of 36.36% to the LsrB-like receptor of *C. saccharobutylicum* (see Figure 11). According to Peirera et al. (2009) [74], both results would indicate low sequence identity. However, they do not yet belong to those proteins with a sequence identity below 36% for which AI-2 binding becomes unlikely [74]. Using BLASTp analysis we also revealed, that the six conserved amino acid residues (Lys_{35}, Asp_{116}, Asp_{166}, Gln_{167}, $Pro_{220,}$ and Ala_{222}) described for the AI-2 binding site of different LsrB-type receptors including the one of *S. enterica* ser. typhimurium [58] (see Figure 11, A, shaded blue) were not identical to those of EF0907 (see Figure 11, B, shaded blue). Instead of Lys_{35}, Asp_{116}, Asp_{166}, Gln_{167}, Pro_{220}, and Ala_{222}, in *E. faecalis* V583 were found Ser_{35}, Ser_{116}, Gly_{166}, Ile_{167}, Asn_{220}, and Pro_{222}. Nonetheless, similar amino acids could be found in the immediate vicinity (shaded green). In contrast to the LsrB-type receptors, no conserved amino acids in the AI-2 binding site of the LsrB-like receptors have been described so far.

Considering the results of the bioinformatic analysis, it cannot be excluded that EF0907 belongs to the family of LsrB-type receptors. Though, due to the low sequence identity and the fact that none of the conserved amino acids of the AI-2 binding site of the LsrB-

type receptors have been found in EF0907 increases the chance that EF0907 might belong to the family of LsrB-like receptors [125]. In order to obtain more evidence on whether EF0907 is able to bind AI-2 and that it belongs to the LsrB-like receptors, further in vitro experiments have to be performed.

>WP_000090737.1 MULTISPECIES: autoinducer 2 ABC transporter substrate-binding protein LsrB **[Salmonella]**
MARHSIKMIALLTAFGLASAAMTVQAAERIAFIPKLVGVGFFTSGGNGAQEAGKALGIDVTYDGPTEPSVSGQVQ
LVNNFVNQGYDAIIVSAVSPDGLCPALKRAMQRGVKILTWDSDTKPECRSYYINQGTPKQLGSMLVEMAAHQVDK
EKAKVAFFYSSPTVTDQNQWVKEAKAKISQEHPGWEIVTTQFGYNDATKSLQTAEGIIKAYPDLDAIIAPDANAL
PAAAQAAENLKRNNLAIVGFSTPNVMRPYVQRGTVKEFGLWDVVQQGKISVYVANALLKNMPMNVGDSLDIPGIG
KVTVSPNSEQGYHYEAKGNGIVLLPERVIFNKDNIDKYDF

>NP_814645.1 peptide ABC transporter peptide-binding protein **[Enterococcus faecalis V583]**
MKLKKSLTFGVITLFSVTTLAACGGGGTSDSSSASGGGKASGEQVLRVTEQQEMPTADLSLATDRISFIALNNVY
EGIYRLDKDNKVQPAGAAEKAEVSEDGLTYKIKLNKDAKWSDGKPVTANDYVYGWQRTVDPATASEYAYLYASVK
NGDAIAKGEKDKSELGIKAVSDTELEITLEKATPYFDYLLAFPSFFPQRQDIVEKYGKNYASNSESAVYNGPFVL
DGFDGPGTDTKWSFKKNDQYWDKDTVKLDSVDVNVVKESPTALNLFQDGQTDDVVLSGELAQQMANDPAFVSQKE
ASTQYMELNQRDEKSPFRNANLRKAISYSIDRKALVESILGDGSIEPNGLVPADMAKDPSGGKDFAKEAGSQIEY
DTKKAKEYWEKAKKELGISTLTMDILSSDADSSKKTVEFVQGSIQDALDGVKVTVSPVPFSVRLDRSNKGDFDAV
IGGWSADYADPSSFLDLFASDNSYNRGRYNNAEFDKFVKAASSADATDPEKRWDDMLNAEKTIMGDMGVVPLFQK
SEAHLRAEKVKDVAVHPAGATYDYKWAYISE

>WP_022746280.1 substrate-binding domain-containing protein **[Clostridium saccharobutylicum]**
MKKKAVALALIGAMIFTTLVGCGSSNTTTDTSTNSSKKGNVTVTFIPKLTGNAFFESANKGAQKYSEQWGFKVDY
EGDANASAASQVSVINKAVQQGTNAICLSSVDAAGVKDALKAAADAGVTVTTWDSDVDPSVRKVMVSQGTPEQLG
QMLVQMGYDSLKERGKDPEKDAIKYCWHYSNATVTDQNSWQVEGEKYIKSKYPNWQNVAPDNYYSNQDAEQAISV
GESILSAHSDIDLIICNDSTALPGQAQAAQNKGLTAKNVTITGFASPNSMKQYCNDGILTRWGLWDCGIQGAMGC
YMAYYIASGNSVKVGDKIEIPTVGTVEVMPNSVLDPKADDSDTSSGVVLLPERTIFTKDNMNNYDF

Figure 11: Amino acid sequences analyzed by BLASTp. [A] Amino acid sequence of the AI-2 binding protein of *S. enterica* ser. *typhimurium*; [B] Amino acid sequence of the EF0907 protein in *E. faecalis* V583; [C] Amino acid sequence of the AI-2 binding protein of *C. saccharobutylicum*. Position of conserved amino acids (shaded blue) and similar amino acid in the immediate vicinity of the conserved amino acids (shaded green).

IV.2. Construction of the recombinant plasmid pQE30::EF0907 and transformation into *E. coli* BL21ΔluxS

In order to recombinantly express the putative AI-2 binding protein EF0907, the Gram-negative overexpression host *E. coli* BL21ΔluxS and the pQE30 expression system were used.

The *ef0907* gene was amplified from the 64th bp, excluding the sequence corresponding to the signal peptide as described in the materials and methods section. As template, the purified DNA of *E. faecalis* V583ΔABC was used. A 1608bp fragment was amplified using the primer pair EF0907_pQE_BamHI / EF0907_pQE30_HindIII (see Figure 12, 1).

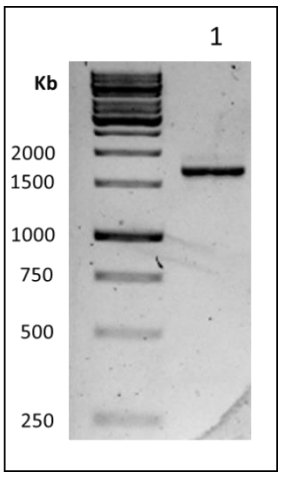

Figure 12: Agarose gel electrophoresis for confirmation for the PCR amplification of the *ef0907* gene. A PCR was performed, using as template the purified DNA of *E. faecalis* V583ΔABC. [1] Primer pair EF0907_pQE_BamHI / EF0907_pQE30_HindIII was used to amplify a 1608bp fragment of the *ef0907* gene.

After purification, the construct was cloned downstream of an IPTG-inducible promotor and a 6xHis-codon sequences in the pQE30 expression vector. After ligation, the recombinant plasmid pQE30::EF0907 was electroporated together with plasmid pREP4 into *E. coli* BL21ΔluxS strain. To verify transformation, colonies grown on LB agar plates supplemented with ampicillin 100µg/mL and kanamycin 50µg/mL were screened for plasmids using the primer pairs pQE30_FW / pQE30_RV and pREP4_FW / pREP4_RV generating a PCR product of 1706bp (see Figure 13, 1–6) and 550bp (see Figure 14, 1–6), respectively. Finally, the cloning was confirmed by DNA sequencing using the primers pQE30_FW, pQE30_RV, EF0907_seq1_FW and EF0907_seq1_RV (data not shown). The resulting strain was named as *E. coli* BL21ΔluxS+pREP4+pQE30::EF0907 and was used for the recombinant production of the EF0907 protein.

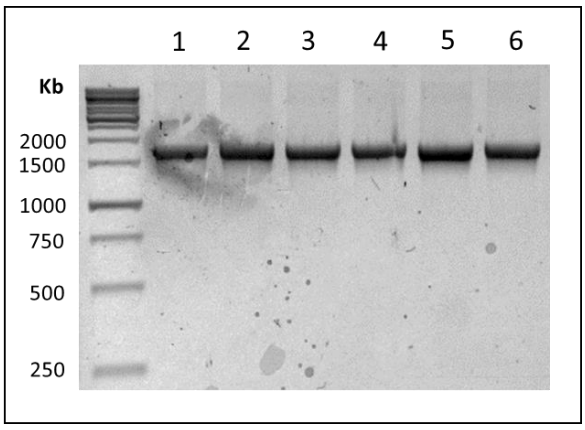

Figure 13: Agarose gel electrophoresis for confirmation of the *E. coli* transformation of the pQE30::EF0907 ligation. [1–6] Integration of EF0907 insert in vector pQE30 in *E. coli*

BL21ΔluxS electrocompetent cells was confirmed by PCR using the primer pair pQE30_FW / pQE30_RV generating a 1706bp product.

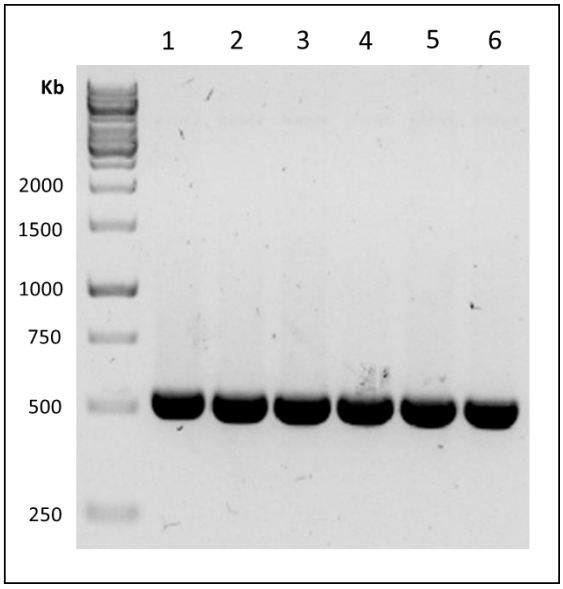

Figure 14: Agarose gel electrophoresis for confirmation of the *E. coli* transformation of the pREP4 plasmid. [1–6] Integration of vector pREP4 in *E. coli* BL21ΔluxS electrocompetent cells was confirmed by PCR using the primer pair pREP4_FW / pREP4_RV generating a 550bp product.

IV.3. Construction of the *E. faecalis* ΔEF0907 and xxxEF2694 mutants

IV.3.1. Construction of the recombinant plasmid pLT06::ΔEF0907 and transformation into *E. faecalis* V583ΔABC

To investigate the role of the *ef0907* gene in *E. faecalis* V583ΔABC as putative AI-2 ABC transporter peptide-binding protein, a site-directed mutagenesis was used.

Restriction sites were used to introduce a complementary sequence in the primers to generate DNA fragments with overlapping ends which can anneal in further ligation reactions (see Figure 15, A). As a result, an 81.3% portion of the *ef0907* gene of *E. faecalis* V583ΔABC was deleted in-frame (see Figure 15, B) as described in the materials and methods section.

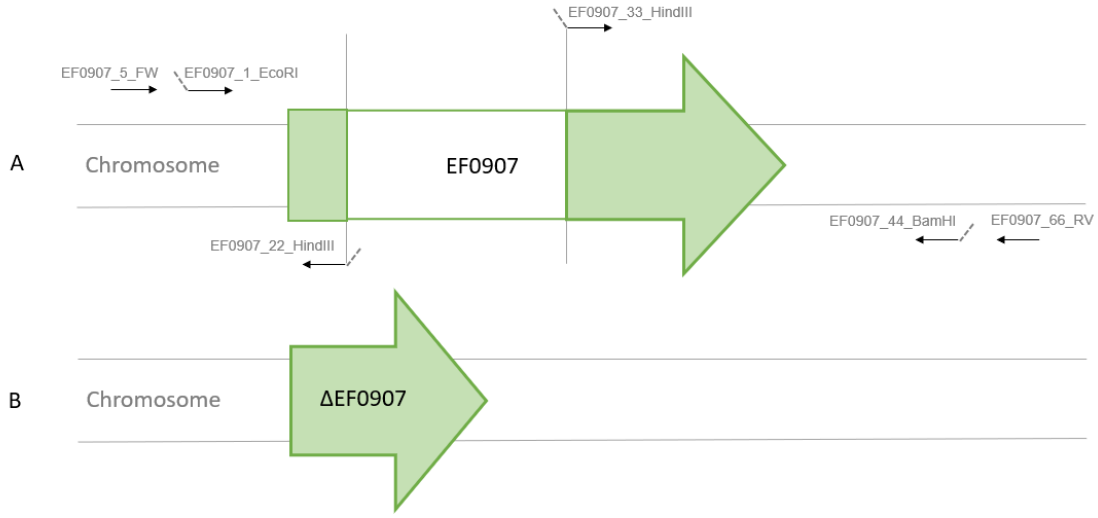

Figure 15: Deletion of the *ef0907* gene using site directed mutagenesis. Schematic representation of the *ef0907* gene with the pairs used for construction of fragments. [A] The wildtype with complete *ef0907* gene; [B] The ΔEF0907 mutant after deletion of 81,3% of the *ef0907* gene.

Independent PCRs were performed, using as template the purified DNA of *E. faecalis* V583. First, a 974bp fragment upstream of the *ef0907* gene (see Figure 16, 3) and then a 1283bp fragment downstream of the *ef0907* gene (see Figure 16, 4) were amplified using the primer pairs EF0907_5_FW / EF0907_22_HindIII and EF0907_33_HindIII / EF0907_66_RV respectively.

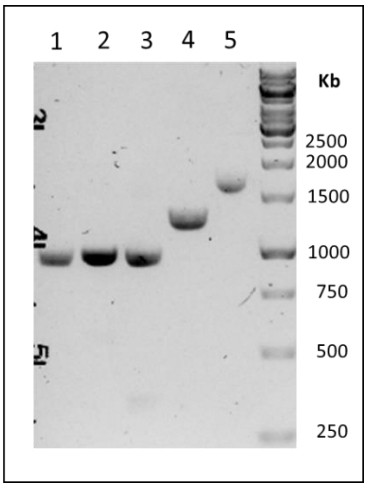

Figure 16: Agarose gel electrophoresis for confirmation of the different PCR amplifications for the different mutagenesis. Independent PCRs were performed, using as template the purified DNA of *E. faecalis* V583. [1] Primer pair EF2694_5_FW / EF2694_2_RV was used to amplify a 967bp fragment upstream of the *ef2694* gene; [2] Primer pair EF2694_3_FW / EF2694_6_RV was used to amplify a 1000bp fragment downstream of the *ef2694* gene; [3] Primer pair EF0907_5_FW / EF0907_22_HindIII was used to amplify a 974bp fragment upstream of the *ef0907* gene; [4] Primer pair EF0907_33_HindIII / EF0907_66_RV was used to amplify a 1283bp fragment downstream of the *ef0907* gene; [5] Primer pair EF0907_FW_pEU327_SalI / EF0907_RV_pEU327_HindIII was used to amplify a 1704bp fragment of the *ef0907* gene.

Amplicons were purified, digested with the restriction enzyme Hind III, and ligated with the T4 DNA Ligase. The ligation product was used as DNA template for a PCR in a 1:10 dilution. A 2093bp fragment was amplified using the primer pair EF0907_1_EcoRI / EF0907_44_BamHI (see Figure 17, 1).

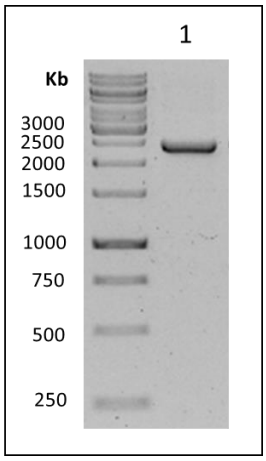

Figure 17: Agarose gel electrophoresis for confirmation of PCR amplification of the ΔEF0907 fragment. The ligation products were used as a DNA template for a PCR. [1] Primer pair EF0907_1_EcoRI / EF0907_44_BamHI was used to generate PCR product of 2093bp.

Amplicons were cloned into the enterococci compatible vector pLT06 as described in the material and method section. Subsequently, the resulting recombinant plasmid pLT06::ΔEF0907 was transformed into *E. coli* DH5α electrocompetent cells. To verify cloning process, blue colonies were screened for recombinant plasmid using the primer pair pLT06_FW / pLT06_RV, generating a PCR product of 2483bp (see Figure 18, 1). Finally, the correct sequence was confirmed by DNA sequencing using the primers pLT06_FW, pLT06_RV, EF0907_seq1_FW, EF0907_seq2_FW, EF0907_seq3_RV, and EF0907_seq4_RV (data not shown). The resulting strain was named as *E. coli* DH5α+pLT06::ΔEF0907.

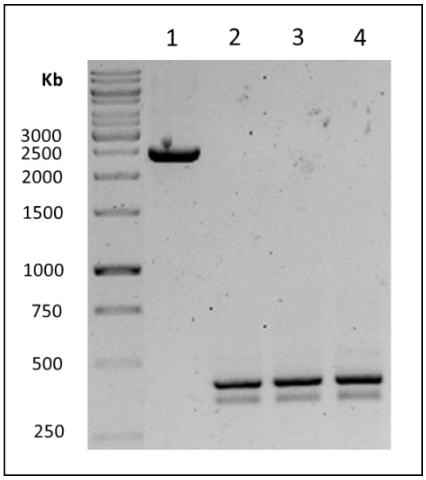

Figure 18: Agarose gel electrophoresis for confirmation of the *E. coli* DH5α transformation with the pLT06::ΔEF0907 ligation. [1] Integration of ΔEF0907 insert in vector pLT06 in *E. coli* DH5α electrocompetent cells was confirmed using the primer pair pLT06_FW / pLT06_RV, generating a PCR product of 2483bp; [2–4] *E. coli* DH5α electrocompetent cells harboring vector pLT06 without insert.

In order to transform recombinant plasmid pLT06::ΔEF0907 into *E. faecalis* V583ΔABC cells by electroporation, the plasmid was extracted from *E. coli* by mini-prep as described in the materials and methods section. To verify the transformation, blue colonies were screened for recombinant plasmid using the primer pair pLT06_FW / pLT06_RV, generating a PCR product of 2483bp (see Figure 19, 1 and 2). The resulting strain was named as *E. faecalis* V583ΔABC+pLT06::ΔEF0907.

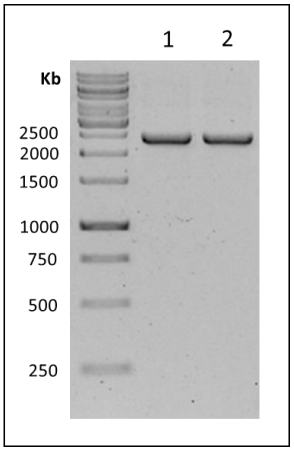

Figure 19: Agarose gel electrophoresis for confirmation of the *E. faecalis* V583ΔABC transformation with the pLT06::ΔEF0907 plasmid. [1, 2] Integration of ΔEF0907 insert in *E. faecalis* V583ΔABC electrocompetent cells was confirmed using the primer pair pLT06_FW / pLT06_RV, generating PCR product of 2483bp.

IV.3.2. Construction of the recombinant plasmid pLT06::xxxEF2694 and transformation into *E. faecalis* V583ΔABC

To construct a negative control (mutant unable to synthesize AI-2) and to further investigate the phenotype of the *ef2694* gene in *E. faecalis* V583ΔABC, encoding for the MTA/SAH nucleosidase, single point site-directed mutagenesis was used.

Three codons on the *ef2694* gene in *E. faecalis* V583ΔABC were single point mutated in-frame (see Figure 20, A) as described in the materials and methods section. Three codons in the first third of the *ef2694* gene were transformed into stop codons by introducing specific mutations in the nucleotide sequence using overlapping primers which already incorporate the respective nucleotide changes (see Figure 20, B).

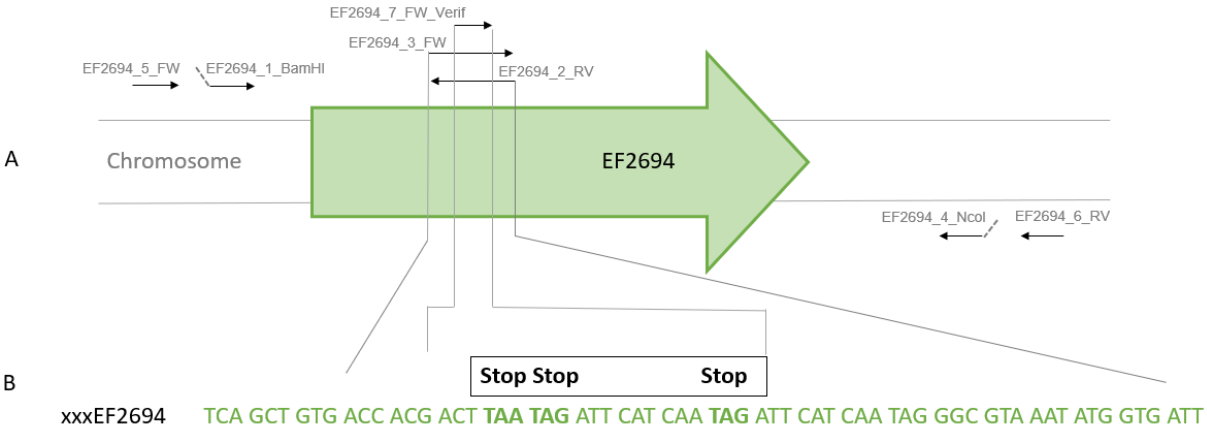

Figure 20: Single point mutation of the *ef2694* gene using site directed mutagenesis. Schematic representation of the *ef2694* gene with the primer pairs used for construction of fragments. [A] The wildtype with complete *ef2694* gene; [B] The single point mutated sequence in the *ef2694* gene.

Independent PCRs were performed, using as template the purified DNA of *E. faecalis* V583. First, a 967bp fragment containing the 5' end of the *ef2694* gene (see Figure 16, 1) and then a 1000bp fragment containing the 3' end of the *ef2694* gene (see Figure 16, 2) were amplified using the primer pairs EF2694_5_FW / EF2694_2_RV and EF2694_3_FW / EF2694_6_RV respectively. Amplicons were purified, mixed on a 1:1 ratio and used as template for a second PCR generating a 1505bp fragment using the primer pair EF2694_1_BamHI / EF2694_4_NcoI (see Figure 21, 1 and 2).

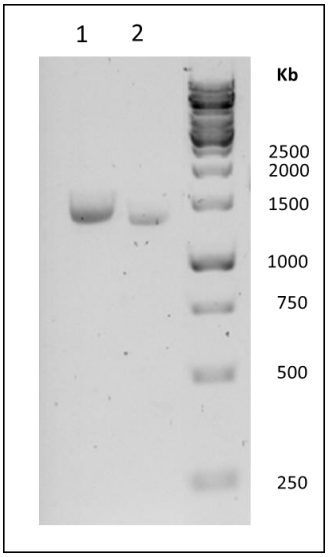

Figure 21: Agarose gel electrophoresis for confirmation of the PCR amplification of the xxxEF2694 fragment. The ligation products from the amplifications with the primer pairs EF2694_5_FW / EF2694_2_RV and EF2694_3_FW / EF2694_6_RV were used as a DNA template for an overlapping PCR. [1, 2] Primer pair EF2694_1_BamHI / EF2694_4_NcoI was used generating PCR product of 1505bp.

Amplicons were cloned into the enterococci compatible vector pLT06 as described in the materials and methods section. Subsequently, the resulting recombinant plasmid pLT06::xxxEF2694 was transformed into *E. coli* BL21 electrocompetent cells. To verify transformation, blue colonies were screened for recombinant plasmid using the primer pair pLT06_FW / pLT06_RV, generating a PCR product of 1723bp (see Figure 22, 1). Finally, the correct sequence was confirmed by DNA sequencing using the primers pLT06_FW, pLT06_RV, EF2694_seq1_FW, and EF2694_seq2_RV (data not shown). The resulting strain was named as *E. coli* BL21+pLT06::xxxEF2694.

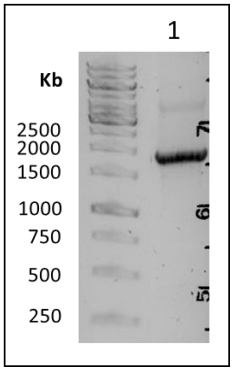

Figure 22: Agarose gel electrophoresis for confirmation of the *E. coli* BL21transformation with the pLT06::xxxEF2694 ligation. [1] Integration of insert xxxEF2694 in vector pLT06 in *E. coli* BL21 electrocompetent cells was confirmed using the primer pair pLT06_FW / pLT06_RV, generating a PCR product of 1723bp. In order to transform recombinant plasmid pLT06::xxxEF2694 into *E. faecalis* V583ΔABC cells by electroporation, the plasmid was extracted from the *E. coli* strain by mini-prep as described in the materials and methods section. To verify the transformation, grown colonies were screened for recombinant plasmid using the primer pair pLT06_FW / pLT06_RV generating a PCR product of 1723bp (see Figure 23, 1–4). The resulting strain was named as *E. faecalis* V583ΔABC+pLT06::xxxEF2694.

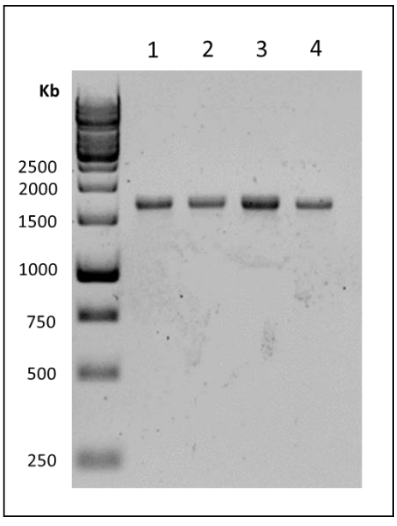

Figure 23: Agarose gel electrophoresis for confirmation of the *E. faecalis* V583ΔABC transformation with the pLT06::xxxEF2694 plasmid. [1–4] Integration of the pLT06::xxxEF2694 plasmid in *E. faecalis* V583ΔABC electrocompetent cells was confirmed using the pair pLT06_FW / pLT06_RV, generating a PCR product of 1723bp.

IV.4. Disruption of the *ef0907* gene by double-crossover

For the first cross-over, positive clones containing the desire pLT06-gene plasmid were cultured at 43°C in 20µg/mL of chloramphenicol over one week as described in the materials and methods section to force the integration of the ΔEF0907 plasmid DNA into the genome of *E. faecalis* V583ΔABC. The second crossover was performed at the permissive temperature of 30°C without antibiotic pressure as described in the material and methods section for several days to get rid of the vector pLT06 after the first crossover. The mutation in the *ef0907* gene was confirmed by PCR using the primer pair EF0907_seq1_FW / EF0907_seq3_RV. For the ΔEF0907 mutant a short PCR product of 715bp was expected (see Figure 24, 1 and 9), for the wildtype a longer PCR product of 2093bp was generated (see Figure 24, 2–8). Loss of vector pLT06 was confirmed by PCR using the primer pair pLT06_FW / pLT06_RV with no PCR products detected in the mutant clones (data not shown). The resulting mutant was named as *E. faecalis* V583ΔABCΔEF0907 (further referred simply as ΔEF0907 mutant).

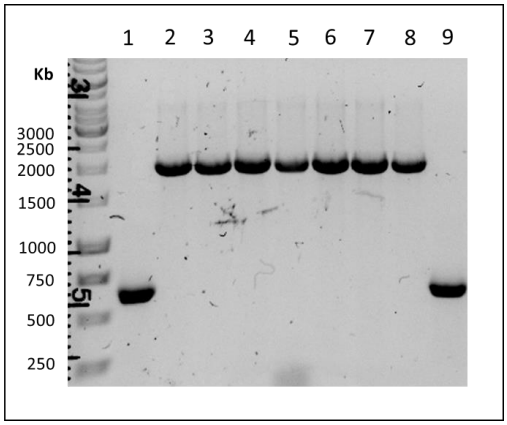

Figure 24: Agarose gel electrophoresis for confirmation of the *E. faecalis* ΔEF0907 mutant. [1, 9] *E. faecalis* ΔEF0907 clone was confirmed using primer pair EF0907_seq1_FW / EF0907_seq3_RV, generating a gene product of 715bp; [2–8] While for the wildtype *E. faecalis* V583ΔABC was generated a gene product of 2093bp.

IV.5. Disruption of the *ef2694* gene by double-crossover

For the first cross-over positive clones containing the desired pLT06-gene plasmid were cultured at 43°C in 20µg/mL of chloramphenicol over one week as described in the materials and methods section to force the integration of the xxxEF2694 plasmid DNA

into the genome of *E faecalis* V583ΔABC. The second crossover was performed at 30°C without antibiotic pressure as described in the material and methods section for several days to get rid of the vector pLT06 after the first crossover. The single point mutations on the *ef2694* gene were confirmed using the primer pair EF2694_7_FW_Verif / EF2694_6_RV generating a PCR product of 988bp (see Figure 25, 1). Loss of vector pLT06 was confirmed by PCR using the primer pair pLT06_FW / pLT06_RV with no PCR products detected in the mutant clones (data not shown).

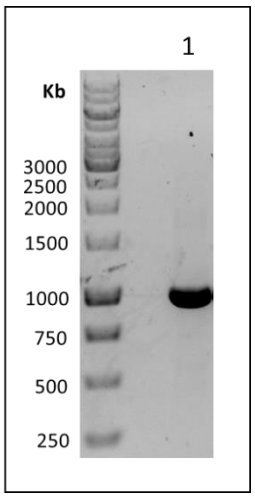

Figure 25: Agarose gel electrophoresis for confirmation of the *E. faecalis* xxxEF2694 mutant. [1] *E. faecalis* xxxEF2694 clone was confirmed using the primer pair EF2694_7_FW_Verif / EF2694_6_RV, generating a gene product of 988bp.

Since there are no differences in the size of the PCR fragments between wildtype and xxxEF2694 mutant, it is necessary to perform further sequence analyses. Therefore, the mutagenesis was confirmed by DNA sequencing using the primers EF2694_seq1_FW and EF2694_seq2_RV (see Figure 26). The resulting mutant was named as *E. faecalis* V583ΔABCxxxEF2694 (further named xxxEF2694 mutant).

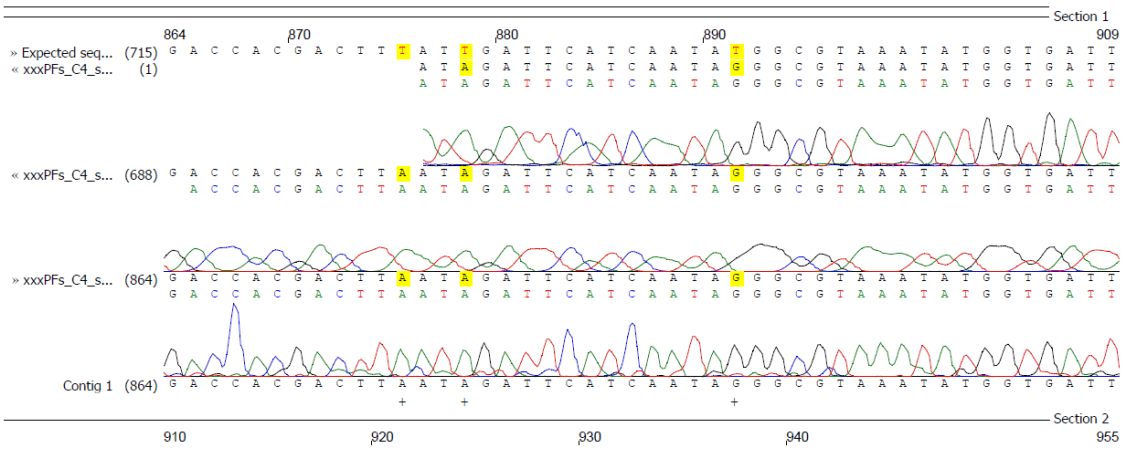

Figure 26: Sequencing chromatogram for confirmation of the xxxEF2694 single point mutations in *E. faecalis* V583ΔABC. PCR and plasmid DNA samples were sent to sequence using the sequencing service of Eurofins Genomics (Germany). Sequencing results were analyzed using Vector NTI 11.0 software. Original (red, shaded yellow) and expected bases (black, shaded yellow).

IV.6. Complementation of the ΔEF0907 deletion mutant using pEU327 plasmid

In order to restore the phenotype of the deleted *ef0907* gene in *E. faecalis* V583ΔABC, plasmid-based complementations of the ΔEF0907 mutant using the pEU327 vector were constructed as described in the materials and methods section.

The pEU327 plasmid was extracted from the *E. coli* Top10+pEU327 strain by mini-prep. The whole *ef0907* gene was amplified by PCR using as template the purified DNA of *E. faecalis* V583. Amplification was started from the 1st bp of the *ef0907* gene including the sequence corresponding to the signal peptide. A 1704bp fragment was amplified using the primer pair EF0907_FW_pEU327_SalI / EF0907_RV_pEU327_HindIII (see Figure 16, 5). After purification, the construct was cloned into shuttle vector pEU327 downstream of the xylose-inducible promoter of the vector using the restriction enzymes SalI and HindIII and the T4 DNA Ligase as described in the materials and methods section. After ligation, the recombinant plasmid pEU327::EF0907 was transformed into *E. coli* Top10 electrocompetent cells. To verify transformation, colonies that grow white in LB agar plates supplemented with 100µg/mL spectinomycin were screened for recombinant plasmid pEU327::EF0907 using the primer pair pEU327_FW / pEU327_RV, generating a fragment of 1820bp (see Figure 27, 3).

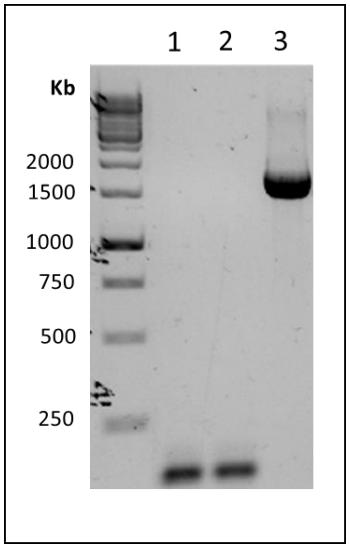

Figure 27: Agarose gel electrophoresis for confirmation of the *E. coli* Top10 transformation with the pEU327::EF0907 ligation. To verify the transformation, grown colonies were screened for recombinant plasmid using the primer pair pEU327_FW / pEU327_RV, generating a PCR

product of 1820bp when the plasmid is harboring the desire insert or generating a PCR product of 136bp when the plasmid is empty. [1,2] *E. coli* Top10+pEU327; [3] *E. coli* Top10+pEU327::EF0907.

Finally, the correct sequence was confirmed by DNA sequencing using the primers pEU327_FW, and pEU327_RV, EF0907_seqPE_FW, and EF0907_seqPE_RV (data not shown). The resulting strain was named as *E. coli* Top10+pEU327::EF0907. The recombinant plasmid pEU327::EF0907 was extracted from *E. coli* cells by mini-prep and consequently transformed into *E. faecalis* ΔEF0907 electrocompetent cells as described in the materials and methods section. Colonies that grow white in TSB agar plates supplemented with 100µg/mL spectinomycin were screened for recombinant plasmid using the primer pair pEU327_FW / pEU327_RV, generating a PCR product of 1820bp (see Figure 28, 1–4). The resulting strain was named as E. faecalis V583ΔABCΔEF0907+pEU327::EF0907 (further named as ΔEF0907+pEU327::EF0907 mutant).

To further ensure that the pEU327 plasmid itself or the spectinomycin, which must be used to guarantee the presence of the plasmid, has no effect on the phenotype of the plasmid-based complementation, the empty pEU327 plasmid was transformed into wildtype *E. faecalis* V583ΔABC and the ΔEF0907 mutant as described in the materials and methods section. To verify transformation, colonies that grow white in TSB agar plates supplemented with 100µg/mL spectinomycin were screened for clones harboring vector pEU327 without the insert using the primer pair pEU327_FW / pEU327_RV, generating a fragment of 136bp (see Figure 28, 5, 6 and 7, 8). The resulting strains were named as *E. faecalis* V583ΔABC+pEU327 and *E. faecalis* V583ΔABCΔEF0907+pEU327 (further named as ΔEF0907+pEU327 mutant).

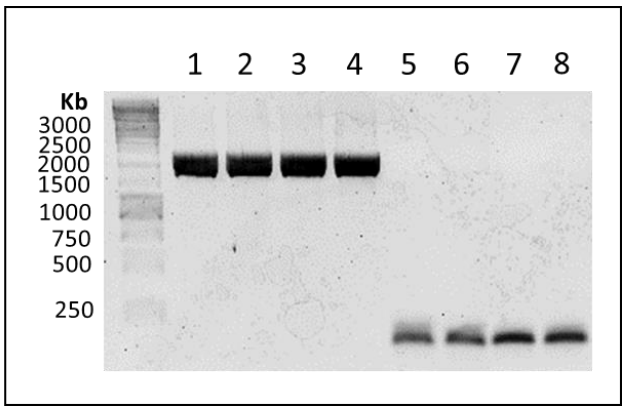

Figure 28: Agarose gel electrophoresis for confirmation of the different *E. faecalis* transformations with the different pEU327 plasmids. To verify the transformation, grown colonies were screened for (recombinant) plasmid using the primer pair pEU327_FW /

pEU327_RV, generating a PCR product of 1820bp when the plasmid is harboring the desire insert or generating a PCR product of 136bp when the plasmid is empty. [1–4] *E. faecalis* ΔEF0907+pEU327::EF0907; [5, 6] *E. faecalis* ΔEF0907+pEU327; [7, 8] *E. faecalis* V583ΔABC+pEU327.

IV.7. Purification of the N-terminally 6xHis-tagged recombinant protein rEF0907 under native conditions using HisTalon Metal Affinity Resin

The recombinant His-tagged protein rEF0907 was overproduced in *E. coli* BL21ΔluxS+pREP4+pQE30::EF0907 strain and purified using a cobalt charged column as described in the materials and methods section.

The rEF0907 was eluted from the resin with 4mL of Elution Buffer. The eluate was collected in 100µL fractions. To find the fraction with the highest yield of protein SDS-PAGE was performed as described in the materials and methods section (see Figure 29). The highest yield of protein was found in the first and second fraction (see Figure 29, black arrows). The molecular weight of the purified fractions corresponds with the 60,88kDa calculated for the EF0907 protein.

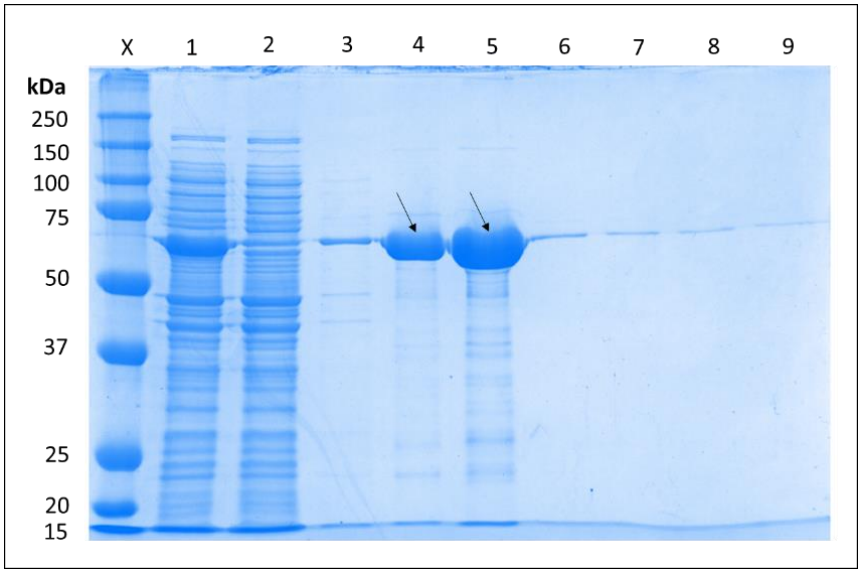

Figure 29: Coomassie blue stained SDS-PAGE (12%) analysis for the purification of the recombinant protein EF0907. Wells were loaded with 10µL of elute of rEF0907 and 3µL of Laemmli Buffer; Run was performed for 50min at 170V. [X] Protein molecular weight marker, [1] Total lysate; [2] Flow through; [3] Column wash; [4] 1st fraction of elution of His-tagged rEF0907; [5] 2nd fraction of elution of His-tagged rEF0907; [6] 3rd fraction of elution of His-tagged rEF0907; [7] 4th fraction of elution of His-tagged rEF0907; [8] 5th fraction of elution of His-tagged rEF0907; [9] 6th fraction of elution of His-tagged rEF0907; arrows are indicating fractions with the highest yield of His-tagged rEF0907.

To quantify the total protein concentration a Bradford standard assay was performed as described in the material and methods section. The absorbance was measured at

590/450nm using CLARIOstar®. The concentration of rEF0907 in the 1st and 2nd fraction are shown below (see Table 24).

Table 24: Concentration of rEF0907 quantified with Bradford standard assay.

	1st fraction [B1]	2nd fraction [B2]
Concentration of rEF0907	3.11 mg/mL	7.5mg/mL

IV.8. Growth curves with TSB and BHI

To determine whether genetic manipulation leads to changes in the growth behavior of wildtype *E. faecalis* V583ΔABC, its mutants ΔEF0907 and xxxEF2694, growth curves in TSB and BHI were performed as described in chapter III.7.1.

As shown in figure 30, no significant differences in growth rate between the wildtype (black line), the ΔEF0907 mutant (red line) and the xxxEF2694 mutant (dark blue line) were observed. Comparing growth behavior in different media used strains reached higher OD when grown in TSB than in BHI (see Figure 30, A and B).

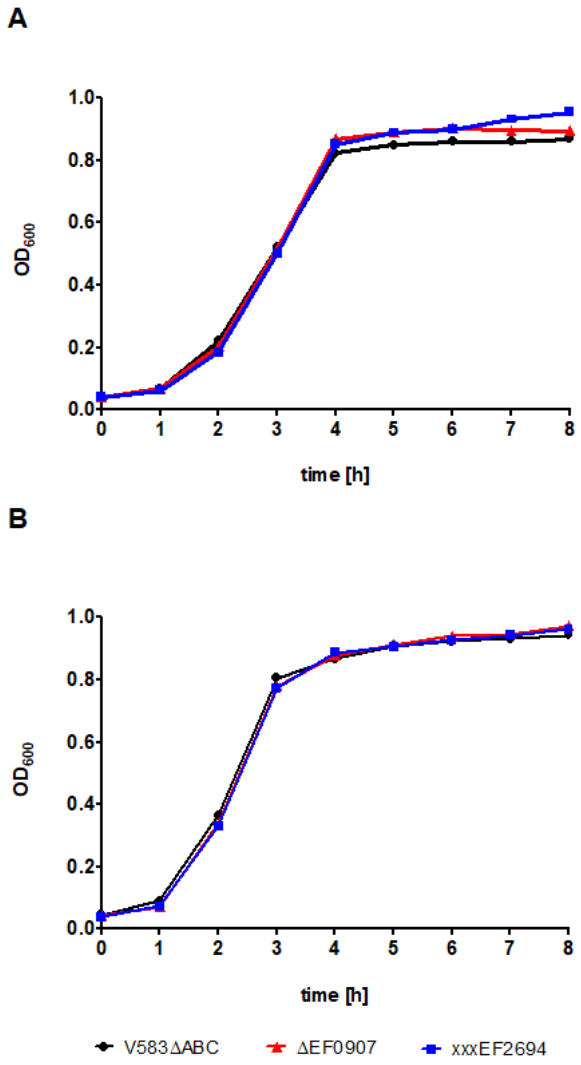

Figure 30: Growth curves of *E. faecalis* V583ΔABC and its mutants in BHI and TSB. Bacteria were incubated in TSB (A) or BHI (B) liquid media at 37°C, optical density was measured at 600nm after 0, 1, 2, 3, 4, 5, 6, 7, and 8h by spectrophotometry. The time points are shown in the abscissa and the measured optical density at 600nm of the bacterial cultures in the ordinate.

IV.9. Growth curves with chemically defined medium

To test whether *E. faecalis* V583ΔABC and its mutants can use AI-2 as a carbon source, growth curves in CDM were performed as described in the materials and methods section. The CDM was prepared without carbon sources to allow bacterial growth only with the addition of a defined energy source. As a carbon source either glucose (positive control) or AI-2 were added. As negative control, Milli-Q-water was used. Spectinomycin was added if needed.

Initially, different volumes of CDM were tested to find the minimum CDM volume required to allow an exact measurement of the OD (data not shown). We observed that a minimal volume of 75µL is required to allow an exact measurement of the optical density.

To further guarantee the same concentration of AI-2 as glucose in CDM, the minimum glucose concentration required to allow an appropriated growth was determined (see Figure 31). Therefore, the wildtype V583ΔABC was cultured in CDM supplemented with different concentrations of glucose (see Figure 31, grey lines with open circles). As shown in figure 31, CDM enriched with equal or lower than 0.07% cannot reach a maximum optical density of at least 0.1, leading to the assumption that growth kinetics in CDM should be studied with glucose equal or more than 0.08%. Therefore, the following experiments were performed with a final glucose concentration of 0.08%.

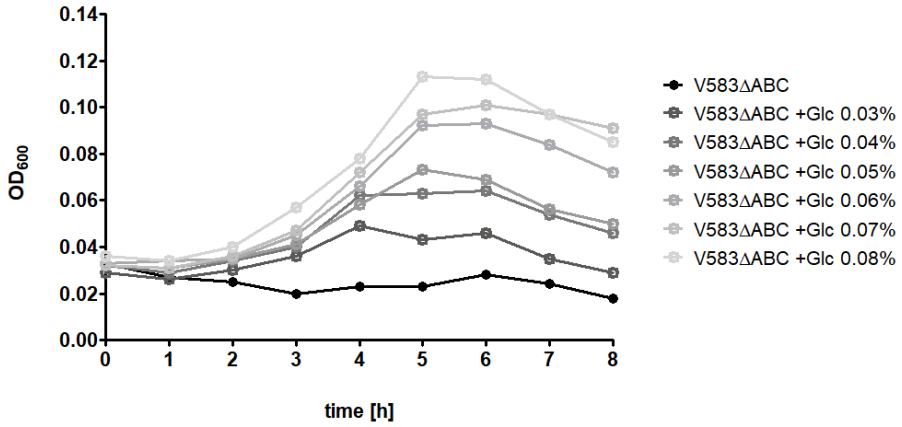

Figure 31: Growth curves of *E. faecalis* V583ΔABC in CDM with different glucose concentrations. Bacteria were incubated in 75µL CDM supplemented with glucose in a final concentration of 0.03–0.08% at 37°C. Optical density was measured in 8.5mm UV cuvettes (Sarstedt) at 600nm after 0, 1, 2, 3, 4, 5, 6, 7, and 8h by spectrophotometry using GENESYS^{TM}20 Vis-Spectrophotometer. The time points are shown in the abscissa and the measured optical density at 600nm of bacterial culture in the ordinate.

To finally test, whether *E. faecalis* can use AI-2 as a carbon source, the derivatives V583ΔABC+pEU327, ΔEF0907+pEU327, and ΔEF0907+pEU327::EF0907 were inoculated at a starting OD_{600} of 0.05 in CDM supplemented with either AI-2 (0,52g/ml; OMM scientific; final concentration of 0.08%) (see Figure 32, dotted lines with half open symbols) or with Milli-Q-Water used as negative control (lines with closed symbols) or with 0.2% glucose (final concentration of 0.08%) used as positive control (lines with open symbols). As seen in figure 32, after 8 hours of incubation at 37°C none of the tested strains could use AI-2 as carbon source. When AI-2 was used, bacterial growth was inhibited the same as with the negative control. Also seen in figure 32, the optical density of bacteria harboring a spectinomycin resistant gene is not negatively influenced by spectinomycin.

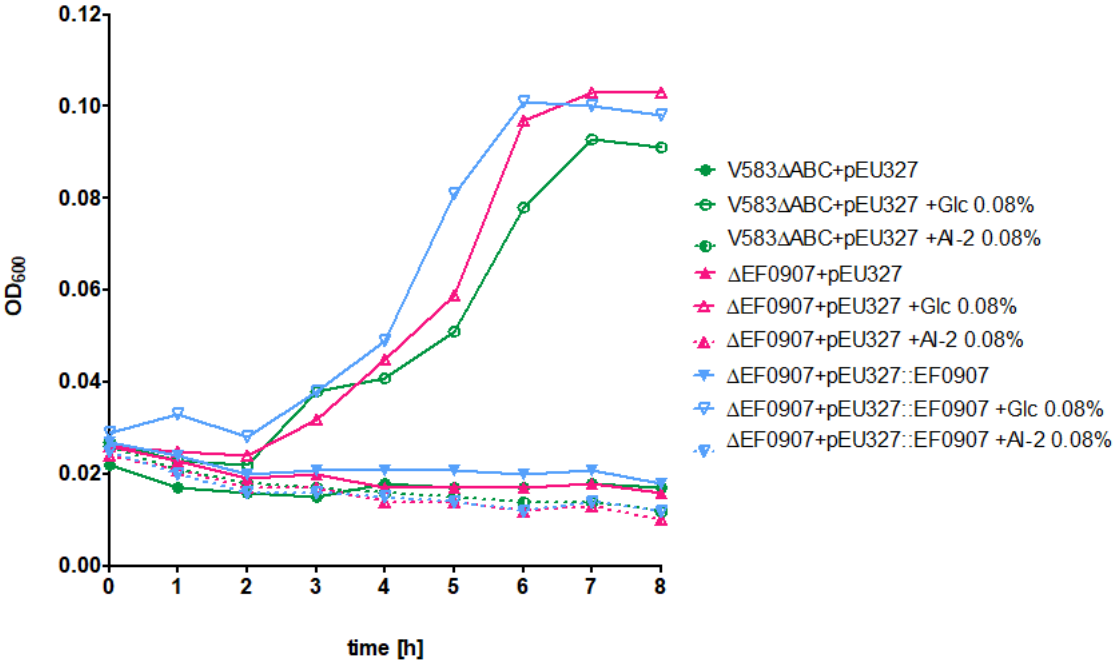

Figure 32: **Growth curves of E. faecalis V583ΔABC+pEU327 and its derivates in CDM using different carbon sources.** Bacteria were incubated in 75µL CDM at 37°C, optical density was measured in 8.5mm UV cuvettes at 600nm after 0, 1, 2, 3, 4, 5, 6, 7, and 8h by spectrophotometry using GENESYSTM20 Vis-Spectrophotometer. As blanc either CDM supplemented with spectinomycin 100µg/mL and AI-2 (Omm scientific) at a final concentration of 0.08% or CDM supplemented with spectinomycin 100µg/mL and glucose at a final concentration of 0.08% or CDM supplemented with spectinomycin 100µg/mL and Milli-Q-Water, were used. The time points are shown in the abscissa and the measured OD of bacterial culture in the ordinate.

IV.10. Isothermal titration calorimetry with rEF0907

To study the role of the *ef0907* gene as a putative binding protein in the AI-2-mediated QS system, ITC measurements were performed using MicroCal™ ITC200 microcalorimeter (Malvern) as described in the materials and methods section.

AI-2 (OMM scientific) at 500µM was injected into 50µM of rEF0907 protein. Measurements were made at 25°C, with a reference power of 10µcal/s, an initial delay of 1200s, an injection every 3min, and a syringe speed of 750rpm. Measurements were evaluated using MicroCal™ ITC200 analysis software. Binding curve shown is representative of one run.

As seen in figure 33 panel A, the binding was detected as temperature difference between sample and reference cell which occur when binding heat is released. Technically, the power (µcal/sec) needed to restore isothermal conditions between the cells was measured and the raw data were integrated over the time (min). Since the peaks in the raw thermogram were negative, we assumed that binding between rEF0907 protein and AI-2

ligand lets to an exothermic reaction. The saturation of rEF0907 protein with AI-2 can be observed as a decreasing in peak size.

As seen in figure 33 panel B, raw data were presented in a Wiseman plot using the Microcal™ ITC200 analysis software: The individual injection heat (kcal mol^{-1} of injectant) was plotted against the molar ratio of the AI-2 and the rEF0907 protein, creating a hyperbola. The resulting binding isotherm was fitted to a one-site binding model to yield the equilibrium association constant (*K*), the reaction stoichiometry (*N*) and the enthalpy (Δ*H*). Subsequently, the entropy (*ΔS*) was calculated [141].

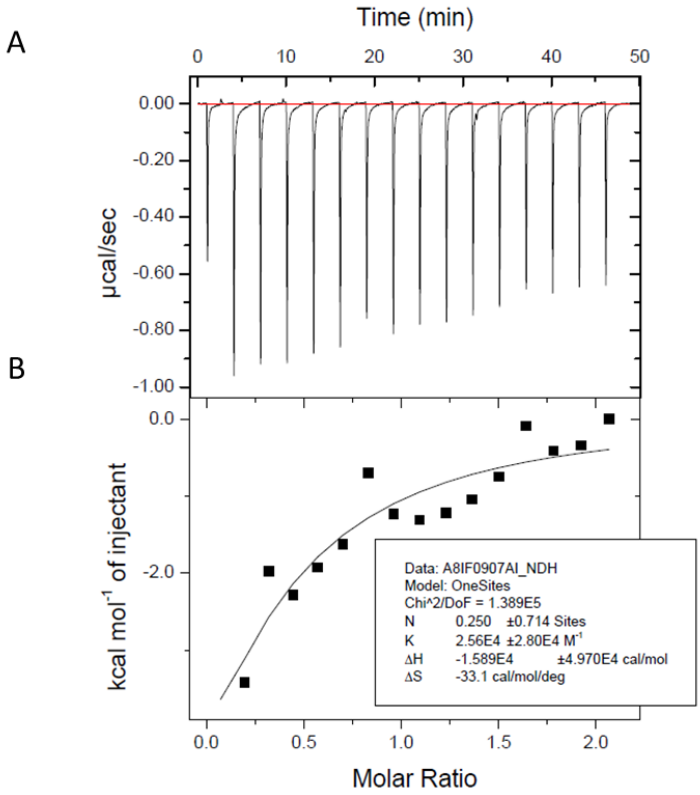

Figure 33: Binding between the rEF0907 protein and AI-2 ligand measured by ITC. [A] Raw thermogram: Temperature differences between the sample and reference cell converted to power (peaks). Baseline (red line); power in µcal/s (ordinate); time in minutes (abscissa). [B] Binding isotherm from the integrated thermogram: The resulting isotherm is fitted to a one-site binding model (black curve) to generate the equilibrium association constant (*K*), the reaction stoichiometry (*N*) and the enthalpy (Δ*H*). From this data is then calculated the entropy (*ΔS*). Measurements were evaluated by MicroCal™ ITC200 analysis software. Individual injection heat in kcal/mol (ordinate); amount of titrated AI-2 to rEF0907 protein in the sample cell as molar ratio (abscissa); injections (black squares).

According to the *K* value ($2.56x10^4 \pm 2.80x10^4$ M^{-1}) which has a concentration of 10^4 the strength of the interaction between rEF0907 and AI-2 would be evaluated as moderate Unfavorable, low *N* value (0.25 ± 0.71 Sites) was determined since we assumed to have a 1:1 binding with an expected *N* value closed to 1. As *N* is strongly correlated with *ΔH*,

the interpretation of *ΔH* is more difficult. Nonetheless negative value in *ΔH* ($-1.59x10^6 \pm 4.97x10^6$cal/mol) suggests that the binding is mainly based on noncovalent interactions (ionic interactions, hydrogen bonds or Van der Waal's Forces) [142]. The negative value in *ΔH* is accompanied by negative value in *ΔS* (-33.1cal/mol/deg) supporting that the binding is mainly based on ionic interactions, H-Bonds or Van der Waal's Forces [143].

IV.11. Fluorescence resonance energy transfer-based AI-2 assay

To confirm our findings, external AI-2 was measured in filter-sterilized supernatants of *E. faecalis* V583ΔABC and its mutants using a LuxP-FRET-based reporter assay as described in the materials and methods section.

Through the dose-dependent FRET signal released after AI-2 binding to the chimeric CFP-LuxP-YFP protein, a FRET ratio (430nm/480nm) was determined. AI-2 samples of known concentration were used to establish a calibration curve (y= -0.054ln(x)+1.4888; and coefficient of the determination [R^2] of 0.99) which was used, in combination with the FRET ratio, to determine the AI-2 concentration of the bacterial supernatants.

As seen in figure 34, the external AI-2 concentrations of wildtype *E. faecalis* V583ΔABC and its mutants showed a growth phase dependent increase. Actually, the AI-2 accumulation of wildtype and ΔEF0907 mutant increased from the mid-exponential phase reaching maximum levels at stationary phase (not significant). While the wildtype reached only a maximum AI-2 concentration of 19.3µM, the ΔEF0907 mutant reached 34.4µM. While the wildtype reached its maximum AI-2 concentration already at 7h, the AI-2 concentration of the ΔEF0907 mutant was still increasing after 8h. After 8h of growing, compared to the wildtype, the maximal external AI-2 concentration of ΔEF0907 mutant was maximum 1.9-fold higher, indicating that EF0907 gene is involved in the internalization of AI-2. As negative control, supernatants of the xxxEF2694 mutant were used, since mutant is no longer able to produce AI-2.

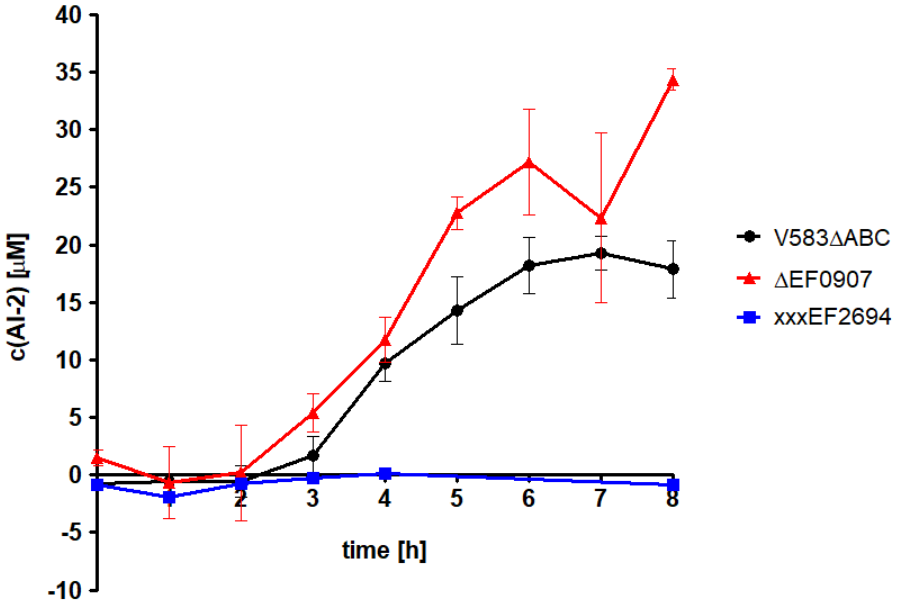

Figure 34: Growth dependent alterations of the external concentration of AI-2 in wildtype *E. faecalis* V583ΔABC and its mutants ΔEF0907 and xxxEF2694 were determined by FRET-based AI-2 assay. Growth dependent alterations of the external concentration of AI-2 were determined over 8h. The time points are shown in the abscissa and the measured AI-2 concentration in the ordinate. Experiments were performed in duplicate. Statistical analysis was done by the nonparametric Mann-Whitney U-Test. Symbols represent the mean of at least two independent results. Error bars represent standard error of the mean.

IV.12. Microtiter plate biofilm assay

In order to assess the competence of wildtype *E. faecalis* V583ΔABC and its mutants ΔEF0907 and xxxEF2694 to produce biofilm on a polystyrene surface, a wet microtiter plate biofilm assay was performed in the presence or absence of AI-2 as described in the materials and methods section.

Absorbance of bacterial culture and crystal violate stained eluted biofilm was measured at 595nm in a polystyrene microtiter plate in an ELISA reader. As negative control TSB supplemented with glucose 1% or AI-2 was used.

As seen in figure 35, statistical significant differences in biofilm formation between the wildtype and the ΔEF0907 mutant were observed after 18h of incubation. The ΔEF0907 mutant produced significantly more biofilm than the wildtype ($p<0.05$), confirming results of previous experiments and indicating that deletion of *ef0907* gene leads to a disturbance in the AI-2 controlled QS system. As well as xxxEF2694 mutant showed statistical significant differences in biofilm formation compared to the wildtype ($p<0.05$). Differences observed between wildtype and mutants cannot be ascribed to variations in

growth as similar growing behavior was observed in growth curves (see Figure 30). To study the effect of AI-2 on biofilm formation, 100µM AI-2 was added in the start of biofilms grown over 18h. After 18h of incubation, no differences in biofilm formation when absented or present 100µM AI-2 were determined. However, a decrease in biofilm was observed when biofilm was grown for 24h with higher AI-2 concentrations (see Figure 36).

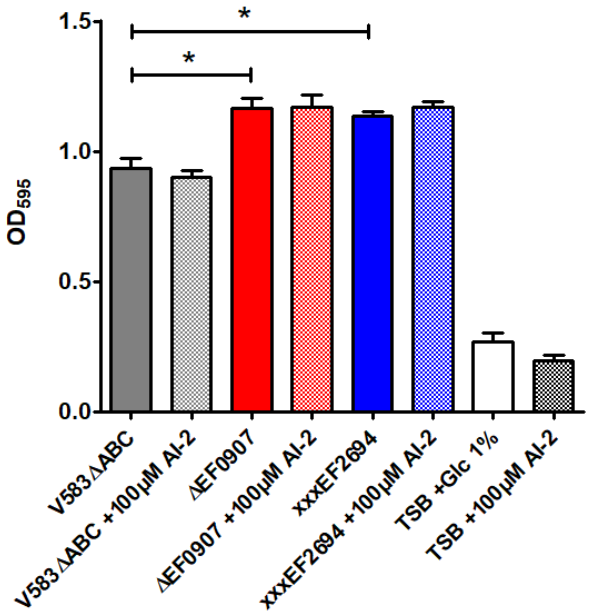

Figure 35: Microtiter plate biofilm assay for the *E. faecalis* V583ΔABC and its mutants with 100µM of AI-2. Crystal violet stained and eluted biofilm was measured in the absence or presence of 100µM AI-2 after 18h of incubation at 595nm. Wet biofilm measurement of wildtype *E. faecalis* V583ΔABC in the absence (grey bar) or presence of 100µM AI-2 (bar with grey dotes). Wet biofilm measurement of *E. faecalis* ΔEF0907 mutant in the absence (red bar) or presence of 100µM AI-2 (bar with red dotes). Wet biofilm measurement of *E. faecalis* xxxEF2694 mutant in the absence (blue bar) or presence of 100µM AI-2 (bar with blue dotes). As negative control TSB supplemented with glucose (white bar) or with AI-2 (bar with black dotes) was used. The used strains are shown in the abscissa and the biofilm optical density at 595nm in the ordinate. Statistical analysis was done by nonparametric Mann-Whitney U-Test. * indicates $p<0.05$. Bars represent the mean of at least four independent results. Error bars represent standard error of the mean.

As seen in figure 36, differences in biofilm formation between the wildtype V583ΔABC and the mutants ΔEF0907 and xxxEF2694 were observed also after 24h of incubation, even if the differences were no longer significant as reported before for an incubation period of 18h (see Figure 35). However, for all tested strains was observed a decrease in biofilm formation when high concentrations of AI-2 were added in the start of the biofilm.

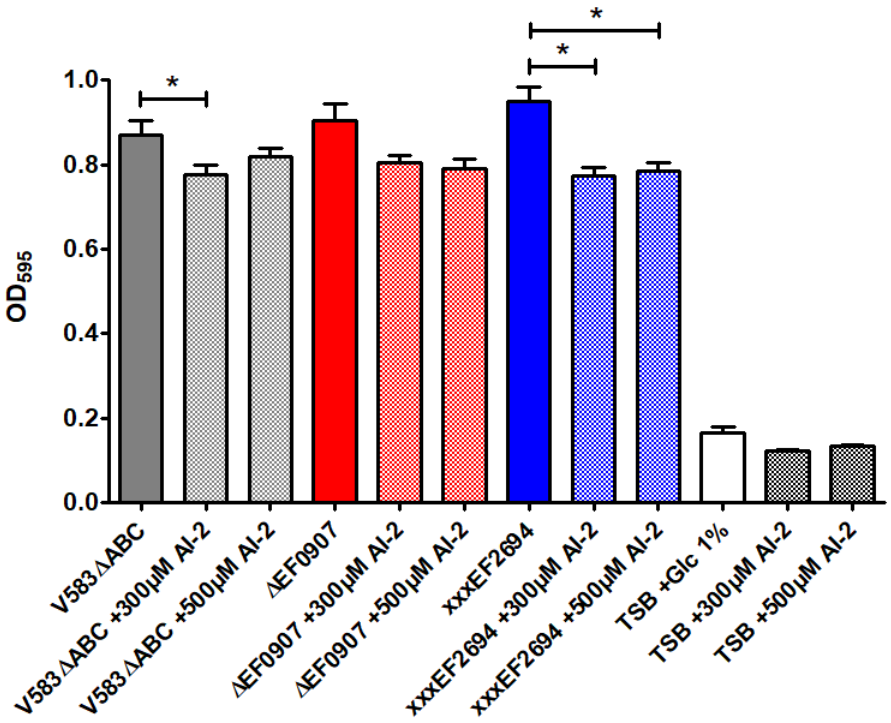

Figure 36: Microtiter plate biofilm assay for the *E. faecalis* V583ΔABC and its mutants with high AI-2 concentrations. Crystal violet stained and eluted biofilm was measured in the absence or presence of 300µM or 500µM AI-2 after 24h of incubation at 595nm. Wet biofilm measurement of wildtype *E. faecalis* V583ΔABC in the absence (grey bar) or presence of AI-2 (bars with grey dotes). Wet biofilm measurement of *E. faecalis* ΔEF0907 mutant in the absence (red bar) or presence of AI-2 (bars with red dotes). Wet biofilm measurement of *E. faecalis* xxxEF2694 mutant in the absence (blue bar) or presence of AI-2 (bars with blue dotes). As negative control TSB supplemented with glucose (white bar) or with AI-2 (white bars with black patterns) was used. The used strains are shown in the abscissa and the optical density at 595nm in the ordinate. Statistical analysis was done by the nonparametric Mann-Whitney U-Test. * indicates $p<0.05$. Bars represent the mean of at least four independent results. Error bars represent standard error of the mean.

IV.13. Opsonophagocytic killing assay

To assess the effect of the deletion in *ef0907* gene on resistance to opsonophagocytosis and to detect putative changes in the bacterial surface of the *E. faecalis* ΔEF0907 mutant and *E. faecalis* xxxEF2694 mutant, an OPA was performed as described in the materials and methods section.

Percent killing (%Killing) (see Figure 37) was calculated by comparing the colony counts at 90min (t90) of a control not containing PMNs (PMNneg) to the colony counts of a tube that contained all four components of the assay using the following formula: {[(mean cfu PMNneg at t90) - (mean cfu at t90)]/(mean cfu PMNneg at t90)}×100 [137]. Rabbit antibodies raised against the lipoteichoic acid from *E. faecalis* 12030 (α-LTA), the whole

of *E. faecalis* V583 bacterium (α-V583) and against whole-bacterium of *E. faecalis* Type 2 (α-T2) were used at 1:100 dilution.

As shown in figure 37, no significant differences between the wildtype and the ΔEF0907 mutant on resistance to opsonophagocytosis were observed, indicating that the knockout of gene *ef0907* does not lead to significant changes to bacterial surface structures involved in the protective immune response. Interestingly statistical significant ($p<0.05$) differences in %Killing for α-LTA were observed between wildtype and xxxEF2694 mutant.

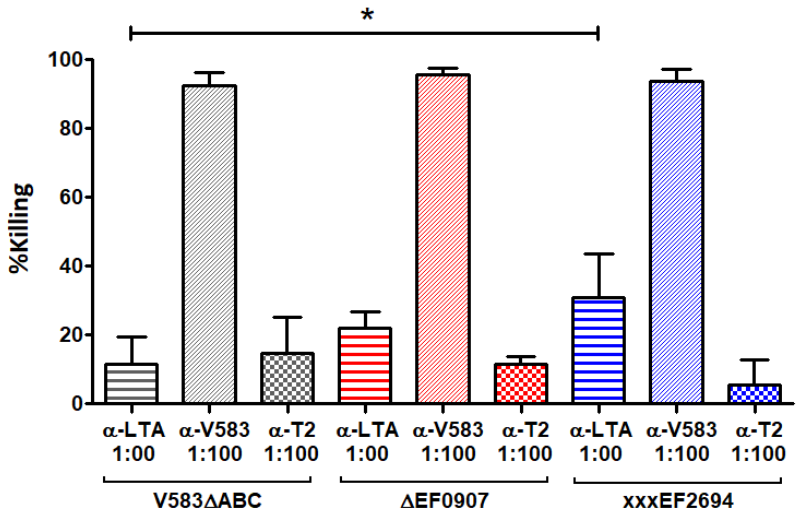

Figure 37: Opsonophagocytic killing assay for the *E. faecalis* V583ΔABC and its mutants. Rabbit sera raised against LTA (α-LTA; horizontal stripes), *E. faecalis* V583 (α-V583; diagonal stripes), and *E. faecalis* Type 2 (α-T2; chess pattern) were directed tested in OPA against different *E. faecalis* strains at 1:100 dilution. Opsonic killing of the *E. faecalis* V583 (bars with grey patterns), *E. faecalis* ΔEF0907 (bars with red patterns), and *E. faecalis* xxxEF2694 (bars with blue patterns). For statistical analysis of the bacterial counts was used the Kruskal-Wallis nonparametric analysis of variance (multigroup comparison) with the Dunn procedure (pairwise comparisons). The dilutions of the sera used in the OPA are shown in the abscissa and the opsonic killing in the ordinate. Bars represent the mean of at least four independent results. * indicate $p<0.05$. Error bars represent standard error of the mean.

V. Discussion

The thesis was focused on the bacterial intra- and interspecies communication system, called Quorum Sensing (QS) [61], and its impact on biofilm formation. In particular, the autoinducer-2 (AI-2) transport in the LuxS/AI-2-type QS system of *E. faecalis* was investigated.

QS was first described by Fuqua et al. in 1994 [1]. Bacteria use QS to coordinate collectives behaviors like biofilm formation depending on cell population density [58,61,62,99]. Therefore, they produce and release low-molecular-weight signaling molecules, called autoinducers [60,61]. By sensing the external autoinducer concentration, information about the number of surrounding bacteria can be shared and the gene expression can be adjusted accordingly [60,61]. From the three different QS systems described so far, only the LuxS/AI-2-type QS system is present in both, Gram-negative and Gram-positive bacteria. The central signaling molecule in the LuxS/AI-2-type QS system is the AI-2 [58]. Remarkably, AI-2 rearranges in solution into different isomers, enabling the bacteria to respond not only to their own AI-2 but also to AI-2 produced by other bacterial species [67]. That makes AI-2 unique among QS signal molecules and universal at the same time [29,59,63,69]. So far, two classes of AI-2 receptors have been characterized: the LuxP-type receptors [73], found only in the *Vibrionaceae* [58], and the LsrB-type receptors [72], best characterized in *S. enterica* ser. typhimurium, *E. coli,* and *Sinorhizobium meliloti* [83,140,144]. Also *E. faecalis*, known as beneficial commensal of the gastrointestinal tract [1] that can cause life-threatening opportunistic and nosocomial infections [29], synthesizes and responds to AI-2 derivates [30, 52,83]. Moreover, it has been shown that AI-2 affects *E. faecalis* biofilm formation [30,103]. However, no genes encoding for the AI-2 transport system in *E. faecalis* have been identified so far.

To identify the AI-2 binding protein in the LuxS/AI-2-type QS system of *E. faecalis* we used the model strain *E. faecalis* V583ΔABC that is a plasmid-free derivate from the first clinical isolate of an *E. faecalis* species with vancomycin resistance in the US [5,39]. In order to determine candidate genes that might encode for the AI-2 binding protein in *E. faecalis* we studied the results of previous unpublished *in silico* analyses of our research group on *E. faecalis* V583ΔABC which revealed genes significantly upregulated 6h after incubation with 100µM AI-2. Among those genes we detected the gene *ef0907* that probably encodes for the substrate binding protein of an ABC transporter. Since we knew from our literature research that LsrB-type receptors also belong to the large family of ABC transporter proteins [140] and that these receptors bind to the boron-free derivate of

AI-2 [74] to which it has already been demonstrated that *E. faecalis* responds [30,52,83], we hypothesized that the *ef0907* gene might encode for the AI-2 binding protein in *E. faecalis*.

In order to obtain more evidence on whether EF0907 protein is able to bind AI-2 ligand we used bioinformatical analysis to find homologies between the amino acid sequence of the protein encoded by the *ef0907* gene (EF0907) of *E. faecalis* V583 with those of the first described LsrB receptor found in *S. enterica* ser. *typhimurium* [72] and the first described LsrB-like receptor found in *C. saccharobutylicum* [125]. Their sequence identity was evaluated according to Peirera et al. (2009) [74] and consequently classified as low, which means EF0907 does not have a typical amino acid sequence for a LsrB- or LsrB-like receptor. However, since sequence identity was over 36%, binding between EF0907 and AI-2 was assumed not to be unlikely [74]. Noteworthy, the Gram-negative Helicobacter pylori can sense AI-2 via the hydrochloric acid chemoreceptor TlpB, although that receptor shares no sequence identity with the already established AI-2 receptors [145].
When we compared the six conserved amino acid residues described for the AI-2 binding site of different LsrB-type receptors [58] we identified that even though they were not identical to those of EF0907 protein similar amino acids could be found in the immediate vicinity. For this reason, we hypothesized that EF0907 protein might not belong to the family of LsrB-type, but to the family of LsrB-like receptors for which is attributed a greater genomic diversity within the AI-2 binding site [125], or even to a novel as yet undiscovered family of AI-2 receptors. For instance, the latter is not unlikely, as new ribose import binding proteins (RbsB) have been recently described to bind AI-2 in *Haemophilus influenzae* and *Aggregatibacter actinomycetemcomitans* which belongs neither to the LuxP-type nor to the LsrB-type nor to the LsrB-like receptors [146,147]. Furthermore, Zhang et al. (2020) claimed to have identified a novel type of AI-2 receptor in *Pseudomonas aeruginosa* which binds AI-2 through a periplasmic double calcium channel and chemotaxis receptor (dCACHE) domain [148]. Meanwhile, dCACHE domain receptors capable to bind AI-2 have been already described for *Rhodopseudomonas palustris* and *Bacillus subtilis* [148].

One of our main concerns was to verify that the EF0907 protein is able to bind AI-2. As verified by SDS-PAGE, we expressed and purified the 60,88kDa EF0907 protein using the overexpression vector pQE30 in the *E. coli* BL21ΔluxS (that is unable to produce AI-2) and a cobalt affinity resin. Subsequently, binding reaction between recombinant protein rEF0907 and AI-2 was tested using isothermal titration calorimetry (ITC). This is

a simple and powerful tool for studying the thermodynamics of protein-ligand interactions in a single experiment [149,150]. Compared to indirect binding assays, ITCs main advantage is the direct and label-free measurement of the binding interaction [150]. Using ITC, we determine that the binding between rEF0907 and AI-2 occurred at micromolar concentrations (*Kd* 40µM). In comparison, the dissociation constant (*Kd*) recently described for the LsrB-like receptor found in *C. saccharobutylicum* differs by a factor of 50 (K*d* 0.8 µM) [125]. Nonetheless, all the other parameters determined by the ITC indicated that EF0907 interacts with AI-2. For instance, the strength of the interaction between rEF0907 and AI-2 was evaluated as moderate (K 10^4 M^{-1}), consisting with the expected association constant for high-affinity substrate-binding proteins (K 0.1–1µM) [151]. Likewise, the fact that the interaction between EF0907 and AI-2 was classified as exothermic which corresponds to what have been described for AI-2 receptors of other bacterial species [125,152]. Furthermore, the observed decrease in peak size in the raw thermogram indicate saturation of rEF0907 [142] which can also be seen as a confirmation of a binding between EF0907 and AI-2. Curiously though, differences in peak size in the raw diagram were relatively small and the errors in the fitting in the 1:1 binding model were relatively large. Probably this could be explained by a mismatch in the concentration of the binding partners [153], especially then when the concentration of the ligand or the protein is to low [153]. Since AI-2 is an inherently unstable molecule that easily degrades [30,58,69] we cannot completely exclude the possibility that too low AI-2 concentrations were used, albeit performing the assay with the recommended 10 times higher ligand concentration than protein concentration (500µM AI-2 was injected into 50µM of rEF0907). A further indication that the ligand concentration may have been too low is the small initial integrated heats (<10µcal/sec) [154], the hyperbolic rather than a sigmoidal binding curve [155], the low value in N and the low values in ΔH (see Figure 34) [153]. Nevertheless, a negative value in ΔH suggests that binding between rEF0907 and AI-2 is mainly based on non-covalent interactions such as ionic interactions, hydrogen bonds or Van der Waal's Forces [142], again supported by negative value in ΔS [143]. This corresponds to what we would expect for a protein-small molecule interaction wherein reversible non-covalent bonds are most frequently observed [156]. While interpreting ITC data it is important to note that the measured overall heat includes not only the heat released or absorbed during binding reaction but also the so called heat of dilution released during mixing the binding partners and their respective buffers in the sample cell [142]. Therefore it is crucial that the two buffers are as similar as possible, favorable identical, otherwise, the heat of interaction will be overwhelmed by the heat of dilution [153,157]. In order to avoid

such a buffer mismatch, it is best to dialyze protein and the ligand against the same dialysis buffer [149]. Unfortunately, it was not possible to dialyze AI-2 since as already mentioned AI-2 is a really unstable small molecule and would probably degrade during the dialysis process [30,58,69]. Instead, we prepared rEF0907 in the same buffer as AI-2 but even this was difficult since the AI-2 available for purchase comes dissolved in an acidic solution with now completely know composition. In fact both companies were we purchase the AI-2 from where unable to provide us with the exact buffer composition for the AI-2 solution. For all these reasons, a possible buffer mismatch must be considered as a contributory cause for our ambiguous ITC results. Due to all the previously mentioned buffer interferences, it was very difficult to produce reliable results using ITC. Therefore, we could not draw final conclusions about the binding between rEF0907 and AI-2, even if results obtained would suggest that rEF0907 moderately binds the AI-2.

To further investigate and characterize the role of *ef0907* gene in the LuxS/AI-2-type QS system of *E. faecalis* V583ΔABC we applied a combination of different genetic, biochemical and biophysical strategies. As shown by PCR, an 81.3% proportion of the *ef0907* gene in *E. faecalis* V583ΔABC was deleted in-frame using site-directed mutagenesis obtaining the *E. faecalis* ΔEF0907 mutant. Additionally, also using site-directed mutagenesis, we constructed a mutant unable to synthesize AI-2 by inserting three single point mutations into the *ef2694* gene as shown by sequencing analysis. The obtained *E. faecalis* xxxEF2694 mutant served primarily as a negative control for FRET-based AI-2 assay. Furthermore, we also included the xxxEF2694 mutant in additional experiments to further investigate the phenotype of the *ef2694* gene in *E. faecalis* V583ΔABC. Moreover, as shown by PCR, we constructed plasmid-based complementations of the ΔEF0907 using the pEU327 vector to partially restore the phenotype of the deleted *ef0907* gene in *E. faecalis* V583ΔABC. By also transforming the empty pEU327 vector into the wildtype and into the ΔEF0907 mutant, we excluded that the pEU327 or the spectinomycin, which must be used to maintain the presence of the plasmid, has no effect on the phenotype of the plasmid-based complementation.

In order to verify ITC results, we tried to demonstrate that the ΔEF0907 mutant is no longer able to internalize AI-2. To our knowledge, this is the first study of the AI-2 activity of an ΔEF0907 mutant. Using FRET-based AI-2 assay, the AI-2 concentration in filtered-sterile supernatants of wildtype *E. faecalis* V583ΔABC, and mutants xxxEF2694 and ΔEF0907 was quantified. As expected, no AI-2 was measured in the supernatants of xxxEF2694 mutant which was supposed to be unable to synthesize AI-2 [158]. Whereas the

AI-2 activity of the wildtype showed a growth phase dependent increase, similar to the results previously reported for *E. faecalis* V583 by Shao et al. [30]. Also AI-2 activity of ΔEF0907 mutant was growth phase dependent, whereby the ΔEF0907 mutant showed a 1.9-fold higher maximum AI-2 concentration compared to the wildtype. The modest difference, which has not been found to be statistically significant, gives rise to the idea of whether *E. faecalis* may have a second AI-2 transport system, as has been already proposed for *S. enterica* ser. typhimurium [146] and *H. influenzae* [147]. As previously mentioned for the ITC experiment also in the FRET-based AI-2 assay one of the major problems was the instability of the AI-2 [30,69], which requires rapid processing of the samples. In addition, the detection range of the FRET-based AI-2 assay varies between different protein samples, which may lead to only small differences in FRET signal [159]. Nevertheless, our results reinforce the assumption that *ef0907* gene is involved in the internalization of AI-2.

Several *E. faecalis* strains are classified as strong biofilm producer including *E. faecalis* V583 [160]. The regulatory role of QS in bacterial biofilm formation is well established [63,161,162]. As well it is known that AI-2 affects enterococcal biofilm formation [2]. Therefore, we decided to investigate how the absence of the EF0907 protein affects the biofilm in *E. faecalis*. To our knowledge this is the first report that investigates the specific role of the *ef0907* gene in biofilm formation. In recent years, several techniques have been tested to quantify biofilm formation (reviewed in [[163]]). The microtiter plate biofilm assay is the most common method, even though there exist a multitude of variants [163]. In the microtiter plate biofilm assay the biofilm can either be quantified when adherend to the bottom of the wells (dry assay) or after being dissolved by ethanol (wet assay) [163]. Clear limitations for both assays, dry and wet, result from the fact that the results are person- or laboratory-dependent [163]. A limitation that only concerns the dry biofilm assay is the possibly incorrect measurement of loosely attached and broken off or otherwise destroyed biofilm. Therefore, we decided to assess the competence of the wildtype *E. faecalis* V583ΔABC and its mutants ΔEF0907 and xxxEF2694 to produce biofilm with the wet microtiter plate biofilm assay as described by Paganelli et al. [136]. Indeed, after 18h of incubation, the ΔEF0907 mutant produced statistically significant more biofilm than the wildtype ($p<0.05$). This suggests that deletion of *ef0907* gene leads to a disturbance in the AI-2 controlled QS system. The same could be observed for the xxxEF2694 mutant, which also produced statistically significant more biofilm compared to the wildtype ($p<0.05$). Consisting with the results previously reported for *luxS* deficient *E. faecalis* mutants,

which are also no longer able to produce AI-2 and showed an increased biofilm formation [30,103] . Nevertheless, Yang et al. observed reduced biofilm formation for *luxS* deficient *E. faecalis* mutants, which may be related to methodological differences between the biofilm assays [55]. Based on the previous studies from our research group reporting that the external supplementation of high concentration of AI-2 mediates the dispersal of biofilm [52], we quantified biofilm of the wildtype *E. faecalis* V583ΔABC and its mutants ΔEF0907 and xxxEF2694 in the presence of AI-2. While Rossmann et al. (2015) [52] observed a dispersion of the biofilm already with 100µM AI-2, we measured a decrease in biofilm formation starting at 300µM. Such differences in the required AI-2 concentration might be explained by the fact that different versions of the microtiter plate biofilm assay were used, while we performed a wet biofilm assay, Rossmann et al. (2015) performed a dry one [52]. Also for other bacteria species, such as *B. cereus*, there are reports that the exogenous supplementation of AI-2 induces the spread of cells from already preformed biofilm [101]. Unexpectedly, the external supplementation of AI-2 led to a decrease in biofilm formation not only in the wildtype and the xxxEF2694 mutant, but also in the ΔEF0907 mutant, which was supposed to be unable to detect external AI-2 concentration. Obviously, we were wondering how the ΔEF0907 mutant was still able to respond to AI-2. Considering the results from the previous experiments, it might be possible that the *ef0907* gene encodes for the AI-2 binding protein which is involved in the internalization of AI-2, but that the sensing of the external AI-2 concentration occurs independently from EF0907 protein. Furthermore, we can imagine that *E. faecalis* possess another AI-2-mediated QS system besides the LuxS/AI-2 QS system, which can also bind and internalize AI-2. Indications for this we derive from the reports about other bacterial species for which more than one Al-2-mediated QS system has already been described [146,147]. And even some bacteria for which only one AI-2-mediated QS system has been described so far, continue to respond to AI-2 although their AI-2 receptors have been knocked out [58]. However, the exact mechanisms have not yet been elucidated.

In Gram-positive bacteria lipoproteins play an important role in immune modulation, pathogenicity and virulence [164,165]. Recently, it could be demonstrated that some *E. faecalis* mutants of surface-associated lipoproteins show differences in the resistance of opsonophagocytosis [89,166]. Since EF0907 is known to be a surface-located lipoprotein [5], the ΔEF0907 mutant could have shown alterations in the resistance of opsonophagocytosis. To our knowledge, this is the first report of the resistance to opsonophagocytosis of ΔEF0907 and xxxEF2694 *E. faecalis* V583ΔABC mutants. OPA

is a reliable tool for testing opsonic antibodies against potential vaccine targets [167] calculating the opsonophagocytic-mediated killing by comparing the number of bacterial units grown on agar plates co-cultured with complement, opsonic antibodies, and phagocytic cells with those of the control [137,168]. Inversely, changes in resistance to opsonophagocytosis may give indications of putative changes in the bacterial surface. Using OPA, the opsonic killing activity (%Killing) of antibodies raised against wildtype *E. faecalis* V583ΔABC and its mutants ΔEF0907 and xxxEF2694 was determined. Even *ef0907* gene encodes a surface-located lipoprotein [5], we could not observe significant differences between the wildtype and the ΔEF0907 mutant in resistance of opsonophagocytosis, suggesting that the knockout of *ef0907* gene does not lead to significant changes to bacterial surface structures. Interestingly, resistance to opsonophagocytosis significantly increased for α-LTA comparing the wildtype with the xxxEF2694 mutant. As *ef2694* gene is encoding for an cytoplasmic located nucleosidase (Pfs) [30,52], we didn't expect to see such differences. However, the interpretation of these results is complicated by the double role of Pfs as enzyme of AI-2 synthesis as well as of the activated methyl cycle. Possibly, an intervention in such a central metabolic pathway as the activated methyl cycle might lead to restrictions of other pathways resulting in changes of the bacterial surface structure. Nevertheless, more experiments are needed to confirm these findings.

V.1. Conclusion and perspectives

Overall, we have demonstrated here that i. according to bioinformatic analysis the probability of binding between EF0907 protein and AI-2 ligand is not unlikely, ii. deletion of *ef0907* gene does not affect bacterial growth behavior, iii. *E. faecalis* cannot use AI-2 as a carbon source, iv. the EF0907 protein seems to interact with AI-2 at a micromolar concentration via non-covalent bonds, v. deletion of *ef0907* gene leads to an accumulation of external AI-2, vi. deletion of *ef0907* gene leads to an increased biofilm formation, vii. The ΔE0907 mutant still responds to AI-2 at high concentrations by reducing its biofilm formation, viii. deletion of *ef0907* gene does not lead to obvious changes in bacterial surface antigens involved in a protective immune response.

In summary, we can conclude that *ef0907* gene is probably involved in the AI-2 controlled QS system. Moreover, the *ef0907* gene seems to encode an AI-2 binding protein in an ABC transport system of *E faecalis*. However, we cannot clearly categorize the EF0907 protein into one of the two known classes of AI-2 receptors (LuxP or LsrB-typ). Most likely, EF0907 can be assigned to the class of LsrB-like receptor as first described in the Gram-positive *C. saccharobutylicum* [125]. Besides, it may also be conceivable that the EF0907 protein belongs to a novel yet undescribed type of AI-2 receptors. The fact that the ΔEF0907 mutant can still react to externally supplemented AI-2 could be explained by two possible causes: The *ef0907* gene encodes for the AI-2 binding protein but not for the protein that senses AI-2, whereby *E. faecalis* would be able to detect the AI-2 concentration in the environment without internalization. Another possibility is that *E. faecalis* possesses more than one AI-2-mediated QS system, as it has already been described for other bacterial species [146,147], that would further ensure AI-2 detection.

In the future, it would be advisable to repeat the ITC experiment with an decreased concentration of rEF0907 or an increased concentration of AI-2 to overcome the putative mismatch in the concentration of the binding partners in order to achieve a better fitting of the binding curve [153]. In addition, it would be important to characterize the other genes involved in this ABC transport system (*ef0909-ef0912*) and the putative regulatory genes (*ef0926, ef0927*) by qRT PCR to better understand transport, sensing and regulation of AI-2 in this opportunistic pathogen. Certainly, it would also be interesting to create a double mutant in which, in addition to the *ef0907* gene, either the *ef0910*, the *ef0912*, the *ef0926* or the *ef0927* [80] are knocked out in order to see a much stronger phenotype in the FRET-based AI-2 assay or in the microtiter biofilm assay. Additionally, we could use

scanning electron microscopy to demonstrate differences in the structure of biofilms between the wildtype and the ΔEF0907 mutant.

VI. Summary

Enterococci are Gram-positive bacteria that usually live as beneficial commensals within the gastrointestinal tract of human and other higher organisms [3]. However, they can cause life-threatening opportunistic and nosocomial infections [29]. *Enterococcus faecalis* and *Enterococcus faecium* are the species with the greatest clinical relevance [32], being responsible for more than 90% of the enterococcal infections [1]. Some of them are strong biofilm producers [160], and therefore it is of great interest to understand how these pathogens regulate the process of biofilm formation. Fuqua et al. (1994) were the first to describe an intra- and interspecies communication system, called Quorum Sensing (QS), which enables bacteria to regulate collective behaviors like biofilm formation [54]. One of the central signaling molecules in the QS system, autoinducer-2 (AI-2), allows bacteria to monitor the cell population density and to adjust their gene expression accordingly [61]. It is already known that *E. faecalis* synthesizes and responds to AI-2 [30,52], and this autoinducer affects biofilm formation [30], but no genes encoding for the AI-2 transport system in *E. faecalis* have been identified so far [169]. Therefore, the aim of the present thesis was to identify the AI-2 binding protein in the LuxS/AI-2-type QS system of *E. faecalis*. Combining results from literature research and our previous unpublished RNA-seq analysis, showing genes up-regulated after incubation with AI-2, we hypothesize that the *ef0907* gene encodes for the AI-2 binding protein. To investigate the role of *ef0907* gene as AI-2 binding protein in the AI-2 QS system of *E. faecalis*, we performed bioinformatic analysis which revealed that EF0907 protein is a possible candidate for such a system. In order to experimentally verify this hypothesis, we recombinantly expressed the EF0907 protein in *E. coli*. Following, binding between recombinant protein rEF0907 and AI-2 was tested by isothermal titration calorimetry indicating a moderate exothermic interaction. To confirm our findings, we constructed an in-frame knock out of the *ef0907* gene in the *E. faecalis* V583ΔABC strain. Subsequently, we measured the concentrations of AI-2 in the supernatants of V583ΔABC and the mutants performing a fluorescence resonance energy transfer assay. We observed an accumulation of AI-2 of ΔEF0907 indicating that the *ef0907* gene is involved in the internalization of AI-2. This correlates with results in a microtiter plate biofilm assay, where an increased biofilm was detected for ΔEF0907. Surprisingly, ΔEF0907 mutant still responds to AI-2 at high concentrations by reducing its biofilm formation. Overall, the *ef0907* gene seems to encode an AI-2 binding protein in the ABC transport system of *E. faecalis*. However, the bacterium may be able to detect the AI-2 concentration in the environment without

internalization. Besides, it is conceivable that *E. faecalis* possesses more than one AI-2-mediated QS system.

VII. Zusammenfassung

Enterokokken sind grampositive Bakterien, die neben ihrer Rolle als nützliche Kommensalen des Gastrointestinaltrakts [3] auch als Verursacher lebensbedrohlicher opportunistischer und nosokomialer Infektionen bekannt sind. Zu den klinisch relevantesten Enterokokken-Spezies zählt man *Enterococcus faecalis* und *Enterococcus faecium* [32]. Zusammen sind sie für mehr als 90% der Enterokokken-assoziierten Infektionen verantwortlich [1]. Einige Enterokokken-Stämme gelten als besonders starke Biofilmproduzenten [160], weshalb es von großem Interesse ist, zu verstehen, wie diese Krankheitserreger den Prozess der Biofilmbildung regulieren. Fuqua et al. (1994) waren die Ersten, die ein bakterielles Kommunikationssystem namens Quorum Sensing (QS) beschrieben haben, welches es Bakterien ermöglicht, kollektive Verhaltensweisen wie Biofilmbildung zu koordinieren [54]. Eines der zentralen QS-Signalmoleküle stellt Autoinducer-2 (AI-2) dar. Durch die Detektion der externen AI-2-Konzentration, ist es Bakterien möglich, ihre Genexpression abhängig von der Zelldichte zu regulieren [61]. Auch für *E. faecalis* konnte eine AI-2-Synthese sowie eine AI-2-abhängige Biofilmbildung nachgewiesen werden [30]. Bislang gelang es jedoch nicht Gene, die für das AI-2-Transportsystem in *E. faecalis* kodieren, zu beschreiben. Das Ziel der vorliegenden Arbeit war es daher das Gen, welches für das AI-2-Bindeprotein im LuxS/AI-2-Typ QS-System von *E. faecalis* kodiert, zu identifizieren. Basierend auf Literaturrecherchen und bisher nicht publizierenten RNA-Seq-Analysen, mithilfe welcher wir Gene detektierten, die nach Inkubation mit AI-2 verstärkt transkribiert wurden, vermuteten wir, dass das *ef0907*-Gen für das AI-2-Bindeprotein kodiert. Um die Rolle des *ef0907*-Gens im LuxS/AI-2-Typ QS-System in *E. faecalis* näher zu untersuchen, führten wir zunächst eine bioinformatische Analyse durch, der zufolge das Protein EF0907 ein potenzielles Bindeprotein in solch einem System ist. Nachfolgend untersuchten wir die Bindung zwischen dem rekombinant überexprimierten Protein rEF0907 und AI-2 mittels isothermer Titrationskalorimetrie und beurteilten die Interaktion als moderat exotherm. Zur Bestätigung der Ergebnisse wurde das *ef0907*-Gen im *E. faecalis* V583ΔABC Stamm in-frame deletiert (ΔEF0907). Anschließend bestimmten wir die AI-2-Konzentrationen in den Kulturüberständen von V583ΔABC und den Mutanten. Die vermehrte Akkumulation von AI-2 in den Überständen von ΔEF0907, weist auf eine Beteiligung des *ef0907*-Gen an der Internalisierung von AI-2 hin. Dies korreliert mit den Ergebnissen im Mikrotiterplatten-Biofilm-Assay, denen zufolge ΔEF0907 signifikant mehr Biofilm produziert. Unerwarteterweise reagiert ΔEF0907 nach wie vor auf external supplementiertes AI-2 in Form einer verminderten Biofilmbildung. Insgesamt vermuten

wir daher, dass das *ef0907*-Gen zwar für ein AI-2-bindendes Protein im ABC-Transportsystem von *E. faecalis* kodiert, jedoch *E. faecalis* in der Lage ist die AI-2-Konzentration auch ohne Internalisierung zu detektieren. Außerdem ist es vorstellbar, dass *E. faecalis* mehr als nur ein AI-2-vermitteltes QS-System besitzt.

VIII. References

1. Fisher, K. & Phillips, C. The ecology, epidemiology and virulence of Enterococcus. *Microbiology* **155**, 1749–1757 (2009).

2. Arntzen, M. Ø., Karlskås, I. L., Skaugen, M., Eijsink, V. G. H. & Mathiesen, G. Proteomic Investigation of the Response of Enterococcus faecalis V583 when Cultivated in Urine. *PLoS One* **10**, e0126694 (2015).

3. Van Tyne, D., Martin, M. J. & Gilmore, M. S. Structure, function, and biology of the Enterococcus faecalis cytolysin. *Toxins (Basel).* **5**, 895–911 (2013).

4. Lawley, T. D. & Walker, A. W. Intestinal colonization resistance. *Immunology* **138**, 1–11 (2013).

5. Paulsen, I. T. *et al.* Role of mobile DNA in the evolution of vancomycin-resistant Enterococcus faecalis. *Science* **299**, 2071–2074 (2003).

6. Simon, A. *et al. Hyg Med.* **29**, (2004).

7. Klare, I., Witte, W., Wendt, C. & Werner, G. Vancomycin-resistente Enterokokken (VRE): Aktuelle Daten und Trends zur Resistenzentwicklung. *Bundesgesundheitsblatt* **55**, 1387–1400 (2012).

8. O'Driscoll, T. & Crank, C. W. Vancomycin-resistant enterococcal infections: epidemiology, clinical manifestations, and optimal management. *Infect. Drug Resist.* **8**, 217–230 (2015).

9. Cetinkaya, Y., Falk, P. & Mayhall, C. G. Vancomycin-resistant enterococci. *Clin. Microbiol. Rev.* **13**, 686–707 (2000).

10. Paganelli, F. L. *et al.* Enterococcus faecium Biofilm Formation: Identification of Major Autolysin AtlA Efm , Associated Acm Surface Localization, and AtlA Efm-Independent Extracellular DNA Release 2013. Enterococcus faecium biofilm formation: identification of major autolysin At. *MBio* **4**, (2013).

11. Brown, D. F. J. *et al.* National Glycopeptide-Resistant Enterococcal Bacteraemia Surveillance Working Group Report to the Department of Health — August 2004. *J. Hosp. Infect.* **62**, 1–27 (2006).

12. Thiercelin, M. E. Sur un diplocoque saprophyte de l'intestin susceptible de

devenir pathogène. *C. R. Séances Société Biol.* **51**, 269–71 (1899).

13. Thiercelin, M. E. & Jouhaud, L. Reproduction de l'entérocoque: taches centrales; granulations périphériques et microblastes. *C. R. Séances Société Biol.* **55**, 686–688 (1903).

14. Andrewes, F. W. & Horder, T. J. A study of the streptococci pathogenic for man. *Lancet* **168**, 775–783 (1906).

15. Sherman, J. M. The Streptococci. *Bacteriol. Rev.* **1**, 3–97 (1937).

16. Schleifer, K. H. & Kilpper-Bälz, R. Transfer of Streptococcus faecalis and Streptococcus faecium to the genus Enterococcus nom. rev. as Enterococcus faecalis comb. nov. and Enterococcus faecium comb. nov. *Int. J. Syst. Bacteriol.* **34**, 31–34 (1984).

17. Ludwig, W. *et al.* The Phylogenetic Position of Streptococcus and Enterococcus. *J. Gen. Microbiol.* **131**, 543–551 (1985).

18. Collins, M. D., Ash, C., Farrow, J. A., Wallbanks, S. & Williams, A. M. 16S ribosomal ribonucleic acid sequence analyses of lactococci and related taxa. Description of Vagococcus fluvialis gen. nov., sp. nov. *J. Appl. Bacteriol.* **67**, 453–60 (1989).

19. Klein, G. Taxonomy, ecology and antibiotic resistance of enterococci from food and the gastro-intestinal tract. *Int. J. Food Microbiol.* **88**, 123–131 (2003).

20. Parte, A. C., Carbasse, J. S., Meier-Kolthoff, J. P., Reimer, L. C. & Göker, M. List of prokaryotic names with standing in nomenclature (LPSN) moves to the DSMZ. *Int. J. Syst. Evol. Microbiol.* **70**, 5607–5612 (2020).

21. DSMZ. Genus: Enterococcus. (2021). Available at: https://www.bacterio.net/genus/enterococcus. (Accessed: 23rd January 2022)

22. Li, Y. Q. & Gu, C. T. Proposal of enterococcus Xinjiangensis Ren et al. 2020 as a later heterotypic synonym of enterococcus Lactis Morandi et al. 2012. *Int. J. Syst. Evol. Microbiol.* **71**, 004716 (2021).

23. Bøhle, L. A. *et al.* Identification of surface proteins in Enterococcus faecalis V583. *BMC Genomics* **12**, 135 (2011).

24. Tacconelli, E. & Cataldo, M. A. Vancomycin-resistant enterococci (VRE): transmission and control. *Int. J. Antimicrob. Agents* **31**, 99–106 (2008).

25. Sava, I. G., Heikens, E. & Huebner, J. Pathogenesis and immunity in enterococcal infections. *Clin. Microbiol. Infect.* **16**, 533–540 (2010).

26. Franz, C. M., Holzapfel, W. H. & Stiles, M. E. Enterococci at the crossroads of food safety? *Int. J. Food Microbiol.* **47**, 1–24 (1999).

27. Benachour, A. *et al.* Identification of secreted and surface proteins from Enterococcus faecalis. *Can. J. Microbiol.* **55**, 967–74 (2009).

28. Aakra, A. *et al.* Transcriptional Response of Enterococcus faecalis V583 to Erythromycin. *Antimicrob. Agents Chemother.* **49**, 2246–59 (2005).

29. Kaper, J. B. & Sperandio, V. Bacterial Cell-to-Cell Signaling in the Gastrointestinal Tract. *Infect. Immun.* **73**, 3197–209 (2005).

30. Shao, C. *et al.* LuxS-dependent AI-2 regulates versatile functions in Enterococcus faecalis V583. *J. Proteome Res.* **11**, 4465–4475 (2012).

31. Reffuveille, F. *et al.* The prolipoprotein diacylglyceryl transferase (Lgt) of Enterococcus faecalis contributes to virulence. *Microbiology* **158**, 816–825 (2012).

32. Vebø, H. C., Snipen, L., Nes, I. F. & Brede, D. A. The Transcriptome of the Nosocomial Pathogen Enterococcus faecalis V583 Reveals Adaptive Responses to Growth in Blood. *PLoS One* **4**, e7660 (2009).

33. Agudelo Higuita, N. I. & Huycke, M. M. *Enterococcal Disease, Epidemiology, and Implications for Treatment*. *Enterococci: From Commensals to Leading Causes of Drug Resistant Infection* (Massachusetts Eye and Ear Infirmary, 2014).

34. McDonald, J. R. *et al.* Enterococcal endocarditis: 107 cases from the international collaboration on endocarditis merged database. *Am. J. Med.* **118**, 759–766 (2005).

35. Hollenbeck, B. L. & Rice, L. B. Intrinsic and acquired resistance mechanisms in enterococcus. *Virulence* **3**, 421–433 (2012).

36. Werner, G., Klare, I., Hübner, J., Ker, W. & Witte, W. Vancomycin-resistente Enterokokken. *Chemother. J.* **17**, 183–193 (2008).

37. Uttley, A. C., Collins, C. H., Naidoo, J. & George, R. C. Vancomycin-resistant Enterococci. *Lancet* **331**, 57–58 (1988).

38. Gastmeier, P., Schroder, C., Behnke, M., Meyer, E. & Geffers, C. Dramatic increase in vancomycin-resistant enterococci in Germany. *J. Antimicrob. Chemother.* **69**, 1660–1664 (2014).

39. Sahm, D. F. *et al.* In Vitro Susceptibility Studies of Vancomycin-Resistant Enterococcus faecalis. *Antimicrob. Agents Chemother.* **33**, 1588–1591 (1989).

40. Mundy, L. M., Sahm, D. F. & Gilmore, M. Relationships between Enterococcal Virulence and Antimicrobial Resistance. *Clin. Microbiol. Rev.* **13**, 513–522 (2000).

41. Oprea, S. F. *et al.* Molecular and clinical epidemiology of vancomycin-resistant Enterococcus faecalis. *J. Antimicrob. Chemother.* **53**, 626–630 (2004).

42. Klare, I. *et al.* Eigenschaften, Häufigkeit und Verbreitung von Vancomycin-resistenten Enterokokken (VRE) in Deutschland – Update 2015/2016. *Epidemiol. Bull.* **46**, 12 (2017).

43. WHO Regional Office for Europe and European Centre for Disease Prevention and Control. Surveillance of antimicrobial resistance in Europe, 2020 data. Executive Summary. *Copenhagen WHO Reg. Off. Eur.* 1–5 (2021).

44. European Centre for Disease Prevention and Control. Surveillance Atlas of Infectious Diseases. (2016). Available at: http://atlas.ecdc.europa.eu/public/index.aspx. (Accessed: 25th January 2022)

45. Robert Koch Institute. ARS - Antibiotika Resistenz Surveillance. (2021). Available at: https://ars.rki.de/Content/Database/Main.aspx. (Accessed: 24th January 2022)

46. Remschmidt, C. *et al.* Continuous increase of vancomycin resistance in enterococci causing nosocomial infections in Germany - 10 years of surveillance. *Antimicrob. Resist. Infect. Control* **7**, 1–7 (2018).

47. Fuqua, W. C., Winans, S. C. & Greenberg, E. P. Quorum Sensing in Bacteria: the LuxR-LuxI Family of Cell Density-Responsive Transcriptional Regulatorst. *J. Bacteriol.* **176**, 269–275 (1994).

48. Parveen, N. & Cornell, K. A. Methylthioadenosine/S-adenosylhomocysteine nucleosidase, a critical enzyme for bacterial metabolism. *Mol. Microbiol.* **79**, 7–20 (2011).

49. Ahmed, N. A. A. M., Petersen, F. C. & Scheie, A. A. AI-2 quorum sensing affects antibiotic susceptibility in Streptococcus anginosus. *J. Antimicrob. Chemother.* **60**, 49–53 (2007).

50. Teixeira, N. *et al.* Drosophila Host Model Reveals New Enterococcus faecalis Quorum-Sensing Associated Virulence Factors. *PLoS One* **8**, e64740 (2013).

51. Silpe, J. E. & Bassler, B. L. A Host-Produced Quorum-Sensing Autoinducer Controls a Phage Lysis-Lysogeny Decision. *Cell* **176**, 268-280.e13 (2019).

52. Rossmann, F. S. *et al.* Phage-mediated Dispersal of Biofilm and Distribution of Bacterial Virulence Genes Is Induced by Quorum Sensing. *PLoS Pathog.* **11**, e1004653 (2015).

53. Singh, P. K. *et al.* Quorum-sensing signals indicate that cystic fibrosis lungs are infected with bacterial biofilms. *Nature* **407**, 762–764 (2000).

54. Davies, D. G. *et al.* The involvement of cell-to-cell signals in the development of a bacterial biofilm. *Science (80-.).* **280**, 295–298 (1998).

55. Yang, Y., Li, W., Hou, B. & Zhang, C. Quorum sensing LuxS/autoinducer-2 inhibits Enterococcus faecalis biofilm formation ability. *J. Appl. Oral Sci.* **26**, e20170566 (2018).

56. Pacheco, A. R. & Sperandio, V. Inter-kingdom signaling: chemical language between bacteria and host. *Curr. Opin. Microbiol.* **12**, 192–198 (2009).

57. Thompson, J. A., Oliveira, R. A. & Xavier, K. B. Chemical conversations in the gut microbiota. *Gut Microbes* **7**, 163–170 (2016).

58. Pereira, C. S., Thompson, J. A. & Xavier, K. B. AI-2-mediated signalling in bacteria. *FEMS Microbiol. Rev.* **37**, 156–181 (2013).

59. Rezzonico, F., Smits, T. H. M. & Duffy, B. Detection of AI-2 receptors in genomes of Enterobacteriaceae suggests a role of type-2 quorum sensing in closed ecosystems. *Sensors* **12**, 6645–6665 (2012).

60. DeLisa, M. P., Wu, C. F., Wang, L., Valdes, J. J. & Bentley, W. E. DNA Microarray-Based Identification of Genes Controlled by Autoinducer 2-Stimulated Quorum Sensing in Escherichia coli. *J. Bacteriol.* **183**, 5239–47 (2001).

61. Miller, M. B. & Bassler, B. L. Quorum Sensing in Bacteria. *Annu. Rev. Microbiol.* **55**, 165–199 (2001).

62. Papenfort, K. & Bassler, B. L. Quorum sensing signal-response systems in Gram-negative bacteria. *Nat. Rev. Microbiol.* **14**, 576–88 (2016).

63. Federle, M. J. & Bassler, B. L. Interspecies communication in bacteria. *J. Clin. Invest.* **112**, 1291–1299 (2003).

64. Federle, M. J. Autoinducer-2-based chemical communication in bacteria: Complexities of interspecies signaling. *Contrib. Microbiol.* **16**, 18–32 (2009).

65. Challan Belval, S. *et al.* Assessment of the Roles of LuxS, S-Ribosyl Homocysteine, and Autoinducer 2 in Cell Attachment during Biofilm Formation by Listeria monocytogenes EGD-e. *Appl. Environ. Microbiol.* **72**, 2644–2650 (2006).

66. Bassler, B. L., Greenberg, E. P. & Stevens, A. M. Cross-Species Induction of Luminescence in the Quorum-Sensing Bacterium Vibrio harveyi. *J. Bacteriol.* **179**, 4043–4045 (1997).

67. Xavier, K. B. & Bassler, B. L. Interference with AI-2-mediated bacterial cell–cell communication. *Nature* **437**, 750–753 (2005).

68. Cao, J. G. & Meighen, E. A. Purification and structural identification of an autoinducer for the luminescence system of Vibrio harveyi. *J. Biol. Chem.* **264**, 21670–21676 (1989).

69. Schauder, S., Shokat, K., Surette, M. G. & Bassler, B. L. The LuxS family of bacterial autoinducers: biosynthesis of a novel quorum-sensing signal molecule.

Mol. Microbiol. **41**, 463–476 (2001).

70. Walsh, J. R., Sen, T. Z. & Dickerson, J. A. A computational platform to maintain and migrate manual functional annotations for BioCyc databases. *BMC Syst. Biol.* **8**, 115 (2014).

71. Doherty, N., G Holden, M. T., Qazi, S. N., Williams, P. & Winzer, K. Functional Analysis of luxS in Staphylococcus aureus Reveals a Role in Metabolism but Not Quorum Sensing. *J. Bacteriol.* **188**, 2885–2897 (2006).

72. Miller, S. T. *et al.* Salmonella typhimurium recognizes a chemically distinct form of the bacterial quorum-sensing signal AI-2. *Mol. Cell* **15**, 677–687 (2004).

73. Chen, X. *et al.* Structural identification of a bacterial quorum-sensing signal containing boron. *Nature* **415**, 545–549 (2002).

74. Pereira, C. S., De Regt, A. K., Brito, P. H., Miller, S. T. & Xavier, K. B. Identification of Functional LsrB-Like Autoinducer-2 Receptors. *J. Bacteriol.* **191**, 6975–6987 (2009).

75. Qin, X., Singh, K. V., Weinstock, G. M. & Murray, B. E. Effects of Enterococcus faecalis fsr genes on production of gelatinase and a serine protease and virulence. *Infect. Immun.* **68**, 2579–2586 (2000).

76. Ali, L. *et al.* Molecular Mechanism of Quorum-Sensing in Enterococcus faecalis: Its Role in Virulence and Therapeutic Approaches. *Int. J. Mol. Sci.* **18**, E960 (2017).

77. La Rosa, S. L., Solheim, M., Diep, D. B., Nes, I. F. & Brede, D. A. Bioluminescence based biosensors for quantitative detection of enterococcal peptide - Pheromone activity reveal inter-strain telesensing in vivo during polymicrobial systemic infection. *Sci. Rep.* **5**, 8339 (2015).

78. Pillai, S. K. *et al.* Effects of Glucose on fsr- Mediated Biofilm Formation in Enterococcus faecalis. *J. Infect. Dis.* **190**, 967–970 (2004).

79. Haas, W., Shepard, B. D. & Gilmore, M. S. Two-component regulator of Enterococcus faecalis cytolysin responds to quorum-sensing autoinduction. *Nature* **415**, 84–87 (2002).

80. Kanehisa, M., Sato, Y., Furumichi, M., Morishima, K. & Tanabe, M. New approach for understanding genome variations in KEGG. *Nucleic Acids Res.* **47**, D590–D595 (2019).

81. Sun, J., Daniel, R., Wagner-Döbler, I. & Zeng, A.-P. Is autoinducer-2 a universal signal for interspecies communication: a comparative genomic and phylogenetic analysis of the synthesis and signal transduction pathways. *BMC Evol. Biol.* **4**, 36 (2004).

82. Gaspar, F. *et al.* Enterococcus faecalis V583 LuxS/AI-2 system is devoid of role in intra-species quorum-sensing but contributes to virulence in a Drosophila host model. *bioRxiv* 344176 [Preprint] (2018). doi:10.1101/344176

83. Xavier, K. B. & Bassler, B. L. Regulation of uptake and processing of the quorum-sensing autoinducer AI-2 in Escherichia coli. *J. Bacteriol.* **187**, 238–248 (2005).

84. Thompson, J. A., Oliveira, R. A., Djukovic, A., Ubeda, C. & Xavier, K. B. Manipulation of the quorum sensing signal AI-2 affects the antibiotic-treated gut microbiota. *Cell Rep.* **10**, 1861–71 (2015).

85. Tay, S. B. & Yew, W. S. Development of quorum-based anti-virulence therapeutics targeting Gram-negative bacterial pathogens. *Int. J. Mol. Sci.* **14**, 16570–99 (2013).

86. Fong, J. *et al.* Combination Therapy Strategy of Quorum Quenching Enzyme and Quorum Sensing Inhibitor in Suppressing Multiple Quorum Sensing Pathways of P. aeruginosa. *Sci. Rep.* **8**, 1155 (2018).

87. Williams, P. Strategies for inhibiting quorum sensing. *Emerg. Top. Life Sci.* **1**, 23–30 (2017).

88. Murugayah, S. A. & Gerth, M. L. Engineering quorum quenching enzymes: progress and perspectives. *Biochem. Soc. Trans.* **47**, 793–800 (2019).

89. Rigottier-Gois, L. *et al.* Large-Scale Screening of a Targeted Enterococcus faecalis Mutant Library Identifies Envelope Fitness Factors. *PLoS One* **6**, e29023 (2011).

90. McShan, W. M. & Shankar, N. The Genome of Enterococcus faecalis V583: a Tool for Discovery. in *The Enterococci* 409–415 (American Society of Microbiology, 2014). doi:10.1128/9781555817923.ch11

91. Reffuveille, F., Leneveu, C., Chevalier, S., Auffray, Y. & Rincé, A. Lipoproteins of Enterococcus faecalis: Bioinformatic identification, expression analysis and relation to virulence. *Microbiology* **157**, 3001–3013 (2011).

92. Chang, C., Bigelow, L., Bearden, J. & Joachimiak, A. Crystal structure of peptide ABC transporter, peptide-binding protein. *Protein Data Bank [To be Publ.]* doi:10.2210/PDB3O6P/PDB

93. Vebø, H. C., Solheim, M., Snipen, L., Nes, I. F. & Brede, D. A. Comparative Genomic Analysis of Pathogenic and Probiotic Enterococcus faecalis Isolates, and Their Transcriptional Responses to Growth in Human Urine. *PLoS One* **5**, e12489 (2010).

94. Beeston, A. L. & Surette, M. G. pfs-dependent regulation of autoinducer 2 production in Salmonella enterica serovar Typhimurium. *J. Bacteriol.* **184**, 3450–6 (2002).

95. Mah, T. F. & O'Toole, G. A. Mechanisms of biofilm resistance to antimicrobial agents. *Trends Microbiol.* **9**, 34–9 (2001).

96. Mohamed, J. A. & Huang, D. B. Biofilm formation by enterococci. *J. Med. Microbiol.* **56**, 1581–1588 (2007).

97. Stewart, P. S. & Costerton, J. W. Antibiotic resistance of bacteria in biofilms. *Lancet* **358**, 135–138 (2001).

98. Hirakawa, H. & Tomita, H. Interference of bacterial cell-to-cell communication: A new concept of antimicrobial chemotherapy breaks antibiotic resistance. *Front. Microbiol.* **4**, (2013).

99. Ch'ng, J. H., Chong, K. K. L., Lam, L. N., Wong, J. J. & Kline, K. A. Biofilm-associated infection by enterococci. *Nat. Rev. Microbiol.* **17**, 82–94 (2019).

100. Hentzer, M., Givskov, M. & Parsek, M. R. Targeting Quorum Sensing for Treatment of Chronic Bacterial Biofilm Infections. *Lab. Med.* **33**, 295–306

(2002).

101. Auger, S., Krin, E., Aymerich, S. & Gohar, M. Autoinducer 2 Affects Biofilm Formation by Bacillus cereus. *Appl. Environ. Microbiol.* **72**, 937–41 (2006).

102. Wang, Y., Liu, B., Grenier, D. & Yi, L. Regulatory mechanisms of the LuxS/AI-2 system and bacterial resistance. *Antimicrobial Agents and Chemotherapy* **63**, (2019).

103. He, Z. *et al.* Effect of the quorum-sensing luxS gene on biofim formation by Enterococcus faecalis. *Eur. J. Oral Sci.* **124**, 234–240 (2016).

104. Nazzaro, F., Fratianni, F. & Coppola, R. Quorum sensing and phytochemicals. *Int. J. Mol. Sci.* **14**, 12607–12619 (2013).

105. Arias, C. A. & Murray, B. E. The rise of the Enterococcus: beyond vancomycin resistance. *Nat. Rev. Microbiol.* **10**, 266–278 (2012).

106. Durfee, T. *et al.* The complete genome sequence of Escherichia coli DH10B: insights into the biology of a laboratory workhorse. *J. Bacteriol.* **190**, 2597–606 (2008).

107. Thurlow, L. R., Thomas, V. C. & Hancock, L. E. Capsular Polysaccharide Production in Enterococcus faecalis and Contribution of CpsF to Capsule Serospecificity. *J. Bacteriol.* **191**, 6203–6210 (2009).

108. Eichenbaum, Z. *et al.* Use of the Lactococcal nisA Promoter To Regulate Gene Expression in Gram-Positive Bacteria: Comparison of Induction Level and Promoter Strength. *Appl. Environ. Microbiol.* **64**, 2763–2769 (1998).

109. Jeong, H. *et al.* Genome Sequences of Escherichia coli B strains REL606 and BL21(DE3). *J. Mol. Biol.* **394**, 644–652 (2009).

110. Hanahan, D. Studies on transformation of Escherichia coli with plasmids. *J. Mol. Biol.* **166**, 557–580 (1983).

111. Taga, M. E. & Xavier, K. B. Methods for Analysis of Bacterial Autoinducer-2 Production. *Curr. Protoc. Microbiol.* **23**, 1C.1.1-1C.1.15 (2011).

112. Zhao, C. *et al.* Role of Methionine Sulfoxide Reductases A and B of

Enterococcus faecalis in Oxidative Stress and Virulence. *Infect. Immun.* **78**, 3889–3897 (2010).

113. Qiagen. *The QIAexpressionist^{TM}: A handbook for high-level expression and purification of 6xHis-tagged proteins, 5th Edition*. (2003).

114. Samuelson, J. Bacterial Systems. in *Production of Membrane Proteins* 11–35 (Wiley-VCH Verlag GmbH & Co. KGaA, 2011). doi:10.1002/9783527634521.ch1

115. Stüber, D., Matile, H. & Garotta, G. System for High-Level Production in Escherichia coli and Rapid Purification of Recombinant Proteins: Application to Epitope Mapping, Preparation of Antibodies, and Structure—Function Analysis. in *Immunological Methods* 121–152 (Academic Press, 1990). doi:10.1016/b978-0-12-442704-4.50014-1

116. Janknecht, R. *et al.* Rapid and efficient purification of native histidine-tagged protein expressed by recombinant vaccinia virus. *Proc. Natl. Acad. Sci. U. S. A.* **88**, 8972–8976 (1991).

117. Schwarz, E., Scherer, G., Hobom, G. & Kössel, H. Nucleotide sequence of cro, cII and part of the O gene in phage λ DNA. *Nature* **272**, 410–414 (1978).

118. Kristich, C. J., Chandler, J. R. & Dunny, G. M. Development of a host-genotype-independent counterselectable marker and a high-frequency conjugative delivery system and their use in genetic analysis of Enterococcus faecalis. *Plasmid* **57**, 131–44 (2007).

119. Behnke, D., Gilmore, M. S. & Ferretti, J. J. Plasmid pGB301, a new multiple resistance streptococcal cloning vehicle and its use in cloning of a gentamicin/kanamycin resistance determinant. *Mol. Gen. Genet.* **182**, 414–21 (1981).

120. Callegan, M. C., Jett, B. D., Hancock, L. E. & Gilmore, M. S. Role of hemolysin BL in the pathogenesis of extraintestinal Bacillus cereus infection assessed in an endophthalmitis model. *Infect. Immun.* **67**, 3357–66 (1999).

121. Hancock, L. E. & Gilmore, M. S. The capsular polysaccharide of Enterococcus faecalis and its relationship to other polysaccharides in the cell wall. *Proc. Natl.*

Acad. Sci. U. S. A. **99**, 1574–1579 (2002).

122. Theilacker, C. *et al.* Glycolipids are involved in biofilm accumulation and prolonged bacteraemia in *Enterococcus faecalis*. *Mol. Microbiol.* **71**, 1055–1069 (2009).

123. Chattoraj, D. K., Snyder, K. M. & Abeles, A. L. P1 plasmid replication: Multiple functions of RepA protein at the origin. *Proc. Natl. Acad. Sci. U. S. A.* **82**, 2588–2592 (1985).

124. Steed, M. E. *et al.* Characterizing vancomycin-resistant Enterococcus strains with various mechanisms of daptomycin resistance developed in an In Vitro pharmacokinetic/pharmacodynamic model. *Antimicrob. Agents Chemother.* **55**, 4748–4754 (2011).

125. Torcato, I. M., Kasal, M. R., Brito, P. H., Miller, S. T. & Xavier, K. B. Identification of novel autoinducer-2 receptors in Clostridia reveals plasticity in the binding site of the LsrB receptor family. *J. Biol. Chem.* **294**, 4450–4463 (2019).

126. Maniatis, T., Sambrook, J., Fritsch, E. F. & Laboratory, C. S. H. *Molecular Cloning: A Laboratory Manual*. (Cold Spring Harbor Laboratory Press, 1982).

127. Dower, W. J., Miller, J. F. & Ragsdale, C. W. High efficiency transformation of E. coli by high voltage electroporation. *Nucleic Acids Res.* **16**, 6127–45 (1988).

128. Ullmann, A., Jacob, F. & Monod, J. Characterization by in vitro complementation of a peptide corresponding to an operator-proximal segment of the β-galactosidase structural gene of Escherichia coli. *J. Mol. Biol.* **24**, 339–343 (1967).

129. Green, M. R. & Sambrook, J. *Molecular Cloning: A Laboratory Manual*. (Cold Spring Harbor Laboratory Press, 2012).

130. Sanger, F. & Coulson, A. R. A rapid method for determining sequences in DNA by primed synthesis with DNA polymerase. *J. Mol. Biol.* **94**, 441–448 (1975).

131. Ho, S. N., Hunt, H. D., Horton, R. M., Pullen, J. K. & Pease, L. R. Site-directed mutagenesis by overlap extension using the polymerase chain reaction. *Gene* **77**,

51–59 (1989).

132. Ladjouzi, R. *et al.* Analysis of the tolerance of pathogenic enterococci and staphylococcus aureus to cell wall active antibiotics. *J. Antimicrob. Chemother.* **68**, 2083–2091 (2013).

133. Laemmli, U. K. Cleavage of Structural Proteins during the Assembly of the Head of Bacteriophage T4. *Nature* **227**, 680–685 (1970).

134. Bradford, M. M. A rapid and sensitive method for the quantitation of microgram quantities of protein utilizing the principle of protein-dye binding. *Anal. Biochem.* **72**, 248–254 (1976).

135. Rajamani, S., Zhu, J., Pei, D. & Sayre, R. A LuxP-FRET-based reporter for the detection and quantification of AI-2 bacterial quorum-sensing signal compounds. *Biochemistry* **46**, 3990–3997 (2007).

136. Paganelli, F. L. *et al.* Enterococcus faecium Biofilm Formation: Identification of Major Autolysin AtlAEfm, associated Acm Surface Localization, and AtlAEfm-Independent Extracellular DNA Release. *MBio* **4**, e00154 (2013).

137. Kropec, A. *et al.* Identification of SagA as a novel vaccine target for the prevention of Enterococcus faecium infections. *Microbiology* **157**, 3429–3434 (2011).

138. Huebner, J. *et al.* Isolation and chemical characterization of a capsular polysaccharide antigen shared by clinical isolates of Enterococcus faecalis and vancomycin-resistant Enterococcus faecium. *Infect. Immun.* **67**, 1213–1219 (1999).

139. Hufnagel, M. *et al.* Serological and genetic diversity of capsular polysaccharides in Enterococcus faecalis. *J. Clin. Microbiol.* **42**, 2548–2557 (2004).

140. Taga, M. E., Semmelhack, J. L. & Bassler, B. L. The LuxS-dependent autoinducer AI-2 controls the expression of an ABC transporter that functions in AI-2 uptake in Salmonella typhimurium. *Mol. Microbiol.* **42**, 777–793 (2008).

141. Núñez, S., Venhorst, J. & Kruse, C. G. Target–drug interactions: first principles and their application to drug discovery. *Drug Discov. Today* **17**, 10–22 (2012).

142. Du, X. *et al.* Insights into Protein-Ligand Interactions: Mechanisms, Models, and Methods. *Int. J. Mol. Sci.* **17**, 144 (2016).

143. Banerjee, D. R. *et al.* Design, synthesis and characterization of novel inhibitors against mycobacterial β-ketoacyl CoA reductase FabG4. *Org. Biomol. Chem.* **12**, 73–85 (2014).

144. Pereira, C. S., McAuley, J. R., Taga, M. E., Xavier, K. B. & Miller, S. T. Sinorhizobium meliloti, a bacterium lacking the autoinducer-2 (AI-2) synthase, responds to AI-2 supplied by other bacteria. *Mol. Microbiol.* **70**, 1223–1235 (2008).

145. Rader, B. A. *et al.* Helicobacter pylori perceives the quorum-sensing molecule AI-2 as a chemorepellent via the chemoreceptor TlpB. *Microbiology* **157**, 2445–2455 (2011).

146. Shao, H., James, D., Lamont, R. J. & Demuth, D. R. Differential Interaction of Aggregatibacter (Actinobacillus) actinomycetemcomitans LsrB and RbsB Proteins with Autoinducer 2. *J. Bacteriol.* **189**, 5559–5565 (2007).

147. Armbruster, C. E. *et al.* RbsB (NTHI-0632) mediates quorum signal uptake in nontypeable Haemophilus influenzae strain 86-028NP. *Mol. Microbiol.* **82**, 836–850 (2011).

148. Zhang, L. *et al.* Sensing of autoinducer-2 by functionally distinct receptors in prokaryotes. *Nat. Commun.* **11**, 1–13 (2020).

149. Duff, M. R., Grubbs, J. & Howell, E. E. Isothermal Titration Calorimetry for Measuring Macromolecule-Ligand Affinity. *J. Vis. Exp.* e2796 (2011). doi:10.3791/2796

150. Falconer, R. J., Penkova, A., Jelesarov, I. & Collins, B. M. Survey of the year 2008: applications of isothermal titration calorimetry. *J. Mol. Recognit.* **23**, 395–413 (2010).

151. Ames, G. F. L. Bacterial Periplasmic Transport Systems: Structure, Mechanism, and Evolution. *Annu. Rev. Biochem.* **55**, 397–425 (1986).

152. Zhu, J. & Pei, D. A LuxP-Based Fluorescent Sensor for Bacterial Autoinducer II.

ACS Chem. Biol. **3**, 110–119 (2008).

153. Freyer, M. W. & Lewis, E. A. Isothermal Titration Calorimetry: Experimental Design, Data Analysis, and Probing Macromolecule/Ligand Binding and Kinetic Interactions. *Methods Cell Biol.* **84**, 79–113 (2008).

154. Tellinghuisen, J. Optimizing Experimental Parameters in Isothermal Titration Calorimetry. *J. Phys. Chem. B* **109**, 20027–20035 (2005).

155. Ciulli, A. Biophysical Screening for the Discovery of Small-Molecule Ligands. *Methods Mol. Biol.* **1008**, 357–388 (2013).

156. Chen, K. & Kurgan, L. Investigation of Atomic Level Patterns in Protein—Small Ligand Interactions. *PLoS One* **4**, e4473 (2009).

157. Bian, X. & Lockless, S. W. Preparation To Minimize Buffer Mismatch in Isothermal Titration Calorimetry Experiments. *Anal. Chem.* **88**, 5549–5553 (2016).

158. Heurlier, K. *et al.* Growth Deficiencies of Neisseria meningitidis pfs and luxS Mutants Are Not Due to Inactivation of Quorum Sensing. *J. Bacteriol.* **191**, 1293–1302 (2009).

159. Keizers, M., Dobrindt, U. & Berger, M. A Simple Biosensor-Based Assay for Quantitative Autoinducer-2 Analysis. *ACS Synth. Biol.* **11**, 747–759 (2022).

160. Rajamani, S. & Sayre, R. Biosensors for the Detection and Quantification of AI-2 Class Quorum-Sensing Compounds. in *Methods in molecular biology (Clifton, N.J.)* **1673**, 73–88 (2018).

161. von Bodman, S. B., Willey, J. M. & Diggle, S. P. Cell-Cell Communication in Bacteria: United We Stand. *J. Bacteriol.* **190**, 4377–4391 (2008).

162. Nadell, C. D., Xavier, J. B. & Foster, K. R. The sociobiology of biofilms. *FEMS Microbiol. Rev.* **33**, 206–224 (2009).

163. Azeredo, J. *et al.* Critical review on biofilm methods. *Crit. Rev. Microbiol.* **43**, 313–351 (2017).

164. Nguyen, M. T. & Götz, F. Lipoproteins of Gram-Positive Bacteria: Key Players

in the Immune Response and Virulence. *Microbiol. Mol. Biol. Rev.* **80**, 891–903 (2016).

165. Kovacs-Simon, A., Titball, R. W. & Michell, S. L. Lipoproteins of Bacterial Pathogens. *Infect. Immunitymmunity* **79**, 548–561 (2011).

166. Romero-Saavedra, F. *et al.* Identification of Peptidoglycan-Associated Proteins as Vaccine Candidates for Enterococcal Infections. *PLoS One* **9**, e111880 (2014).

167. Kropec, A. *et al.* Identification of SagA as a novel vaccine target for the prevention of Enterococcus faecium infections. *Microbiology* **157**, 3429–3434 (2011).

168. Anderson, P., Whitin, J. C. & Keyserling, H. L. Standardization of an Opsonophagocytic Assay for the Measurement of Functional Antibody Activity against Streptococcus pneumoniae Using Differentiated HL-60 Cells. *Clin. Diagn. Lab. Immunol.* **4**, 415–422 (1997).

169. Yi, L., Dong, X., Grenier, D., Wang, K. & Wang, Y. Research progress of bacterial quorum sensing receptors: Classification, structure, function and characteristics. *Sci. Total Environ.* **763**, 143031 (2021).

Acknowledgements

First, I would like to give my deepest gratitude to my supervisors Prof. Dr. med. Johannes Hübner, head of the Infectiology Department of the Dr. von Hauner Children's Hospital of the Ludwig-Maximilians-University in Munich, and Dr. Luis Felipe Romero Saavedra, postdoc in the Dr. von Hauner Children's Hospital, who accompanied and supported me during all stages of this work.

Lieber Johannes, ich weiß es sehr zu schätzen, dass ich Teil deiner Arbeitsgruppe sein durfte, es war eine so lehrreiche und wunderbare Zeit. Im Besonderen möchte ich dir für deine Freundlichkeit und deine konstante Erreichbarkeit danken. Ich bewundere deine positive Herangehensweise, sowohl als Arzt, als auch als Wissenschaftler. Du bist zu einem Mentor für mich geworden. Danke, dass du mich unterstützt und deine überaus wertvollen Erfahrungen mit mir teilst.

Dear Felipe, thank you for always answering any of my questions so patiently. Some of the drawings, you made for a better understanding, still decorate my pinboard. I will never forget how we carried our samples to the Department of Biology in Martinsried in wind and weather and how both you and Diana prepared a delicious Colombian dinner for our research group. It was so much fun working with you.

It is important for me to kindly thank Dr. Diana Laverde, a postdoc in the Dr. von Hauner Children’s Hospital, for her invaluable help during my work in the Kubus. Thanks also for the nice conversations and the good coffee we enjoyed together after lunch.

I owe my regards to all those who supported me in the completion of this project. For manifold support, I am especially connected to our collaborator Prof. Dr. Kirsten Jung from the Department of Microbiology of the Ludwig-Maximilians-University in Munich assisting us with the Fluorescence resonance energy transfer-based assay. A sincere thanks also to our collaborator Prof. Dr. Ralf Heermann for your support in isothermal titration calorimetry.

Thanks also to the research group of Prof. Dr. med. Dr. sci. nat. Christoph Klein for sharing the laboratory facilities and instruments. Also, I would like to thank the members of the doctoral committee for evaluating my work presented in this thesis.

Zuletzt möchte ich mich bei meinen Eltern bedanken, die mich immer unterstützen.

Affidavit

Riedl, Victoria

Name, Vorname

Ich erkläre hiermit an Eides statt,
dass ich die vorliegende Dissertation mit dem Titel

Identification of the AI-2 binding protein in the Quorum Sensing system of *E. faecalis*

selbständig verfasst, mich außer der angegebenen keiner weiteren Hilfsmittel bedient und alle Erkenntnisse, die aus dem Schrifttum ganz oder annähernd übernommen sind, als solche kenntlich gemacht und nach ihrer Herkunft unter Bezeichnung der Fundstelle einzeln nachgewiesen habe.

Ich erkläre des Weiteren, dass die hier vorgelegte Dissertation nicht in gleicher oder in ähnlicher Form bei einer anderen Stelle zur Erlangung eines akademischen Grades eingereicht wurde.

München, 07.11.2023	Victoria Riedl
Ort, Datum	Unterschrift Doktorandin

List of Publications

V. Riedl, F. Romero-Saavedra, D. Laverde, R. Heermann, K. Jung, J. Huebner (2017, June). Identification of the AI-2-binding protein in the Quorum Sensing system of Enterococcus faecalis. Poster presentation for the 1st i-Target Kubus Conference, 2017, Munich, Germany.

V. Riedl, F. Romero-Saavedra, D. Laverde, R. Heermann, K. Jung, J. Huebner (2016, November). Identification of the AI-2-binding protein in the Quorum Sensing system of Enterococcus faecalis. Poster presentation for the Annual Meeting DZIF - German Center for Infection Research, 2016, Cologne, Germany.